Deutsches Geodätisches Forschungsinstitut

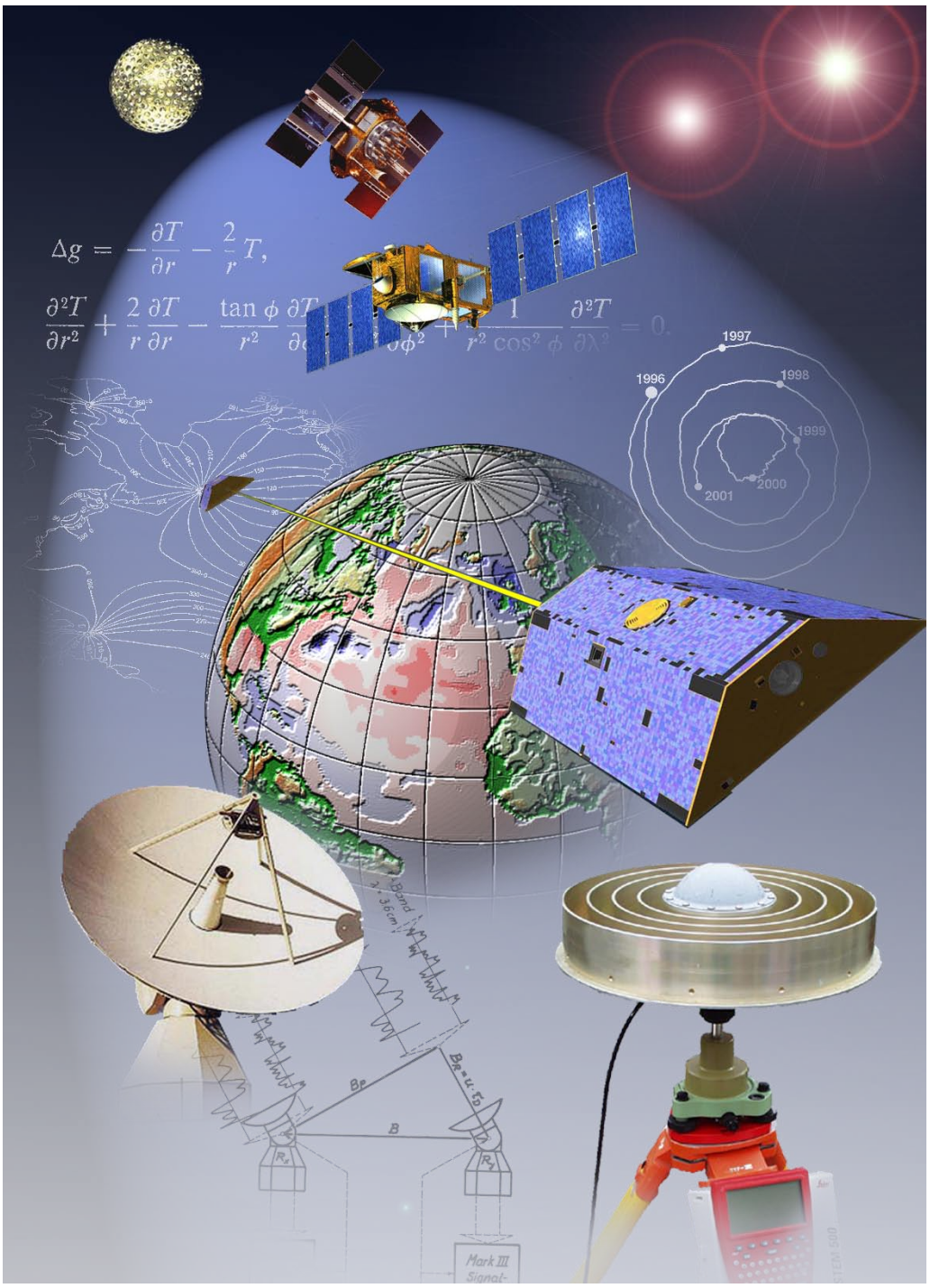

ANNUAL REPORT 2003/2004

Deutsches Geodätisches Forschungsinstitut (DGFI)
Marstallplatz 8, D-80539 München
Tel.: 089 23031-1107 Fax: 089 23031-1240
E-mail: mailer@dgfi.badw.de Internet: http://www.dgfi.badw.de

ANNUAL REPORT 2003/2004

Table of Contents

1st Edition

The Institute

The German Geodetic Research Institute (Deutsches Geodätisches Forschungsinstitut, DGFI) is an autonomous and independent research institution located in Munich. It is supervised by the German Geodetic Commission (Deutsche Geodätische Kommission, DGK) at the Bavarian Academy of Sciences. The research covers all fields of geodesy and includes the participation in national and international research projects as well as functions in international bodies.

The Programme

The long-term research programme of DGFI is based on the general theme „Fundamentals of Geodetic Reference Systems“. The definition of geodetic reference systems is studied and methods for their realization with modern space geodetic techniques are developed. Geodetic observations are analysed, approaches for the data processing are set up, tested and exemplarily applied.

Reference Systems

Reference systems are the necessary basis for the representation of geometrical or physical quantities, e.g., coordinates of points at the Earth’s surface or parameters describing the Earth’s outer gravity field. They are needed to transform geodetic observations into these parameters used in all kinds of precise positioning on Earth for geodesy, cadastre, engineering, geodynamics etc. But also geo-information systems, land management, navigation on land, in the sea and in air, and space research use the geodetic reference systems. Neighbouring disciplines like astronomy and geophysics apply geodetic reference systems for the orientation of spatial parameters. In general, geodetic reference systems are fundamentals for the global spatial infrastructure.

Motivation

The reason for the increasing importance of geodetic reference systems is the extensive use of space observation techniques in all fields of geodesy and neighbouring disciplines. Classical reference systems were defined and realised locally, e.g., by fixing a fundamental point with its coordinates and a local orientation. This was sufficient because the observation techniques were also locally oriented. Nowadays we need global reference systems to use appropriately the global observations.

Modern Reference Systems

To use the modern space techniques, e.g. satellite observations and radio astrometry, we need a geometric terrestrial reference system covering the whole globe. The Earth’s gravity field is represented by physical reference surfaces, e.g. the geoid as an equipotential surface or the sea level as a natural surface in a state of nearly equilibrium. To understand the geometrical and physical systems as well as their variations in space and time we have to study and model dynamic processes which influence the geodetic observations and parameters.

Practical Applications

The research programme of DGFI forms the basis for many practical applications in various fields of geodesy and surveying. The realizations of global reference systems as terrestrial reference frames, like the ITRF, allow the integration of continental and national systems, e.g. the German Satellite Positioning Service, SAPOS, as regional densifications. Theoretical studies on physi-

cal reference surfaces and monitoring of the time-dependent sea level are fundamentals for the definition and realization of height systems. These vertical reference systems have got an increasing importance because heights are today more and more determined by space techniques (e.g. GPS) rather than by terrestrial methods (e.g. levelling).

International Cooperation

The international geodetic community has developed an excellent cooperation during the last decades. Generally needed fundamentals, e.g. global reference systems, are studied jointly and established and maintained by mutual efforts. The International Association of Geodesy (IAG) as the most important body has installed several scientific services dealing with this problem and providing most important products free of charge. DGFI recognizes the outstanding role of these services for geodetic practice and research and cooperates in various of these services as data, analysis and research centre. Members of the DGFI staff have taken leading positions in the IAG and other organizations.

Neighbouring Disciplines

Geodetic parameters, e.g. from the realization of reference frames, may be used, analysed and interpreted in other disciplines like astronomy, geophysics, hydrology, meteorology, oceanography etc. DGFI seeks the contact to these disciplines and provides all the data and results to the neighbouring sciences. Several research projects are carried out in close cooperation with scientists and institutions from these disciplines.

Structure of the Research Programme

The present research programme for the years 2003/2004 was set up on the basis of the above described arguments. It was reviewed by the scientific council of the German Geodetic Commission (DGK) and approved by the DGK General Assembly in October 2002. It is divided into four long-term major topics consisting of 21 projects as well as the information systems and scientific transfer. The major topics are:

A Geometric reference systems
B Physical reference surfaces
C Dynamic processes
D International services and projects
E Information systems and scientific transfer

Research Group Satellite Geodesy

The projects related to satellite geodesy are carried out in the frame of the research programme of the Research Group Satellite Geodesy (Forschungsgruppe Satellitengeodäsie, FGS) which is a cooperation of the Institute of Astronomical and Physical Geodesy (IAPG), the Research Establishment Satellite Geodesy (FESG), both at the Technical University Munich, the Geodetic Institute of the University Bonn (GIUB), the Federal Agency for Cartography and Geodesy (BKG), and the German Geodetic Research Institute (DGFI).

A Geometric Reference Systems

The principal task of geodesy is the measurement and mapping of the Earth's surface and its variations in time. Global reference systems provide the framework for scientific investigations of the Earth's system (e.g. plate tectonics, sea level change, Earth orientation excitation), as well as for many practical applications (e.g. surveying and navigation). Today space geodetic observation techniques, such as the Global Navigation Satellite System (GNSS), Satellite Laser Ranging (SLR) and the Very Long Baseline Interferometry (VLBI), allow to determine geodetic parameters (e.g. station coordinates, Earth rotation parameters) with a precision of a few millimeters. However, high accuracy is not reflected by current realizations of the terrestrial reference system. A major error source are biases between different space geodetic solutions. DGFI studies mathematical and physical models for the different space geodetic observations to understand the origin of remaining discrepancies and to improve the consistency. Furthermore each of the different space techniques has its strengths and weaknesses concerning the determination of various geodetic parameters, and thus it is a major goal to develop optimal integration and combination methods that provide highly accurate and consistent results.

A1 Modelling for GNSS

The investigations concentrated again on aspects related to the height determination using GPS. A study performed during the previous year showed that vertical site displacements caused by atmospheric pressure loading are particularly large at high northern latitudes, e.g. in Fennoscandia. As this area experiences also uplift due to postglacial rebound, an analysis was performed determining the vertical velocities of permanent GPS stations.

Postglacial uplift in Fennoscandia

The observations of a network comprising 20 Fennoscandian and 7 fiducial stations during the period October 2000 - September 2003 were processed on a daily basis using the Bernese software version 4.2. A subsequent adjustment based on daily ellipsoidal height solutions and their full variance/covariance matrices solved for the following parameters: Ellipsoidal heights referring to a reference epoch and a reference pressure, linear vertical velocities and their annual variations, height discontinuities due to hardware changes, local snow effects and pressure loading parameters. Solution variations demonstrated the sensitivity to the strategy applied for realizing the reference frame. The figure A1.1 displays the resulting vertical velocities.

Vertical velocities of European tide gauge sites

As DGFI is involved in the IGS TIGA pilot project (see D3), which aims at achieving progress in determining the vertical velocities of tide gauge sites with GPS, observations from permanent GPS stations at European tide gauge sites were analysed. In view of the good data quality at mid latitudes, this study could assess the achievable accuracy. The analysed data set included 30 tide gauge sites and 8 fiducial stations and covered the period January 2001 - February 2004. Figure A1.2 shows the network (▲) and also an extension realized for further pressure and ocean loading studies (●).

Two solutions were performed, one based on the time series of daily network solutions (strategy I), the other one on the accumulated daily free network normal equations (strategy II). Table A1.1 gives for some tide gauge sites the vertical velocity estimates from the two strategies. Standard deviations are only giv-

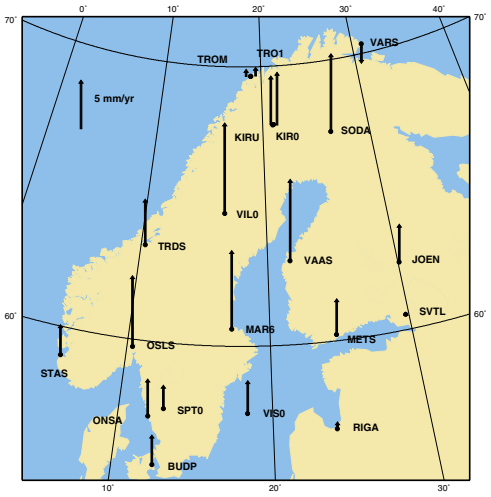

Fig. A1.1 Uplift rates in Fennoscandia due to postglacial rebound

Tab. A1.1 Examples of vertical velocities of European tide gauge sites in the ITRF 2000

Station	Days	Vertical Velocity (mm/yr)	
		Strategy I	Strategy II
ALAC	1118	0.6 ± 0.10	0.7
ALME	1105	1.3 ± 0.10	1.5
BORK	1130	-0.9 ± 0.09	-0.9
GAIA	973	-2.0 ± 0.11	-1.8
HELG	1120	-0.2 ± 0.09	-0.2
MALL	1141	-1.0 ± 0.10	-0.8
REYK	1109	-3.8 ± 0.13	-3.7
VAAS	1095	8.1 ± 0.10	8.0

Fig. A1.2 Analysed European network

en for the first strategy, because those resulting from the normal equation solution are unrealistically small because of the stochastic modelling in the GPS data processing. The differences between the two solutions reflect modelling differences: Annual signals and pressure loading coefficients were estimated only in the first approach.

Atmospheric pressure loading

The software developments for estimating site dependent vertical atmospheric pressure loading coefficients and amplitudes and phases of diurnal and semidiurnal ocean loading constituents from GPS observations with the Bernese software were already initiated during the previous year. Since then software refinements and the application to much larger data sets have been realized. As for pressure loading, the extended network of 61 stations shown in figure A1.2 was analysed on a daily basis from January 2001 to February 2004. Table A1.2 gives some examples of estimated loading parameters for continental sites as well as coastal and island locations. The pressure anomalies were derived from sea level pressure data with 1° x 1° and 6 hours spacing. The results indicate firstly that due to the larger pressure variations the effect is better determined at higher than at mid latitudes, and secondly that stations at coastlines or islands require individual modelling. As the total range of pressure variations at

Tab. A1.2 Examples of estimated vertical pressure loading coefficients Δh_p

Continental Sites			Coastal / Island Sites		
Station	**Days**	**Δh_p (mm/hPa)**	**Station**	**Days**	**Δh_p (mm/hPa)**
BUCU	1053	-0.49 ± 0.004	**BORK**	1043	-0.20 ± 0.002
GLSV	1046	-0.44 ± 0.003	**GAIA**	890	-0.24 ± 0.004
JOEN	1001	-0.45 ± 0.002	**HELG**	1033	-0.08 ± 0.002
PENC	1026	-0.35 ± 0.003	**LAMP**	977	-0.22 ± 0.005
SODA	1001	0.53 ± 0.002	**MALL**	1050	-0.18 ± 0.004
VIL0	1043	-0.43 ± 0.002	**REYK**	1028	-0.17 ± 0.002

high latitudes is 80 hPa or even more, the peak to peak vertical displacements may reach as much as 4 - 5 cm.

Ocean tide loading

The same network as above was used for estimating ocean loading constituents. However, in this case only 180 days of observations almost evenly distributed over the two years 2002 and 2003 were processed. This time span is sufficient to separate all partial tides from each other. Various solutions were performed, e.g. applying different a priori models based on the FES99 or the CSR4.0 ocean tide models or using orbits generated at the University of Berne instead of the official IGS orbits. The results achieved so far can be summarized as follows:

- The estimates do not significantly depend on the selected orbits nor on the a-priori loading model;
- GPS is capable of solving for the main constituent M2 and for N_2, O_1 and Q_1;
- The estimates for S_2, K_2, K_1 and P_1 suffer probably from aliasing effects, e.g. with the orbital periods.

As the O_1 and Q_1 contributions do not exceed very few millimetres, table A1.3 gives only the estimated M_2 and N_2 amplitudes for some coastal sites in comparison to the FES99 and CSR4.0 models. The standard deviations of the GPS estimates are well below 0.1 mm.

Tab. A1.3 Examples of M_2 and N_2 vertical amplitudes (mm)

Site	M_2			N_2		
	FES99	**CSR4.0**	**GPS**	**FES99**	**CSR4.0**	**GPS**
ALME	11.8	11.4	11.5	2.5	2.4	3.2
BRST	43.7	39.8	42.8	9.0	8.2	10.2
LAGO	32.0	31.0	32.5	7.0	6.6	8.0
REYK	23.8	20.5	21.9	4.6	4.0	4.9
SFER	23.7	21.4	23.1	5.1	4.6	6.0
VARS	13.1	10.4	12.1	2.8	3.2	4.2

A2 Modelling for SLR

The processing of Satellite Laser Ranging (SLR) observations yields time series of solved-for parameters, such as

- weekly coordinates of the tracking stations (see D4),
- daily Earth orientation parameters (EOP), expressed as polar motion and UT1 variation,
- weekly geopotential coefficients of degree 2 which are directly related to the orientation of the coordinate basis of the tracking stations.

Such time series allow to identify modelling deficits and to establish the mathematical form of refined models.

Time series of J_2

As a result of reprocessing all SLR tracking data since 1981 (see D4) two time series of the geopotential coefficient J_2 ($= -C_{20}$) for the satellites LAGEOS1 and LAGEOS2 were generated. Among the parameters of weekly satellite arcs, J_2 was solved simultaneously with EOP's and station coordinates. To remove the ambiguities of the coordinate basis, we added a no-net-rotation condition for the ILRS core stations and fixed one UT1-value per arc. Figure A2.1 shows the time series of absolute unnormalized J_2 values from 1981 to 2004 relative to J_2 = 0.0010826. It can be seen that in accordance with the worse orbit precision from 1981 to 1984, the J_2 values have a higher noise level. Why there is again a higher noise in the LAGEOS1 series from 2000 to 2004 is not yet clear and needs further analysis. A combined series will be available together with the final SLR solution of DGFI by the end of 2004.

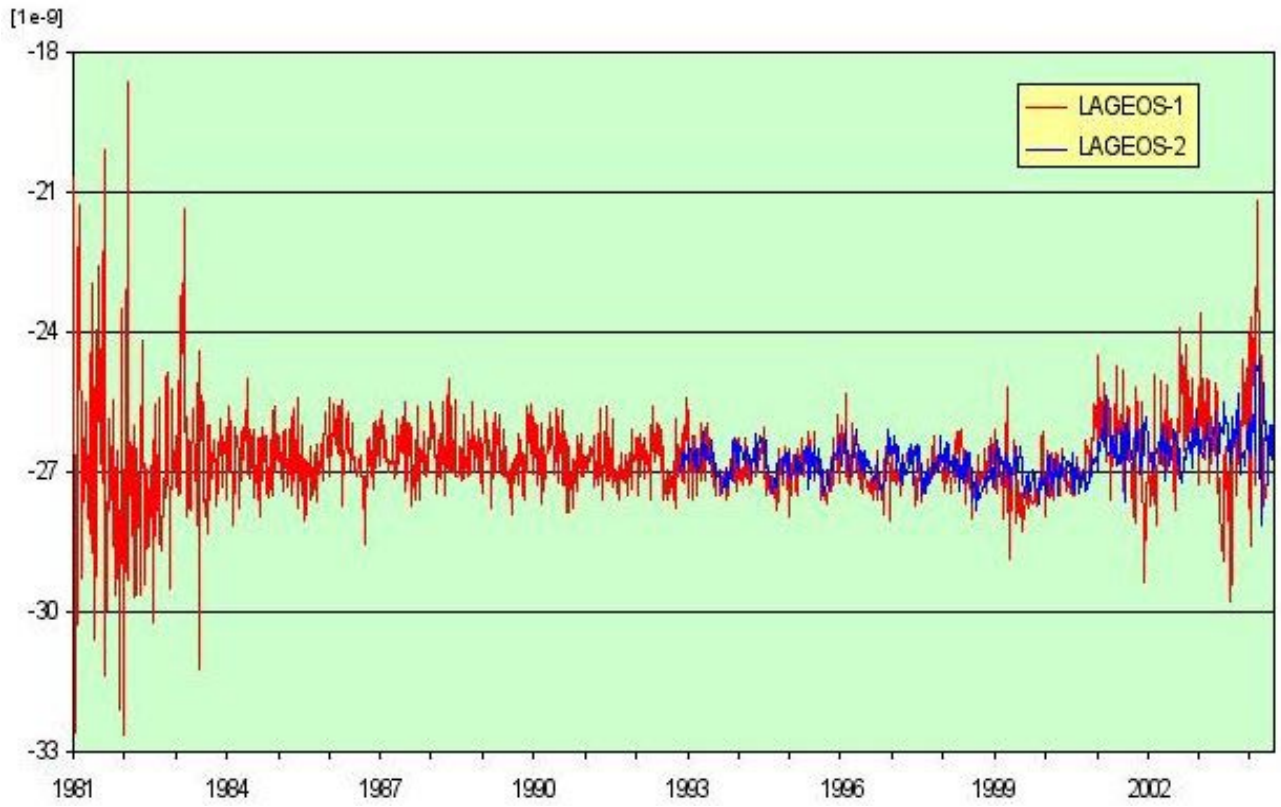

Fig. A2.1 Weekly J_2-values relative to J_2 = 0.0010826 for LAGEOS1 and LAGEOS2.

Time series of EOP parameters

The time series of the Earth orientation parameters (pole coordinates *x*, *y* and UT1-variation) are an indispensable input to the processing of space observations. All the official products provide these series by their 0h UTC values. These values are interpolated using different polynomial representations (linear, Lagrange, Bessel, Hermite, spline, ...) of 1st or 3rd degree. Thus, the EOP values required at observation time are a continuous linear function of the given 0h UTC values. These circumstances allow any linear estimation program to correct the given time series - independent of the chosen interpolation algorithm. So the EOP correction is implemented in the DGFI Orbit and Geodetic Parameter Estimation Software (DOGS-OC), according to three alternative interpolation algorithms. Other software packages – used for GPS, SLR or VLBI observations – solve for a diurnal linear correction to a 1st to 3rd degree polynomial representation which is deduced from the given 0h UTC values.This correction is expressed by offset and drift at 12h UTC. For a multi-day solution, the linear correction is either not continuous at the days boundaries if both offsets and drifts are solved for independently, or the resulting variance matrix is singular if the diurnal offsets are solved for and the drift is computed afterwards. When combined to an official IERS pole series, the EOP functions are remodelled again with knots at 0h UTC.

In order to compare the results of different analysis centres, the pilot projects of the ILRS and the IERS prescribe the delivery of 12h UTC values for the time series of the EOP parameters and/ or their derivatives. For that reason the DOGS software must be able to transform time series of parameters solved for from 0h to 12h-sampling and to differentiate those series. This can be done either before or after the linear correction process. Since the estimated satellite orbits always start and end at 0h UTC, it is better to have the knots at 0h UTC – otherwise there is at each of the arc boundaries a half-day interval without observations. Thus, the change of knots and, if necessary, the differentiation is made after the solution. The software developed for that purpose was generalized to the module cs_trasi of DOGS-CS which is designed for singular transformations of the parameter space of observation equations, normal equations, or solutions with variance matrix, respectively. The singularity of the transformation results from the fact that the number of given knots usually differs from the number of computed knots. In case of observation and normal equations, a generalized inverse of the transformation matrix has to be applied.

Bias database at DGFI

One of the quality checks performed during the weekly reprocessing of SLR data is the computation of pass-wise range and time biases. The result of these computations is available from the DGFI homepage: http://ilrsac.dgfi.badw.de. For each observed pass of the satellites LAGEOS1/2 and ETALON1/2 over all SLR stations the computed range and time biases are reported (table A2.1). A comparision with an intended ILRS data base was not yet possible.

Tab. A2.1: Example of the DGFI weekly bias reports.

Station	year	mm	dd	hh mm	range-bias [cm]	sigma	time-bias [microsec.]	sigma	prec.est. [cm]	no of observ.
Grasse__	2004	10	6	21:02	2.08	2.46	-24.37	40.83	0.25	12
Grasse__	2004	10	7	19:42	0.96	3.45	30.34	39.13	0.14	10
Graz____	2004	10	4	09:48	-0.27	1.21	-2.44	21.06	0.21	12
Graz____	2004	10	4	13:26	-1.62	2.03	-4.29	19.30	0.24	18
Graz____	2004	10	4	16:46	0.75	2.33	-3.85	18.87	0.16	13
Graz____	2004	10	4	20:52	-0.37	12.07	-5.38	54.72	0.06	3
Maidanak	2004	10	4	16:30	1.38	1.46	-10.05	22.76	0.75	8
Maidanak	2004	10	5	15:04	0.56	2.08	13.63	30.50	2.15	6
Maidanak	2004	10	7	15:52	-2.77	6.70	-7.59	41.29	2.33	4
Maidanak	2004	10	8	14:30	3.88	2.51	21.76	39.59	2.22	11
Wettzell	2004	10	3	14:58	-0.99	3.69	-7.04	29.38	0.59	5
Wettzell	2004	10	3	18:14	1.40	1.98	-7.77	21.86	0.56	12
Wettzell	2004	10	3	21:48	-2.95	4.23	-10.11	31.06	0.07	6
Wettzell	2004	10	4	10:00	2.00	1.77	7.75	22.49	0.39	7
Beijing_	2004	10	3	10:54	8.27	5.51	2.79	39.42	0.85	8
Beijing_	2004	10	3	14:22	9.75	2.73	-2.37	29.85	0.65	12
Shanghai	2004	10	8	14:20	-7.79	3.96	2.48	41.79	0.50	11
Changchu	2004	10	3	10:38	1.23	3.03	12.66	37.33	0.48	12
Changchu	2004	10	3	14:16	0.46	3.48	9.82	29.97	0.66	7
Greenbel	2004	10	4	01:24	-1.22	1.17	15.66	46.70	0.16	14
Greenbel	2004	10	5	00:02	-0.86	1.40	2.32	35.62	0.24	25
Yarragad	2004	10	6	12:56	-0.38	2.00	17.41	34.02	0.36	9
Yarragad	2004	10	6	16:22	-1.71	4.57	12.27	32.59	0.14	9
Yarragad	2004	10	7	15:00	-1.73	1.70	29.04	32.49	0.22	9
Yarragad	2004	10	7	18:36	-3.50	5.48	26.95	37.38	0.24	10
Mount_St	2004	10	4	12:10	-1.13	2.29	-14.38	21.40	0.19	11
Mount_St	2004	10	4	15:34	-3.25	4.10	-23.55	21.29	0.32	11
Mount_St	2004	10	4	18:56	3.90	4.40	-21.20	25.38	0.45	7
Mount_St	2004	10	5	11:00	-0.80	5.70	-2.99	33.73	0.59	3
Mount_St	2004	10	5	14:10	-3.01	4.07	-14.38	31.27	0.42	5

As an example, figure A2.2 shows the range biases in 2004 for the Australian station Yaragadee. The biases show that the quality of the tracking data is at present quite reasonable, and only a very few stations produce significant biases. Thus, the biases represent local systematic errors and are not generated by a wrong adaption of the satellite orbit.

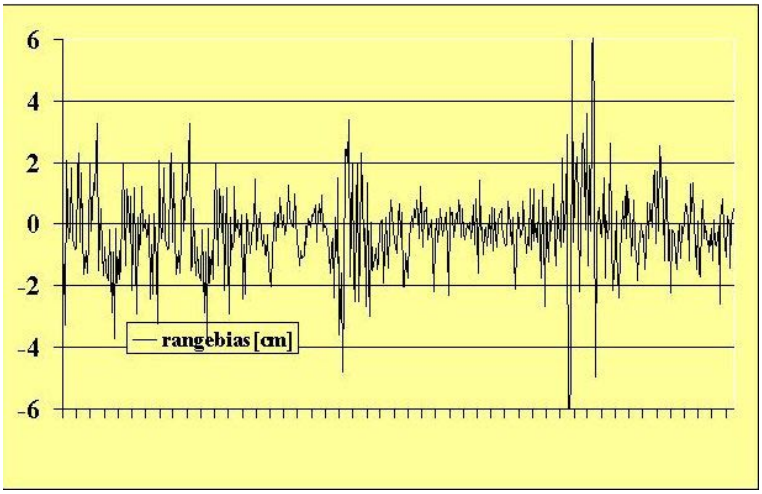

Fig. A2.2: Range biases at the station Yaragadee in 2004.

A3 Modelling for VLBI

Consistent Reference Frames

During 2003/04, a terrestrial reference frame (TRF), the EOP and a celestial reference frame (CRF) were estimated simultaneously by a VLBI solution. The geodetic datum was realized applying no-net-rotation (NNR) and no-net-translation (NNT) conditions for the TRF and NNR for the CRF. Such a solution is completely free of biases due to fixing reference frames (which might not be modelled consistently) or other relevant parameters of the observation equations. Due to two reasons, VLBI is especially suitable to perform such a task: Firstly, there are only several million VLBI observations which can very easily be reprocessed in one common solution although they cover already more than 20 years. Secondly, the celestial VLBI reference frame consists of quasi pointlike objects (radiosources) and not of dynamic orbits which are quite difficult to model and valid for several days only. Hence, a major task of VLBI is to provide the link between the celestial and the terrestrial frame, including fully consistent time series of parameters to transform between the frames (pole coordinates and their first derivatives, dUT1 and LOD, as well as daily corrections to a precession-nutation model).

Until now, for 2565 sessions between 1984 and 2004, each about 24h long, normal equations were set up with the VLBI software OCCAM 6.0 (modified to allow to estimate source positions). These data include a total of 49 telescopes (of which 47 are part of ITRF2000) observing 887 sources (of which 572 are part of ICRF-Ext1). The auxiliary parameters (for troposphere and clocks) are reduced for each session. All prereduced session-wise normal equations are then accumulated to one equation system with the DGFI software DOGS-CS and solved with an appropriate datum, namely NNR and NNT for 25 stable stations w.r.t. ITRF2000 and NNR for 199 stable sources w.r.t. ICRF-Ext1.

Figure 3.1 shows very clearly that ITRF2000 is not fully consistent with ICRF-Ext1: the differences of the source position estimates in declination (dDE) show a systematic shape if ITRF2000 is kept fixed. This is not the case if both the celestial and the terrestrial frame are estimated simultaneously (figure 3.2).

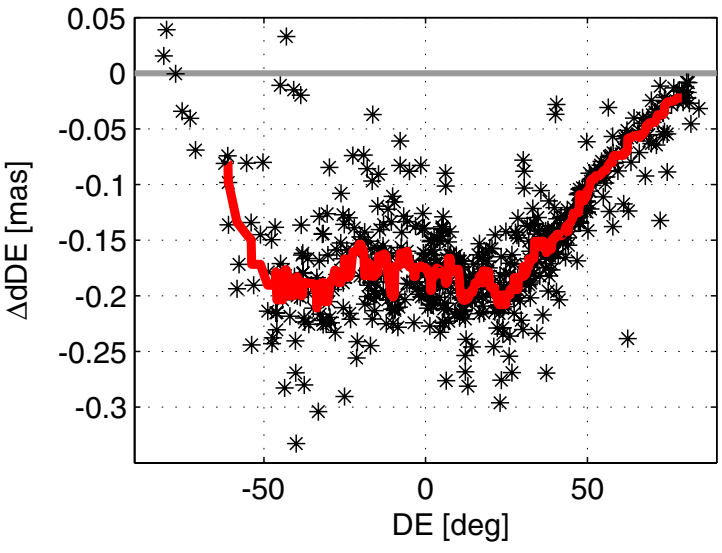

Fig. 3.1: Differences between source position estimates of two solutions: one was computed with the TRF fixed to ITRF2000 and the other estimating the TRF. In both solutions, the CRF was estimated with a NNR condition of 199 stable sources w.r.t. ICRF-Ext1.

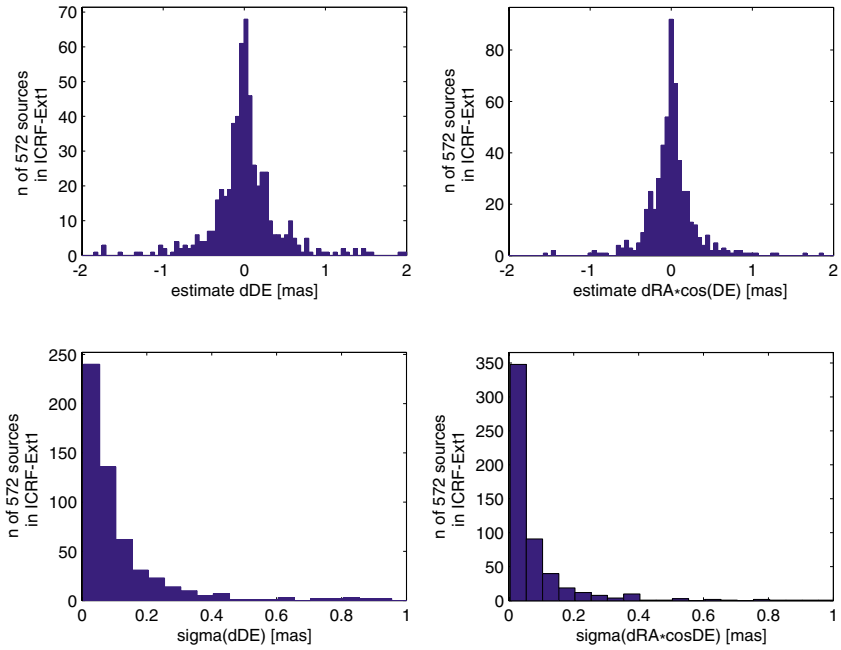

Fig. 3.2: Histograms of the source position estimates w.r.t. ICRF-Ext1 and their formal errors of a solution where both the celestial and the terrestrial frame are estimated simultaneously. Here, 96% of the sources have estimates smaller than 2 mas w.r.t. ICRF-Ext1, 98% of their formal errors are smaller than 1 mas.

Besides a terrestrial (TRF) and a celestial reference frame (CRF), the solution provides time series of the EOP, referenced to the ITRF2000 and the ICRF-Ext1, as well as time series of session-wise station and source positions. Such position series should not directly be interpreted as "real" spatial movements of stations or quasars, but provide the basis for an advanced analysis of shortcomings in the modelling, such as neglected non linear station motion or apparent motion of the quasars due to jets etc.

Advanced Stochastic Model for VLBI Observations

Further refinements of the functional representation of the geometric-physical properties of the VLBI observations mostly need big efforts and are not possible with any precision. Although the stochastic model is an important part of the VLBI observation equations, the stochastic properties of VLBI observations have not been studied in detail so far. The idea is to interpret discrepancies between the functional model and the observations as variances of the observations. In particular, the modelling of station and elevation dependent influences is of limited precision (in general, for present standard VLBI-solutions, correlations between observations were found to be negligible).

In contrast to earlier investigations, all of the 57 stochastic properties (station and elevation dependent portions of variance of VLBI observations), estimated by means of variance covariance component estimation, can be considered as stable and reliable estimates (more data was used). When applying the advanced stochastic model to parameter estimations, care has to be taken regarding indirect effects which are mainly connected with:

- the weights and the respective impact of the pseudo observations for the constraints of auxiliary clock and tropospheric

parameters (to be overcome by readjusting the weights of the constraints),
- the power of outlier tests which compare observation residuals with their formal errors (to be overcome by readjusting the criterion for outlier rejection),
- the influence of observations under very low elevations, which can decisively affect the variances of the tropospheric parameters as well as their correlations with station positions, EOP and station clock parameters (to be overcome by readjusting the cut off angle).

One of the major motivations for investigating the stochastic VLBI model was to improve VLBI solutions. In table 3.1 and 3.2, one can find tests concerning the repeatability of estimated station position time series and similarity of EOP from simultaneous NEOS-A and CORE-A sessions.

	$\frac{RMS_{new}}{RMS_{old}}$	$\frac{WRMS_{new}}{WRMS_{old}}$
latitude	95.9%	97.4%
longitude	95.8%	96.6%
radial	96.8%	99.9%

Tab. 3.1: Repeatability of estimated station positions, determined from 2211 sessions between 1984 and 2001. The rms values in this test assume that the smaller (or the less significant in case of wrms) the residual position estimates are, the better is the modelling of the corresponding observations.

	$\frac{RMS_{new}}{RMS_{old}}$	$\frac{WRMS_{new}}{WRMS_{old}}$
XP	99.2%	98.6%
YP	88.0%	87.2%
dUT1	95.4%	94.0%
PSI	83.6%	88.7%
EPS	99.8%	98.8%

Tab. 3.2: Similarity of EOP from 67 pairs of simultaneous NEOS-A and CORE-A sessions. The rms values in this test assume that the better the modelling of the observations is, the smaller (or the less significant in case of wrms) are the differences between the estimated EOP determined from the two networks.

Both tests indicate clearly that by using the advanced stochastic model, many target parameters improve and become more realistic concerning their formal errors. But, one has to consider that further progress in the functional modelling of the VLBI observations (like, e.g., the modelling of tropospheric influences) may have a significant effect on the corresponding stochastic attributes.

Rigorous Combination Using the VLBI CONT02 Campaign

The data of the IVS-initiated VLBI campaign ‘CONT02’ during 15 days of October 2002 are especially suitable to study the effect of combining normal equations of different space techniques on the stabilty of estimated parameters. In 2003/2004, many investigations were carried out in close cooperation with the Research Establishment Satellite Geodesy (FESG) at the Technical University of Munich, using the CONT02 VLBI data set for advanced combination studies (see project D1).

Update of the VLBI-Software OCCAM

The VLBI software OCCAM was updated to allow to estimate source positions on the highest level of quality. Further efforts were made on the automation of many processes in VLBI data analysis like post-fit analysis. This is indispensable for the contribution of DGFI to the IVS as an operational analysis center (see project D6), which is planned for the near future.

A4 Combination of Geodetic Space Techniques

Investigations of an optimal combination of geodetic space techniques for the creation of highly accurate and reliable terrestrial and celestial reference frames have been continued. Individual technique solutions such as GPS, SLR, VLBI and DORIS differ from each other in the geodetic datum, in systematic and stochastic error behaviour and in the mathematical modelling of the physics. These differences must be analysed before and consistently homogenized during combining. Furthermore, the combination procedure is to be developed towards automated processing. The activities regarding various combination issues are presented below.

Datum Realization

Each individual space technique solution has its own characteristic influence on the geodetic datum of the combined solution. The datum is dependent on the type of observations - e.g. distances may determine the scale of the reference frame - , but also on the modelling of the specific physics. In order to investigate these influences, numerical test quantities may help to find out the type and the strength of geodetic datum parameters. Here, three quantities are introduced: eigenvalues of the unconstrained normal equation matrix $\mathbf{N}_{unc}$, the zero quantity $\mathbf{z}_i$ as the *i*-th diagonal element of $\mathbf{Z} = \mathbf{G}^T \mathbf{N}_{unc} \mathbf{G}$ ($\mathbf{G}$ beeing the coefficient matrix of the seven Helmert transformation parameters) and the loose constraint quantity $\mathbf{l}_i$ as the square root of the *i*-th diagonal element of $\mathbf{L} = (\mathbf{G}^T \mathbf{C}^{-1}_{loose} \mathbf{G})^{-1}$ ($\mathbf{C}_{loose}$ beeing the covariance matrix of the loose constraints solution. The numerical values of an example are presented in table A4.1.

Tab. A4.1: Eigenvalues, z_i and l_i quantities for a space distance network (test net) and a GPS solution (CONT02 project). z_i and l_i quantities are computed for translations in the direction of the x (t_x), y (t_y), and z axis (t_z), for the rotations about these axes (r_x, r_y, r_z), and for the scale factor sc. The loose constraints of C_{loose} taken here correspond to a-priori standard deviations of 100 m for the coordinates.

i	Eigenvalues		i	z_i		l_i	
	DIST	GPS		DIST	GPS	DIST	GPS
1	$1 \cdot 10^{-17}$	$1 \cdot 10^{-14}$	t_x	$5 \cdot 10^{-12}$	$5 \cdot 10^{5}$	73.	$1 \cdot 10^{-3}$
2	$2 \cdot 10^{-17}$	$5 \cdot 10^{-14}$	t_y	$6 \cdot 10^{-11}$	$5 \cdot 10^{5}$	80.	$1 \cdot 10^{-3}$
3	$3 \cdot 10^{-17}$	$2 \cdot 10^{-12}$	t_z	$5 \cdot 10^{-11}$	$3 \cdot 10^{5}$	57.	$2 \cdot 10^{-3}$
4	$1 \cdot 10^{-16}$	$8 \cdot 10^{-5}$	r_x	$9 \cdot 10^{-9}$	$9 \cdot 10^{-5}$	12.	10.
5	$2 \cdot 10^{-16}$	$1 \cdot 10^{-4}$	r_y	$1 \cdot 10^{-9}$	$7 \cdot 10^{-5}$	11.	10.
6	$3 \cdot 10^{-16}$	$2 \cdot 10^{-4}$	r_z	$1 \cdot 10^{-9}$	$4 \cdot 10^{-3}$	15.	9.
7	0.02	$3 \cdot 10^{-3}$	sc	$1 \cdot 10^{8}$	$2 \cdot 10^{7}$	$3 \cdot 10^{-4}$	$2 \cdot 10^{-4}$

The test net solution DIST is purely geometric without any modelling of physics. Theoretically, its normal equation system should have a rank defect of 6 (3 for translation and 3 for rotation). The 6 smallest eigenvalues should be zero. This is verified by the eigenvalues of table A4.1. Theoretically, the GPS solution has 3 rotational degrees of freedom leading to 3 zero eigenvalues, which is confirmed by the results displayed in table A4.1. The quantities $\mathbf{z}_i$ are close to zero for the respective rank deficiencies. The loose constraints quantity $\mathbf{l}_i$ is constructed so that the values may be interpreted as standard deviations of the datum parameters. The scale values reflect, according with theory, the loose estimability of the translational and rotational geodetic parameters in the case of DIST and of the rotational parameters in the case of GPS.

The correlation matrix of **L** may also help to interpret the estimability of the datum parameters. An example is presented in figure A4.1 where the GPS solution is identical to that of table A4.1.

Fig. A4.1 Correlation matrix of the L and l_i quantities

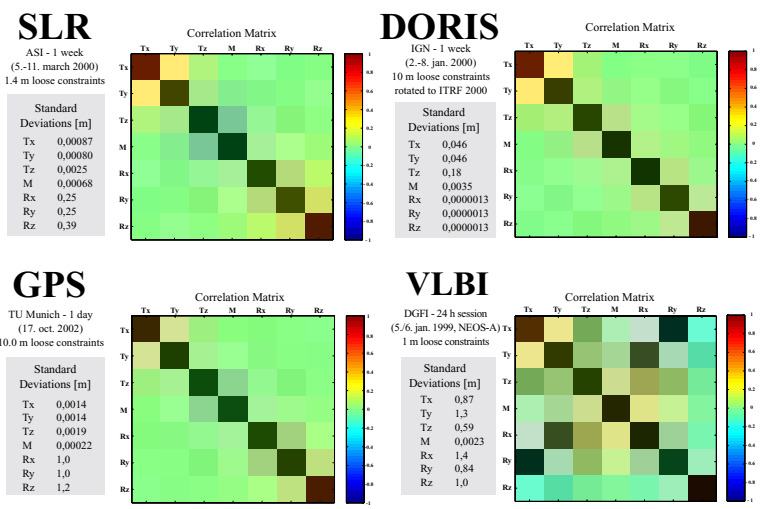

For SLR and GPS a high correlation between the translation in *z* direction and the scale factor is evident - which is a known fact. The rotations of the DORIS solution are assumed to be constrained because of their small correlations and their small standard deviations. For VLBI, only the scale factor is well determined and not correlated with the other datum parameters - as theory requires.

Towards Rigorous Combination

DGFI has continued the CONT02 activities in cooperation with the Research Establishment Satellite Geodesy (FESG) at the Technical University of Munich, aiming at a rigorous combination of space geodetic observations. Identical models and parametrizations were adapted for the analysis of GPS data (with Bernese at FESG) and CONT02 VLBI data (with OCCAM at DGFI, see A3). The combination was performed on the level of unconstrained normal equations, and all parameters were considered that are common to GPS and VLBI (e.g. daily station positions, 2-hourly EOPs, tropospheric and nutation parameters). In additon, SLR normal equations resulting from 15-day arcs to LAGEOS1 and -2 were included. Due to relatively sparse SLR tracking and different characteristics of the optical laser ranging observations compared to microwave techniques the parametrization is different from GPS and VLBI (table A4.2). Results of this quasi-rigorous combination are presented in D1.

Tab. A4.2: Parametrization for CONT02 combination

Parameters	VLBI	GPS	SLR
Station coordinates	daily	daily	15-days
EOPs (x, y, UT1-UTC)	2 h	2 h	daily
Nutation offsets	daily	daily	-
Troposphere zenith delays	2 h	2 h	-
Troposphere gradients	daily	daily	-

SLR Intra-Technique Combination

The methodology of the automated intra-technique combination with SLR input solutions was described in the last annual report. Meanwhile, DGFI has been selected as the official ILRS Backup Combination Centre. That means that DGFI must compute every week a combined solution following the requirements specified in the ILRS Call for Participation "pos+eop". The description of official tasks and products is given in D4.

A first comparison of the DGFI results with those of the official Primary Combination Centre ASI (Agenzia Spaziale Italiana) revealed discrepancies which could be significant. The most critical differences between the solutions of both centres seem to be the methods of scaling the normal or covariance matrices of the input solutions. DGFI applies a scaling method which is based on the hypothesis that solutions with nearly identical observation sets produce a similar precision level for well-covered stations. This leads to scale factors $\mathbf{fd}_i$ for the *i*-th solution. ASI assumes the stochastic hypothesis that the sum of the individual variance factors multiplied by the scale factors $\mathbf{fa}_i$ to be estimated in an iterative process should yield 1, and that all variance factors multiplied by the scale factor should become equal. Taking this stochastic assumption as valid - what may be argued about - the rigorous variance component estimation (VCE) may also be applied also resulting in the scale factors $\mathbf{vf}_i$ with their variances $\mathbf{var}(\mathbf{vf}_i)$. An example of the three scaling methods is presented in table A4.2.

AC	i	vf_i	$var(vf_i)$	fd_i	fa_i
ASI	1	16.4	0.5	16.4	16.4
DGFI	2	4.2	0.8	5.4	11.4
GFZ	3	7.6	0.4	16.0	11.2
JCET	4	2.7	0.1	8.2	4.8
NERC	5	5.3	0.2	5.4	9.0

Tab. A4.3 Methods for scaling the covariance matrices of the input solutions. AC: Analysis Centre, ASI: Agenzia Spaziale Italiana, DGFI: Deutsches Geodätisches Forschungsinstitut, GFZ: Geoforschungszentrum Potsdam, JCET: The Joint Center for Earth Systems Technology, NASA, NERC:The Natural Environmental Research Council, GB, vf_i : i-th variance factor of rigorous VCE, $var(vf_i)$: variance of vf_i, fd_i : relative scaling factors (DGFI method), fa_i : relative scaling factors (ASI method):

All three methods lead to significantly different scale factors which influence the combination results. Hence, further investigations on the scaling methods are necessary.

Inter-technique Combination

The DGFI combination methodology on the level of unconstrained normal equations of the different space geodetic observation techniques was applied for TRF computations (see D1). The "conventional" strategy based on the combination of multi-year solutions provides TRF results that do not preserve the high accuracy of the space geodetic observations. Major error sources are systematic biases between techniques and non-linear effects in site positions and datum parameters. To minimize these biases and to consider non-linear effects, the time series of station positions and datum parameters were analysed (see C3, D1), and a refined TRF realization was computed based on epoch (daily/weekly) normal equations of the different space techniques. First results are presented in D1.

Extended Modelling with Variance Component and Robust Estimation

The extended combination modelling as defined by DGFI was presented in the last annual report. This year, the general basic model $E[\mathbf{p}_o] = \mathbf{f}(\mathbf{p})$ (E beeing the expectation vector, $\mathbf{p}_o$ the para-

meter vector of the input solutions, **f** a nonlinear function vector, and **p** the output parameter vector) is specified for first investigations. The linearization of the basic model leads to the Gauss-Markov-Model in step 1 of figure A4.5 in the last report. The parameter row vectors $\mathbf{p}_o$ and **p** are now defined for weekly combination solutions : $\mathbf{p}_o = [\ {}_k\mathbf{p}_o\ {}_l\mathbf{x}_o\ {}_k\mathbf{e}_d]$ where ${}_k\mathbf{p}_o$ is the input parameter vector (positions and EOP) in the *k*-th reference frame, ${}_l\mathbf{x}_o$ local tie position vectors in the *l*-th frame. The reference frames *k* and *l* differ in number, reference epochs, and geodetic datum. The vector ${}_k\mathbf{e}_d$ contains the daily input EOP for the *k*-th frame. The output vector **p** is modelled as **p=[x, e, h, b]**, where **x** represents the position vectors of the stations for the same reference epoch and **e** the daily EOP for the same daily epoch. Note that ${}_k\mathbf{p}_o$ and ${}_k\mathbf{e}_d$ may also have slightly different time epochs within the same *k*-th reference frame. The Helmert transformation parameter vector **h** may be inserted in case the geodetic datum of frame *k* differs from the datum of the combined solution reference frame. The bias parameter vector **b** may be required for analysis and test purposes and is only allowed in the final combined solution if it can be interpreted physically. The software to this specified modelling is beeing developed.

Variance Component Estimation

The Variance Component Estimation (VCE) can be regarded as an absolute estimation method for scaling the covariance matrices of the input solutions. Meanwhile, several versions of VCE are available: A direct version, in which the full matrices must be stored in RAM. This version works well in the intra-technique combination of ILRS project “pos+eop”, but it may fail for larger matrices. Hence, a second version is developed, which only needs storage capacity for one individual input solution. Both versions are tested. The application for inter-technique combinations is under investigation.

Combination Software Updating

DOGS-**AS** (**A**nalysis **S**oftware): The main new features are:

- direct VCE version;
- minimal storage VCE version;
- validation software for individual and combined solutions (comparison, plotting, test criteria);
- automated version for SLR intra-technique combination applied at the ILRS Backup Combination Centre.

DOGS-**CS** (**C**ombination and **S**olution) software has been updated in the following items:

- The DOGS-**CS** module was extended: (1) Condition equations for local ties can now be expressed also in topocentric coordinates (North-East-Up); (2) The no-net-rotation conditions were extended to radio sources which are represented by spherical latitudes and longitudes.
- In the module cs_inpar, the set up of velocities (estimated together with position coordinates) was extended to velocities which are periodic in time with a prescribed frequency.
- The Hermite interpolation was introduced as an additional interpolation model into the program module cs_trasi.

A5 Modelling the Celestial Intermediate System

Two problems arising with the introduction of the new precession and nuation model were dealt with: the use of Eulerian precession angles and the definition of the ecliptic.

Eulerian precession angles

The precession matrix

$$\mathbf{P} = \mathbf{R}_3(-z)\mathbf{R}_2(\theta)\mathbf{R}_3(-\varsigma)$$

with three small Euler angles ζ, θ, z transforms from the fixed mean equator system of epoch to the mean equator system of date. That is remarkable; for, in general, a small rotation cannot be described by three small Euler angles.

However, if the precession of the mean pole is assumed to be a strictly conical motion around a fixed ecliptic normal (so that the vertical angle ω is constant), the rotation vector of the mean equator system is the ecliptic normal vector, which is perpendicular to the mean equinox direction and consequently has no component along the first axis. Therefore, the Euler representation with three small angles ζ, θ, z around the third and second axes is indeed possible (where $\zeta = z$, and they vanish at the epoch t_0).

Actually, however, the angle $\omega = \varepsilon_0 + \delta\omega$ between the fixed ecliptic normal of epoch and the mean pole of date is not strictly constant. (ε_0 is the constant obliquity at the epoch, and $\delta\omega$ is the slightly varying difference.) Then one finds as a first order approximation

$$\varsigma = \arctan\frac{-\delta\omega}{\sin\varepsilon_0\psi},$$

$$z = \arctan\frac{\delta\omega}{\sin\varepsilon_0\psi} - \chi,$$

where ψ is the lunisolar precession and χ is the planetary precession angle. Since both ψ and $\delta\omega$ tend to zero at the epoch t_0, these expressions become indefinite. Thus the zero order terms of the power series of ζ and z are according to de l'Hospital's rule

$$\varsigma(t_0) = \arctan\frac{-\dot{\omega}(t_0)}{\sin\varepsilon_0\dot{\psi}(t_0)},$$

$$z(t_0) = \arctan\frac{\dot{\omega}(t_0)}{\sin\varepsilon_0\dot{\psi}(t_0)} - \chi(t_0).$$

These angles become very large if $\dot{\omega}$ has the same order of magnitude as the derivative $\dot{\psi}$ of the lunisolar precession ($\dot{\psi} \approx 50''\,a^{-1}$).

As the precession of the mean pole is, though not strictly, but approximately conical, $\dot{\omega}$ is considerably smaller than $\dot{\psi}$. According to the old IAU1976 precession model, $\dot{\omega}(t_0) = 0$ (only the higher derivatives of ω are not equal to zero), and according to the new IAU2000 precession model, $\dot{\omega}(t_0) = -0.00025''a^{-1}$ holds. Thus the fractions in the arctan arguments are small so that ζ and z are small angles, namely in the case of the old precession model $\zeta(t_0) = -z(t_0) = 0$, and in the case of the new precession model $\zeta(t_0) = -z(t_0) = 2.60''$. Therefore, in both precession models, the precession matrix **P** can conveniently be described by small Euler angles ζ, θ, z.

However, the ICRS is, unlike the former FK5 system, not identical with the mean equator of epoch. Therefore, a rotation $\mathbf{R}_3(\gamma)\mathbf{R}_2(\beta)\mathbf{R}_1(\alpha)$ with three very small constant angles α, β, γ has to be added. If the resulting precession matrix $\bar{\bar{\mathbf{P}}}$ is to be expressed in an analogous way by three Euler angles $\bar{\varsigma}, \bar{\theta}, \bar{z}$,

$$\bar{\bar{\mathbf{P}}} = \mathbf{P} \cdot \mathbf{R}_3(\gamma)\mathbf{R}_2(\beta)\mathbf{R}_1(\alpha) = \mathbf{R}_3(-\bar{z})\mathbf{R}_2(\bar{\theta})\mathbf{R}_3(-\bar{\varsigma}),$$

the zero order terms of the power series of $\bar{\varsigma}, \bar{z}$ are

$$\bar{\varsigma}(t_0) = \arctan\frac{\alpha}{\beta},$$

$$\bar{z}(t_0) = -\arctan\frac{\alpha}{\beta} - \chi.$$

Since α, β are both of the same order of magnitude 0.01", $\bar{\varsigma}$ and $\bar{z}$ become very large. Therefore, for representing the extended precession matrix $\bar{\bar{\mathbf{P}}}$, only a parametrization by Cardan angles instead of Euler angles is appropriate.

The definition of the ecliptic

Although the equinox as an axis of the intermediate celestial system has been replaced by the celestial ephemeris origin, the ecliptic still plays a role in the transformation from the ICRS to the ITRS because the new IAU2000 nutation model continuously describes the direction of the celestial intermediate pole (CIP) by the parameters $\Delta\psi$,$\Delta\varepsilon$, which are the differences of the longitude and latitude of the CIP with respect to the ecliptic of date from those of the mean pole. Recent papers on precession (e.g. by Fukushima) distinguish between the ecliptic orientation parameters "in the inertial sense" and those in the "rotational sense".

The ecliptic can on the one hand be defined as the mean plane in which the position vector $\underset{\sim}{r}$ of the barycentre of the earth and the moon with respect to the barycentre of the solar system performs its annual revolution. On the other hand, it can be defined as the mean plane which is always spanned by the position vector $\underset{\sim}{r}$ and the velocity vector $\underset{\sim}{v}$ of the barycentre of the earth and the moon with respect to the barycentre of the solar system. "Mean plane" means that periodic changes of the orientation of the respective plane are subtracted so that in both definitions the ecliptic has only secular rotations. The two definitions turn out to be incompatible with each other.

The "conventional" ecliptic is obtained by adjusting observations of the position vector $\underset{\sim}{r}$ at numerous instants of time under the condition that the orientation parameters of the ecliptic change only secularly. The adjusted postion vector $\underset{\sim}{r}$ is thus always within the secularly rotating conventional ecliptic.

The velocity vector $\underset{\sim}{v} = \dot{\underset{\sim}{r}}$, however, is not within the conventional ecliptic. For it is the sum of the time derivative of $\underset{\sim}{r}$ with respect to the conventional ecliptic (which is, of course, always within the conventional ecliptic) and the vector product of the position vector $\underset{\sim}{r}$ and the rotation vector of the conventional ecliptic. The latter part is obviously outside the conventional ecliptic.

Therefore, the “true” ecliptic, which is spanned by the position vector $\underset{\sim}{r}$ and its time derivative $\underset{\sim}{v}$, is not identical with the conventional ecliptic. Its rotation consists of secular and periodic (semiannual) parts. By splitting off the periodic parts, one obtains the “mean” ecliptic, which, like the conventional ecliptic, rotates only secularly. But it is not identical with the conventional ecliptic.

So there are three different ecliptics: The conventional ecliptic rotates purely secularly, and it always contains the (adjusted) position vector $\underset{\sim}{r}$, but not its derivative $\underset{\sim}{v}$. The true ecliptic rotates both secularly and periodically, and it contains the (adjusted) position vector $\underset{\sim}{r}$ as well as its derivative $\underset{\sim}{v}$. The mean ecliptic rotates purely secularly, and it contains neither the (adjusted) postition vector $\underset{\sim}{r}$ nor its derivative $\underset{\sim}{v}$.

These considerations assume that the ecliptic is determined by adjusting only position vectors. By adjusting both position and velocity vectors, one gets directly the mean ecliptic (in the “inertial sense”). But the ecliptic which is traditionally described by the IAU precession models is the conventional ecliptic (in the “rotational sense”). The orientations of these two ecliptics differ by an angle of 0.0374".

A6 Actual Plate Kinematic Models (APKIM)

The deformation of the Earth's crust can be modelled from surface point motions observed by space geodetic observations. We may split the motions into the rigid tectonic plate rotations which are completely determined by each one geocentric rotation vector per plate and the continuous deformations which occur in particular in the plate boundary zones. This latter deformation is not included in the geologic-geophysical models, like NUVEL-1A, but it affects significantly the geodetic modelling. It is essential for the realization of a kinematic reference frame with no net rotation (NNR). The NNR condition requires the integral of all point rotations over the entire Earth surface, including rigid plates and deformation zones, to become zero.

DGFI has released in the past a series of such **A**ctual **P**late **Ki**nematic and deformation **M**odels (APKIM) covering nearly all the Earth surface. A problem is the correct modelling of the deformation zones along the extended orogens like the Mediterranean and Andean mountain belts. During the last year a sophisticated analysis of all existing geodetic observations in South America has been done, and a continuous deformation model of all the continent has been developed.

The input data of the model were the following station velocities:

- 26 continuously observing GPS stations processed by the IGS Regional Network Associate Analysis Center for South America (RNAAC-SIRGAS, Seemüller et al. 2002, Drewes et al. 2004)
- 21 stations of the South American Geocentric Reference frame (SIRGAS, Drewes et al. 2004)
- 27 stations of the Central and South America (CASA) geodynamics project in Venezuela (Kaniuth et al. 1999)
- 44 stations of the CASA project in Costa Rica, Panama, Colombia, and Ecuador (Trenkamp et al. 2002)
- 44 stations of the South America – Nazca Plate Motion Project (SNAPP, Norabuena et al. 1998)
- 97 stations of the Central Andes Project (Bevis et al. 2001, Brooks et al. 2003, Kendrick et al. 2001)
- 102 stations of the South America Geodynamics Activities (SAGA, Khazaradze and Klotz 2003, Klotz 2001)

Altogether there were 329 site velocities, some stations being identical in different data sets.

All the velocities were transformed by identical stations to a common kinematic datum relative to the stable South American plate which was realized by 16 RNAAC-SIR stations in the eastern part of the continent. For the modelling of deformations we used two different approaches:

- A Least Squares Collocation (LSC) with empirically determined covariance functions of the velocity vectors
- The Finite Element Method (FEM) for an elastic material with three different numbers of the Young modulus for the stable part of the plate, the Andean deformation zone and a contact zone in between.

The r.m.s. deviations between the two models are ±1,0 mm/a in latitude and ± 1,7 mm/a in longitude direction. The combined model is shown in figure A6.1.

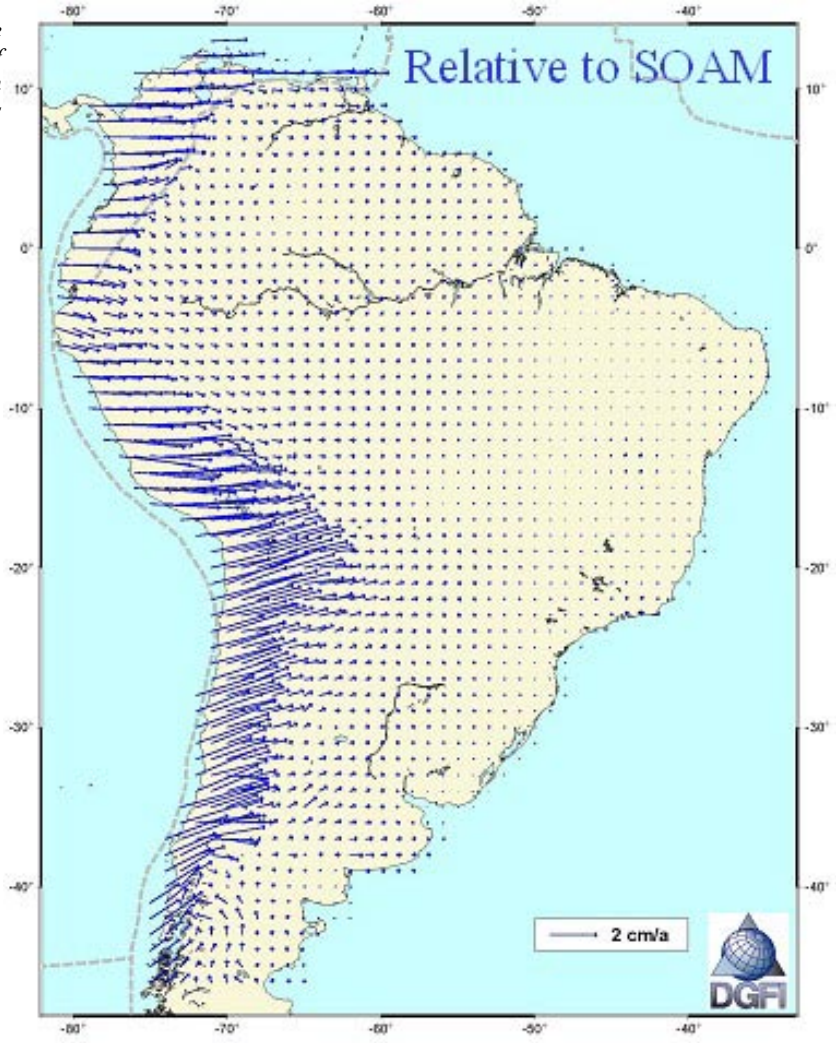

Fig. A6.1: Deformation model of the South American crust from a combination of least squares vector collocation and elastic finite element methods

B Physical Reference Surfaces

The Earth gravity field determines the most important physical reference surfaces which reflect the irregular distribution of masses on and inside the Earth. The Earth gravity field also affects satellite orbits and is important for the surveying of the Earth. Heights, for example, should refer to a unique global height reference surface. Only a precise knowledge of the gravity field allows to determine point positions and heights with the utmost accuracy. DGFI investigates high resolutions and improved representations of the Earth gravity field and contributes to the evaluation of new and upcoming gravity field missions (CHAMP, GRACE and GOCE). The sea level adjusts itself to the gravity field. It is, however, also affected by temperature, air pressure and ocean circulations. Surveying the sea level and analysing temporal sea level changes gives information on general processes within the system Earth. By satellite altimetry sea surface heights can be obtained with centimetre precision. DGFI also determines temporal sea level changes, compares them with tide gauge records and investigates their influence on the gravity field and on the Earth´s rotation.

B1 Analysis of Global Gravity Field Variations

In August 2004 the first time series of *monthly* GRACE gravity field solutions was released by GeoForschungsZentrum (GFZ), Potsdam, and the Centre of Space Research (CSR), Texas. The solutions for the static gravity fields already demonstrated a dramatic improvement for the medium and long wavelength structure of the Earth gravity field. However, as already indicated in the previous annual report, all CHAMP and GRACE models suffer until now from a pronounced "trackiness", which becomes visible if the gradient of the geoid is computed and artificially illuminated as a synthetic relief (figure B1.1). This "trackiness" is still present in the latest GRACE-only gravity model, EIGEN-GRACE02S, published by GFZ. The cause for these meridional patterns are not completely understood. The inter-satellite observation of the two GRACE satellites is primarily sensitive to the along-track component of the gravity gradient, V_{xx}. It seems that V_{xx} of neighbouring tracks is not consistently treated.

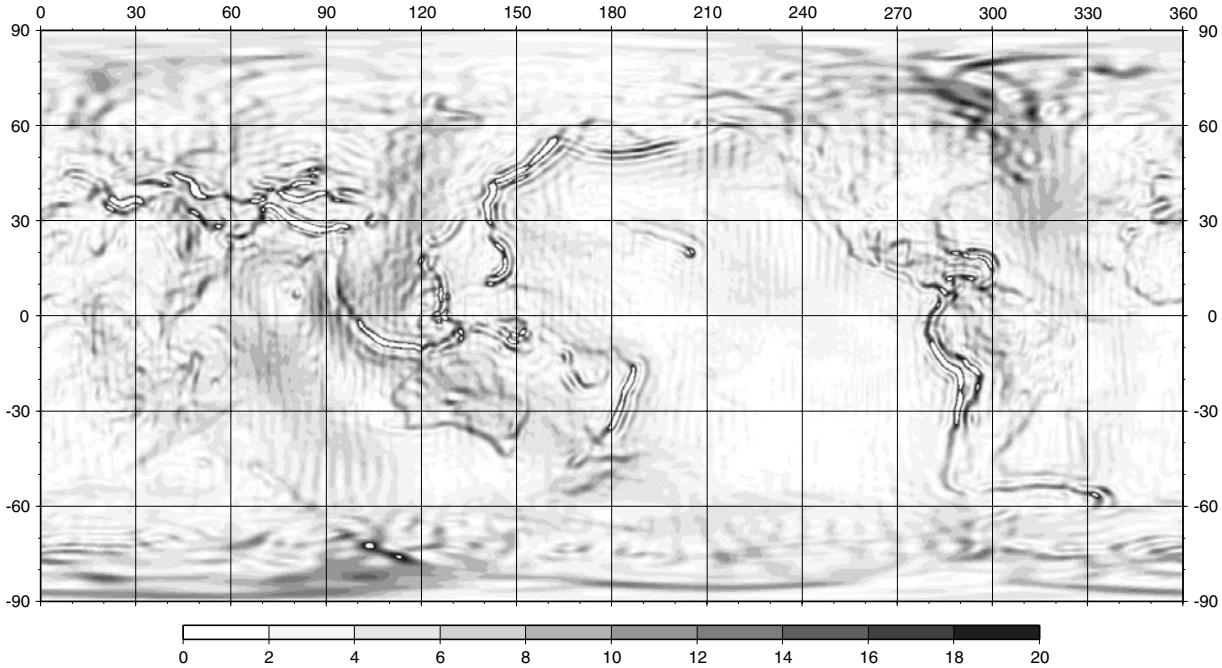

Fig. B1.1: The latest GRACE-only gravity field still exhibits a pronounced "trackiness". The figure shows artificially illuminated gradients of EIGEN-GRACE02S. Gradients of EIGEN-GRACE01S and GGM01S look very similar. The "trackiness" (most likely caused by inconsistent treatment of neighbouring tracks) implies that only smoothed versions of these gravity field models can be used to validate the long wavelength of the marine gravity data.

The new GRACE-only gravity fields were analysed in order to

- investigate the variation in the time series of monthly GRACE gravity fields, and to
- validate high resolution surface gravity data, which is to be combined with the satellite-only gravity field models.

PCA of 20 monthly GRACE gravity fields

Up to now CSR published 20 monthly GRACE-only gravity field solutions. In order to avoid that the variation between these models is dominated by the "trackiness", the monthly gravity fields were smoothed by truncating the spherical harmonic series at degree 36. This corresponds to a spatial resolution of about 550 km. The truncated gravity fields were used to compute geoid heights on a 2°×2° grid. Mean and standard deviations of these models were computed and residual monthly geoid heights were produced by subtracting the mean geoid from the monthly geoid heights. The residual monthly geoid heights were then analysed by principal component analysis (PCA) – to identify the most dominant spatial structures of variability and determine their temporal evolution by time dependent coefficients – the principal components. The results are shown in figure B1.2. The significant secular change between polar and equatorial gravity (captured by the dominant mode 1) requires further investigations.

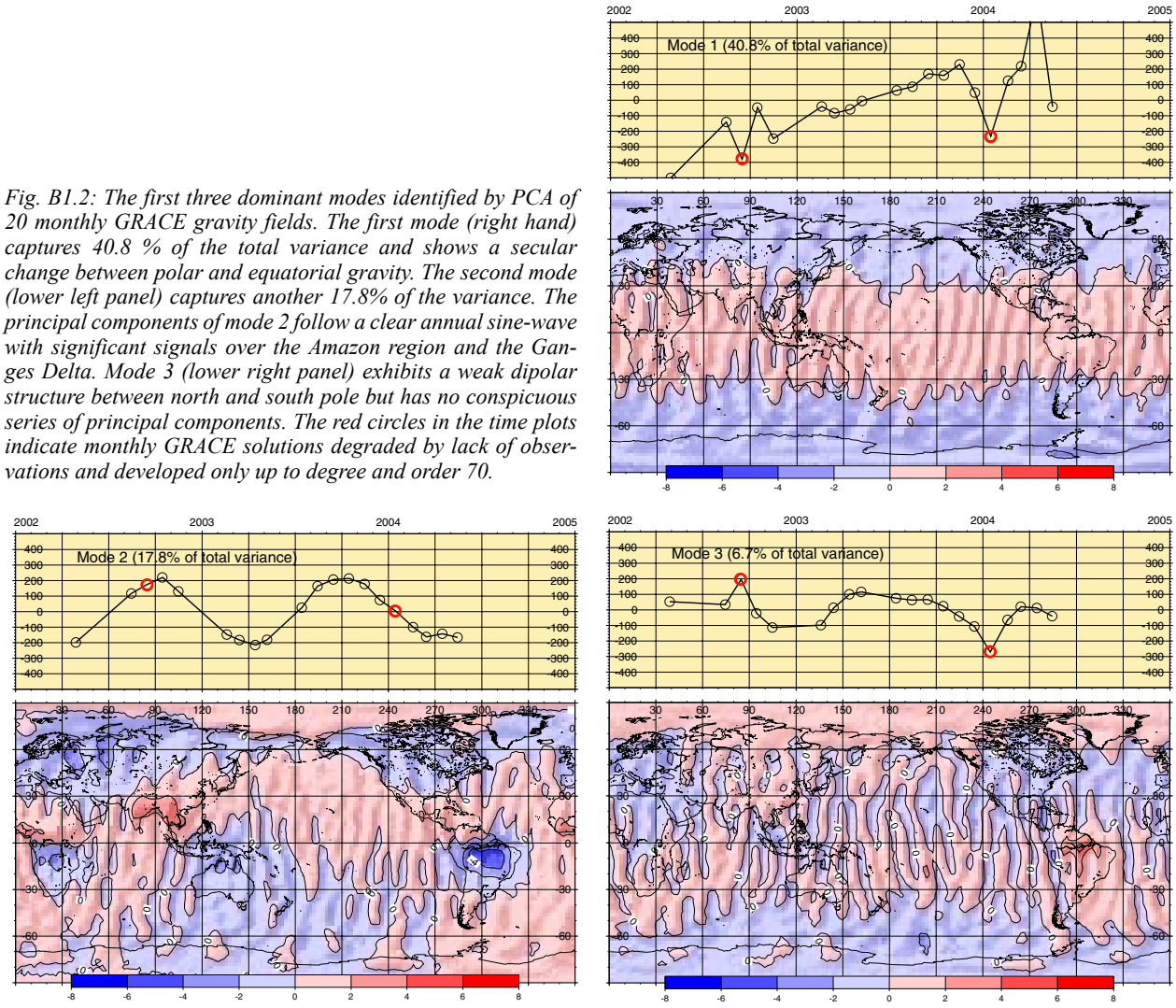

Fig. B1.2: The first three dominant modes identified by PCA of 20 monthly GRACE gravity fields. The first mode (right hand) captures 40.8 % of the total variance and shows a secular change between polar and equatorial gravity. The second mode (lower left panel) captures another 17.8% of the variance. The principal components of mode 2 follow a clear annual sine-wave with significant signals over the Amazon region and the Ganges Delta. Mode 3 (lower right panel) exhibits a weak dipolar structure between north and south pole but has no conspicuous series of principal components. The red circles in the time plots indicate monthly GRACE solutions degraded by lack of observations and developed only up to degree and order 70.

Long and medium wavelength errors of marine gravity data

The latest static GRACE-only gravity field, EIGEN-GRACE02S, is used to investigate if high resolution marine gravity data exhibit medium or long wavelength errors. The recovery of marine gravity data from altimetry is rather sensitive to errors: the inversion of Stokes or Vening-Meinesz formulas, realised either by Least-Squares-Collocation (LSC) or Fast Fourier Techniques (FFT), is applied to a sequence of local areas in order to avoid – in case of LSC – the inversion of huge matrices or to ensure the validity of planar approximations in case of FFT.

Most recent data sets of marine gravity data provide a spatial resolution of 2′×2′ (there are even versions with 1′×1′ resolution) and are derived from the so-called geodetic phases of the Geosat and ERS-1 altimeter missions:

- Version 11.2 of Sandwell & Smith marine gravity data (further on abbreviated as SSv11.2) including re-tracked ERS-1 data, and
- KMS2002 marine gravity provided in 2003 by Anderson & Knudsen.

Within the common latitude range of ±72°, the global agreement between these two data sets is rather good: For 6′×6′ block mean values a mean difference of 0.06 ± 4.58 mGal was found.

Comparison in the space domain

Gravity anomaly differences were then generated between EIGEN-GRACE02S and the two marine gravity data sets. To circumvent the “trackiness” of the GRACE gravity field these differences were smoothed to 3° and 4° block mean values. Figure B1.3 shows the differences with the marine gravity of SSv11.2 (the differences to KMS2002 look very similar). Only if smoothed to at least 4° block mean values (corresponding to a harmonic series up to degree and order 45) the “trackiness” disappears.

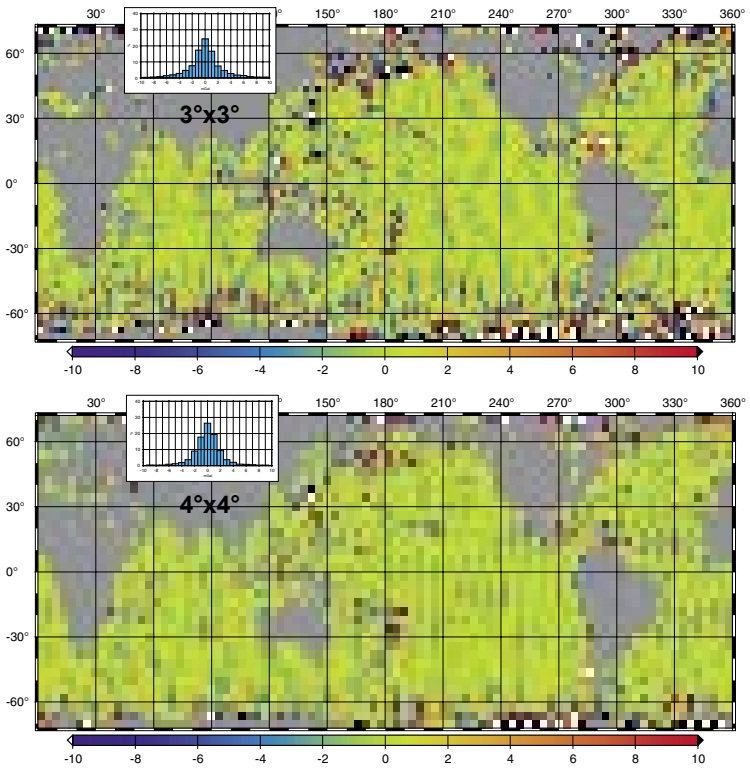

Fig. B1.3: Spatially smoothed gravity anomaly differences [mGal] between EIGEN-GRACE02S and Sandwell & Smith, Version11.2 marine gravity. The top panel shows 3° block mean values which seem to reproduce the EIGEN-GRACE02S meridional pattern in the southern ocean - above all around 55°S. Only when smoothed to 4° block mean values (lower panel), most of these meridional patterns of the anomaly differences disappear.

Comparison in the spectral domain

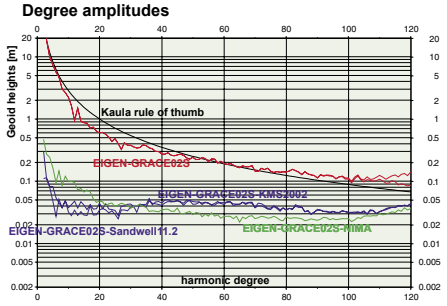

Fig. B1.4: Degree amplitudes, expressed as geoid height [m] for EIGEN-GRACE02S (red) and the differences to SSv11.2 and KMS2002 (blue).

Because block mean values at higher latitude do not account for the convergence of the meridians, a comparison in terms of spherical harmonics is more appropriate. The differences between EIGEN-GRACE02S and the marine gravity data were expanded into spherical harmonics up to degree and order 120 (this is far beyond the harmonic degree relevant for medium and long-wavelength structures). Figure B1.4 shows the degree amplitudes of the difference spectra. Remarkably, the difference spectra show a nearly constant power between degree 5 and 120. It is therefore difficult to choose the most appropriate truncation. The comparison in the spatial domain indicates: above degree 40 the power of the difference spectra is already influenced by the "trackiness" of the GRACE model. The harmonic series of anomaly differences were therefore truncated at degree 40 and transformed back to both, anomaly differences and geoid height differences. Figure B1.5 shows the results.

The SSv11.2 data set exhibits slightly higher anomaly differences in the southern ocean (compare the upper plots of figure B1.5). However, if the difference spectra for both data sets is transformed to geoid height differences, large scale patterns of geoid height differences appear with amplitudes up to about ±0.4 m – located differently for SSv11.2 (lower left plot of figure B1.5) and KMS2002 (lower right plot of figure B1.5).

In summary, the "trackiness" of GRACE-only gravity field models makes it difficult to identify the right cut-off degree for the spherical harmonic representation of anomaly differences.

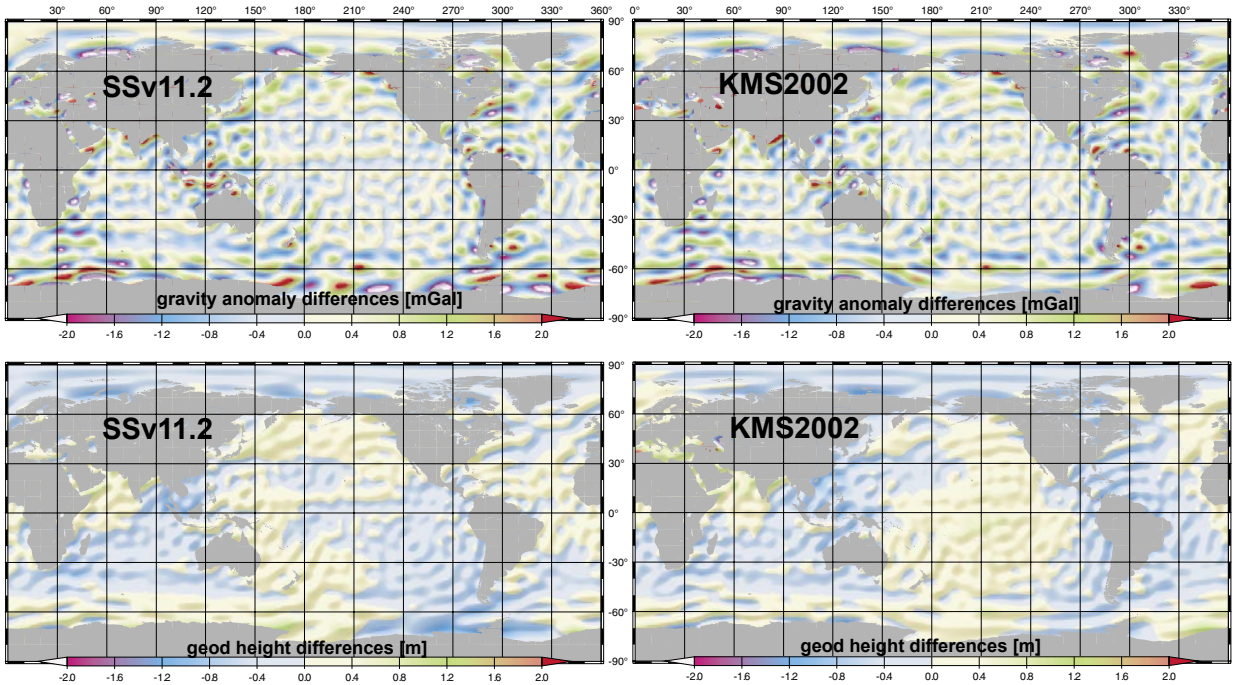

Fig. B1.5: Gravity anomaly differences [mGal], top panels, and geoid height differences [m], bottom panels, for the difference spectra EIGEN-GRACE02S minus SSv11.2 (left hand) and minus KMS2002 (right hand), truncated at degree and order 40.

B2 Multi-Scale Representation of the Gravity Field

The basic idea of a multi-scale (multi-resolution) representation is to decompose a given input signal into spectral components by successive low-pass filtering. In the so-called combined approach, explained in the last year's annual report, the gravity field of the Earth is split into a global trend model (e.g. a spherical harmonics expansion up to a certain degree) and a number of detail signals. Each detail signal is related to a certain frequency band, i.e. resolution level. To be more specific, detail signals of lower (higher) levels represent the low(high)-frequency parts or the coarser (finer) structures of the field. They are calculable from data sets by parameter estimation or numerical integration techniques. Since different measurement types cover different parts of the frequency spectrum, it seems reasonable to calculate the detail signals of the lower levels from satellite data and the detail signals of the higher levels mostly from surface (terrestrial and/or airborne) data. In between there is an overlapping part, in which the detail signals have to be evaluated from both satellite and surface data.

Blackman wavelet function

In order to achieve a multi-scale representation based on wavelet theory, we introduce the spherical *Blackman wavelet function* (figure B2.1) derived from the Blackman window, which is well-known in signal analysis. Although the Blackman wavelet is – like spherical harmonics – a global function, it is quasi-compactly supported in space (panels a,b) und therefore well suited to model regional structures of the gravity field. In the frequency

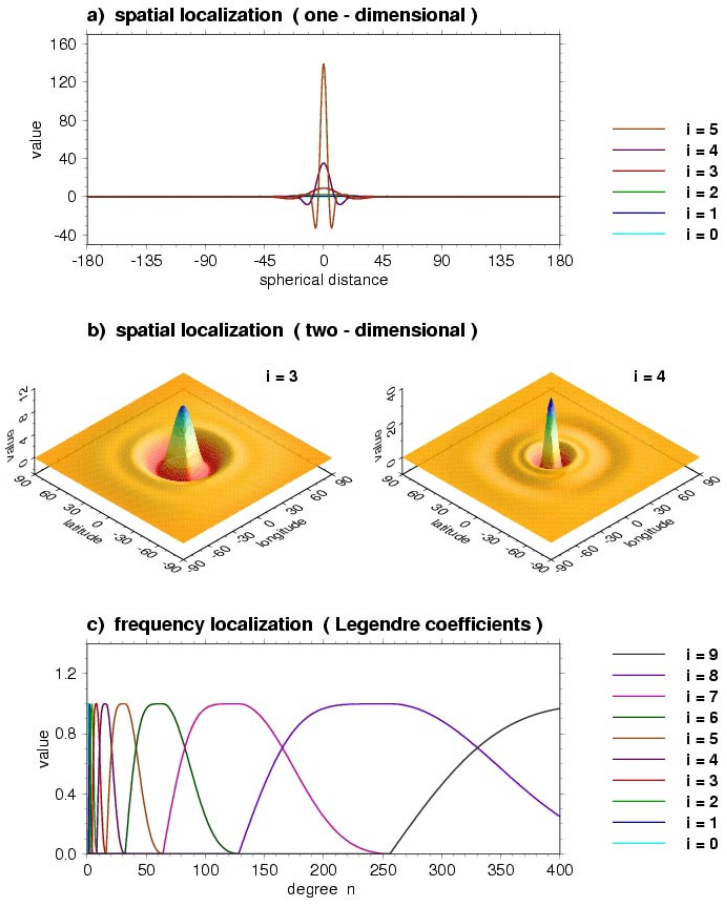

Fig. B2.1: Blackman wavelet function
a) 1-D spatial domain,
b) 2-D spatial domain,
c) frequency (degree) domain

(degree) domain, the function is compactly supported, i.e. band-limited (panel c). Note that a wavelet function gener-ally acts as a bandpass filter.

Regional satellite-only wavelet model of gravity

The objective of our investigation is to compute a *regional high-resolution gravity model* based on satellite and surface data. To be more specific, we first apply the combined approach to calculate a correction to a reference gravity model (EGM96 complete up to degree 120, hereafter referred to as EGM96 (120)) from new regional satellite data. In the second step we extend this multi-scale representation up to a high level by evaluating high-resolution surface data. Geographically we choose a rectangular area in the northern part of South America between 270° and 315° in longitude and -20° and +17° in latitude.

For the preparation of a regional satellite geopotential data set, we analysed kinematic CHAMP orbits, which were kindly provided by D. Svelha and M. Rothacher, TU Munich. These orbits cover a two-year time span between day 70/2002 and day 70/2004. They were converted by the energy balance approach into a time series of geopotential values by J. Kusche and J. van Loon from the Delft University of Technology. After subtracting the reference gravity model EGM96 (120), the resulting residual geopotential data were approximately continued downward or upward to a mean orbital sphere. This *CHAMP residual geopotential data set*, shown in figure B2.2, is the input signal of the following multi-scale analysis including the downward continuation to a sphere close to the Earth's surface. As shown in the last year's annual report on page 29, the downward continuation can be performed until level 6 without considering additional regularisation techniques. Here we carried out the downward continuation until both level 5 and level 6. In general, the sum of the detail signals means an approximation of the signal under consideration. The panel on the left-hand side of figure

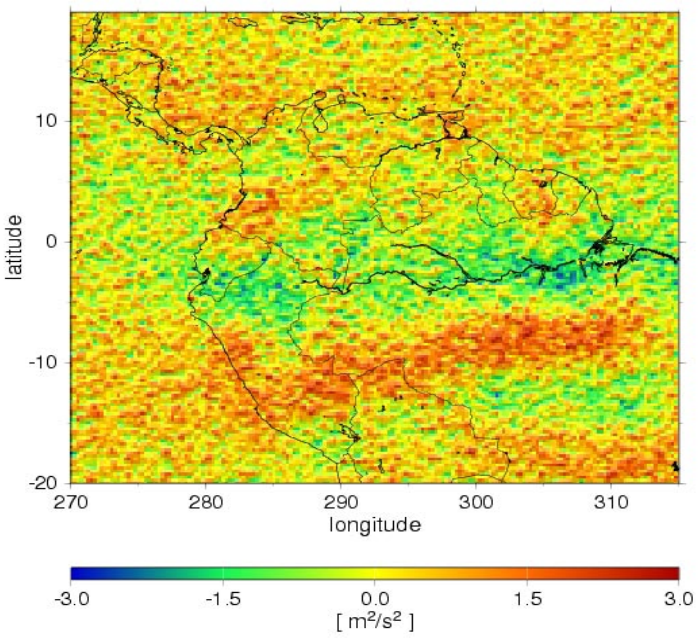

Fig. B2.2: Residual geopotential at mean orbital sphere over northern part of South America, derived from CHAMP data, EGM96 (120) reduced, in [m²/s²]

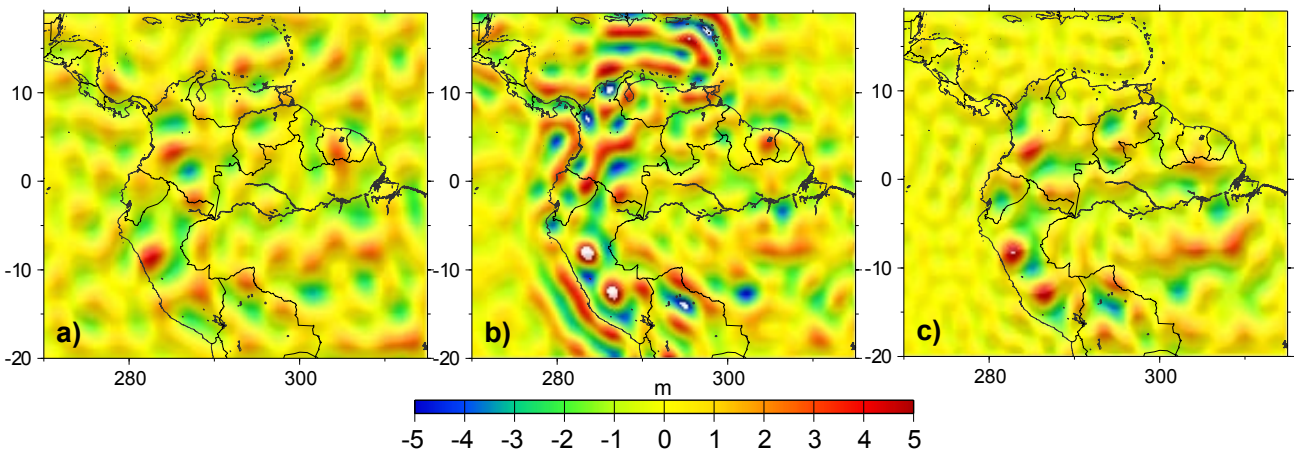

Fig. B2.3: a) WMG-S of residual geoid undulations, b) EIGEN3P model , EGM96 (120) reduced, c) EIGEN-GRACE 02S model , EGM96 (120) reduced, all data in [m]

B2.3 shows the residual geoid undulations as the result of our Wavelet Model of Gravity (WMG-S) using the CHAMP residual geopotential data. Recall that this output signal represents "more or less" the differences between the regional CHAMP data and EGM96 geoid undulations up to degree 120.

The other two panels in figure B2.3 display the corresponding values of the satellite-only models EIGEN3P and EIGEN-GRACE02S from GFZ Potsdam after subtracting the reference model EGM96 (120). There is obviously a much better agreement between WMG-S and EIGEN-GRACE02S than with EIGEN3P, although the latter is computed from CHAMP data, too. This statement is underlined by the numbers given in table B2.1, which presents the rms differences between the aforementioned models.

Tab. B2.1: Rms values of geoid undulations between different satellite-only models, in [m]

model	EIGEN3P	EIGEN-GRACE02S
EIGEN3P		1.26
WMG-S up to level 5	1.37	0.66
WMG-S up to level 6	1.36	0.82
WMG-S up to levels 5/6		0.65

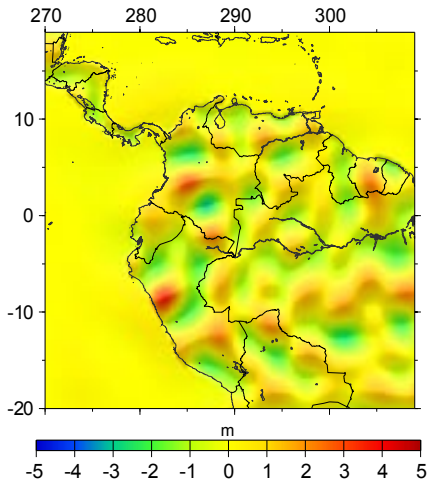

Fig. B2.4: Multi-level WMG-S of residual geoid undulations, model consists of detail signals up to level 5 over oceanic regions and up to level 6 over continental regions, in [m]

The value in the last row is slightly smaller than the other ones. The expression "WMS-S up to levels 5/6" means the construction of a so-called multilevel wavelet model, which considers detail signals up to level 6 over land, but only up to level 5 over the oceans (figure B2.4). This reasonable procedure demonstrates the flexibility of the multi-scale representation using band-limited wavelet functions (building block principle).

As mentioned before, the computation of a *high-resolution gravity model* requires the common evaluation of satellite and surface data. Especially band-limited wavelet functions allow the combination of detail signals computed from different data sources. Our present modelling neglects the overlapping part mentioned in the beginning. Hence, an additional bias between the detail signals computed from satellite data and from surface data may

Comparison with other satellite-only models

occur. But this bias can be determined approximately from the remaining residuals of the decomposition of the surface data. To be more specific, in our modelling the CHAMP satellite data was complemented by a high-resolution data set of Faye anomalies, derived from terrestrial, airborne and altimetry observations and kindly provided by L. Sanchez from the Instituto Geografico Augustin Codazzi, Bogota/Colombia (figure B2.5). Again the refer-

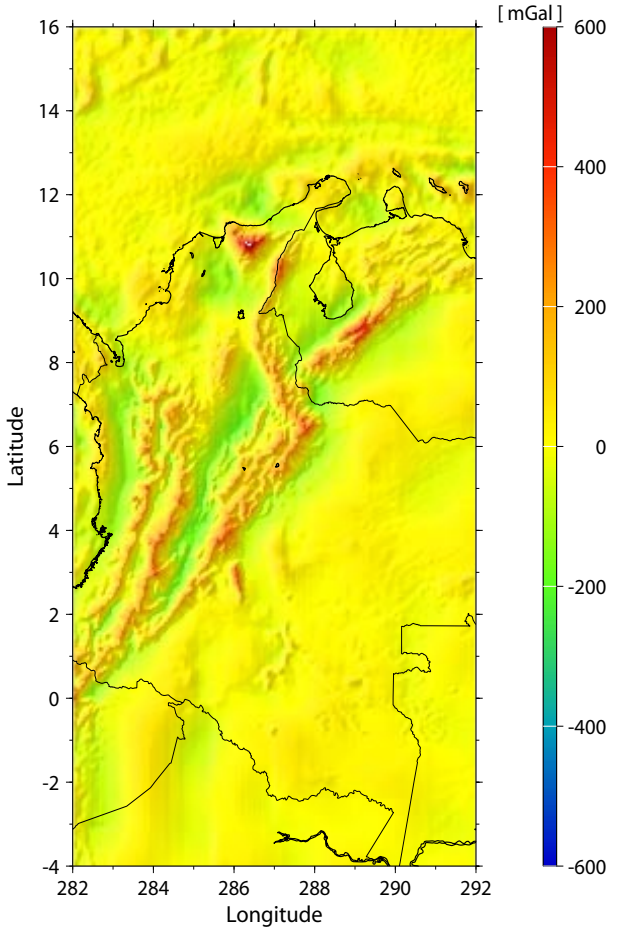

Fig. B2.5: Residual Faye anomalies of Colombia, EGM96 (120) reduced, in [mGal]

ence gravity model EGM96 (120) was subtracted before starting the decomposition process based on the Blackman wavelet function and considering the Stokes operator. The numerical value for the bias mentioned before was neglectable. After all, figure B2.6 demonstrates the stepwise construction of the desired regional high-resolution gravity model by adding

- EGM 96 geoid undulations up to degree 120,
- the residual geoid undulations computed with WMG-S and
- the detail signals for levels 7 to 11 of the residual geoid undulations computed from surface data.

Rejoined high-resolution wavelet model of gravity

The final high-resolution model, shown in the panel on the right-hand side contains frequencies up to degree 4095. This is much higher than the upcoming global gravity model EGM05 with highest degree 2160 will provide. Whereas a comparable spher-

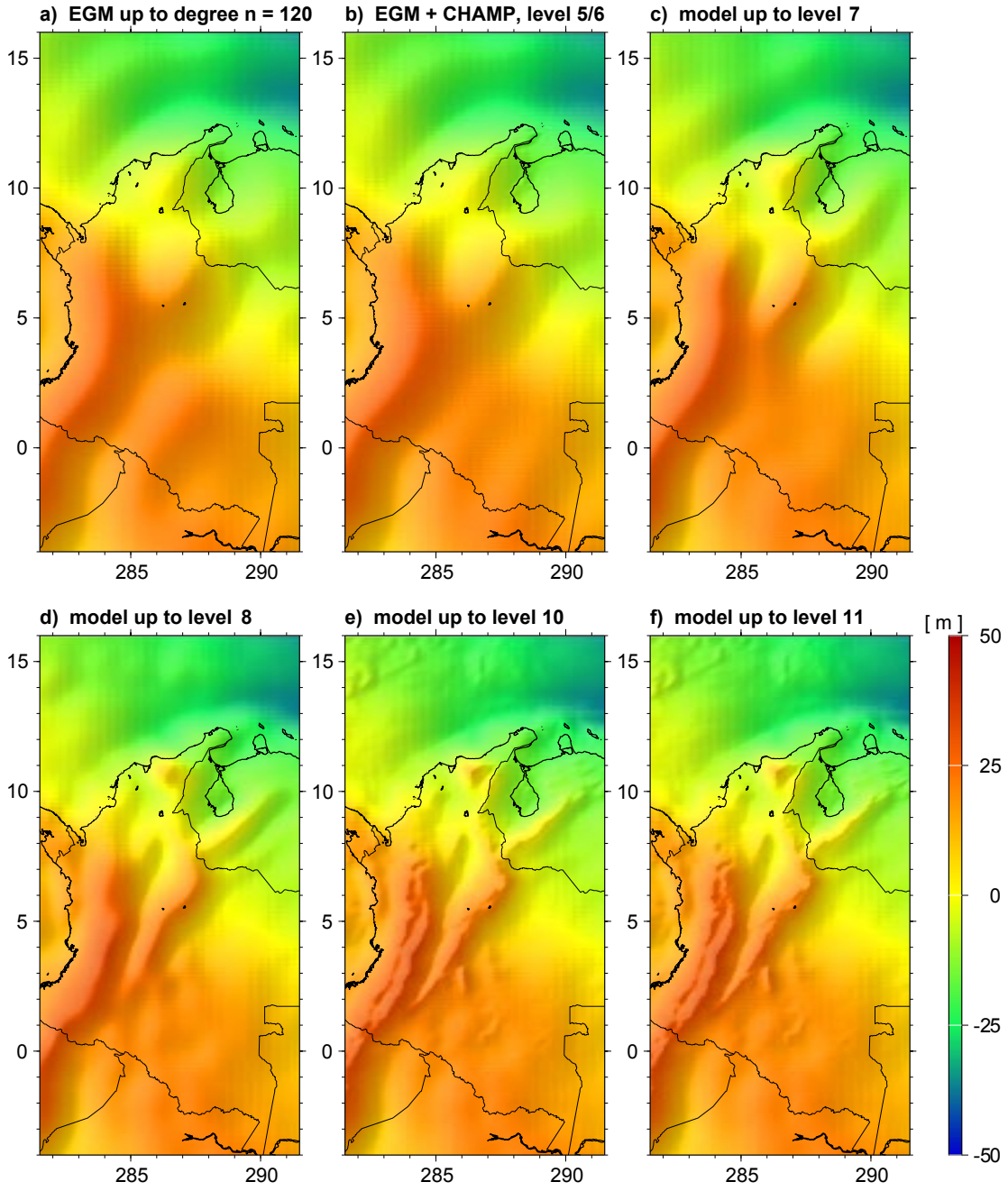

Fig. B2.6: Stepwise construction of the high-resolution gravity model WMG-S/T of Colombia shown in the panel on the right-hand side, all data in [m]

ical harmonics model would require almost 17 million coefficients, our regional model needs just about 0.2 million wavelet coefficients.

Due to the neglect of an effective combination of satellite and surface data within the overlapping detail levels, we denote the final *high-resolution gravity model* by the abbreviaton WMG-S/T, which means that the detail signals altogether are computed either by satellite (S) or by surface, i.e. “terrestrial”(T), data. The consideration of the overlapping model part is subject to future work in project B2.

B3 Modelling the Sea Surface with Multi-Mission Altimetry

The cross-calibration between ERS-2 and ENVISAT performed in the context of the ESA project AO416 (reported in the last annual report) was extended in order to demonstrate the feasibility to perform a *common* crossover adjustment of *all* contemporary altimeter missions. The rationales for this extension are

- the many years with three, four or even five altimeter systems operating simultaneously (namely ERS-2, TOPEX/Poseidon, GFO, later on also Jason1 and ENVISAT),
- the numerous nearly simultaneous crossover events between different contemporary altimeter systems providing a dense network with high redundancy that should allow to estimate reliable radial errors for each of the altimeter systems.

The crossover adjustment takes advantage of the fact that the sea surface height at the intersection of two groundtracks is observed twice. Both heights should coincide if the sea surface would not change. In reality, the difference of sea surface heights (the so-called *crossover differences* Δx_{ij}) does not vanish due to radial orbit errors, insufficient modelling of environmental conditions, and the sea surface variability. If the intersecting ground tracks are observed close in time (with a short time difference Δt_{ij}) the sea surface variability can be neglected and the crossover differences indicate errors of the radial component only.

Discrete crossover analysis

For the multi-mission cross-calibration, a new analysis technique has been developed. The approach (an extension of a method suggested in 1983 by Cloutier) can be characterized as a discrete crossover analysis (DCA). It does not imply any functional model for the radial error component. Instead, the error of the radial components x_i and x_j for the observation times i and j of all crossover differences Δx_{ij} are taken as solve-for parameters. To ensure a certain degree of smoothness for the radial error, the consecutive differences between successive error components x_i and x_{i+1} are minimized in parallel to the residuals of the crossover differences Δx_{ij}.

$$\min_{k'x=0} \left\| \begin{bmatrix} D \\ A \end{bmatrix} x = \begin{bmatrix} 0 \\ d \end{bmatrix} \right\|_P^2$$

$$D = \begin{bmatrix} 1 & -1 & 0 & \dots & \dots & 0 \\ 0 & 1 & -1 & 0 & \dots & 0 \\ \vdots & \ddots & \ddots & \ddots & \ddots & \vdots \\ 0 & \dots & 0 & 1 & -1 & 0 \\ 0 & \dots & \dots & 0 & 1 & -1 \end{bmatrix}$$

$$A = \begin{bmatrix} 1 & 0 & \dots & 0 & -1 & 0 \\ 0 & 1 & -1 & 0 & \dots & 0 \\ \vdots & \vdots & \vdots & \vdots & \vdots & \vdots \\ 0 & \cdots & 0 & 1 & 0 & -1 \end{bmatrix}$$

$$Qx = AW_d b$$

$$Q = D'W_v D + A'W_d A + k\,k'$$

The least squares approach may thus be written as indicated in the left margin where the coeffcient matrix D describes the consecutive differences between successive error components x, which are assumed to be ordered according to their observation time. A is the coefficient matrix for the crossover differences which are compiled into the vector d. Neither the matrix D nor the matrix A has full column rank. The rank defect of the augmented system is 1, because fixing a single error component would determine – by means of the consecutive differences – all other error components. To make the system regular, a single linear combination of error components, $k'x = 0$, is necessary and sufficient and is introduced as a constraint.

Diagonal weight matrices W_d for the crossover differences and W_v for the consecutive differences are used to balance their influence. The error components x are finally obtained as solution of the normal equation system shown in the left margin where the coefficient matrix Q is composed of the weighted Gauss transforms of D and A and the condition equation.

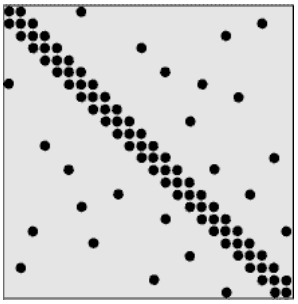

Fig. B3.1: The structue of the normal equation matrix Q is composed of a tridiagonal matrix and a sparse structure with as many off-diagonal non-zero elements as there are crossovers.

In general, the normal equation system is huge. A simultaneous adjustment of crossovers between contemporary missions may involve (as will be shown below) 40000 crossover events. The number of unknowns x is twice as large as the number of crossovers. Thus the systems to be solved have about 80000 unknowns. A rigorous solution for systems of this size is not possible. The only way to solve them is to apply an iterative procedure such as the conjugate gradient projection (CGP) algorithm.

Fortunately, the matrix of the normal equations to be solved have a rather specific structure. Due to the simple form of the matrices D and A, the normal equation matrix Q is composed of a tridiagonal and a sparse part (figure B3.1). The CGP algorithm requires repeated multiplications of the matrix Q and a vector. This can be considerably speeded up if the products with the tridiagonal matrix and the remaining sparse matrix are treated seperately. The CGP algorithm was modified accordingly with the effect that the iterative solution becomes very fast and has very low storage requirements.

Common crossover adjustment of ENVISAT, Jason1, T/P-EM, and GFO

In order to demonstrate the DCA, a common adjustment of the radial components of four altimeter systems, namely ENVISAT, Jason1, T/P-EM and GFO, was performed for a 14-day period. To exclude sea level variability, only single and dual satellite crossovers with a time difference $\Delta t_{ij} < 2$ days were used. As an example, figure B3.2 shows how the coverage of ENVISAT crossovers increases by adding dual satellite crossovers that ENVISAT performs with the other three altimeter missions.

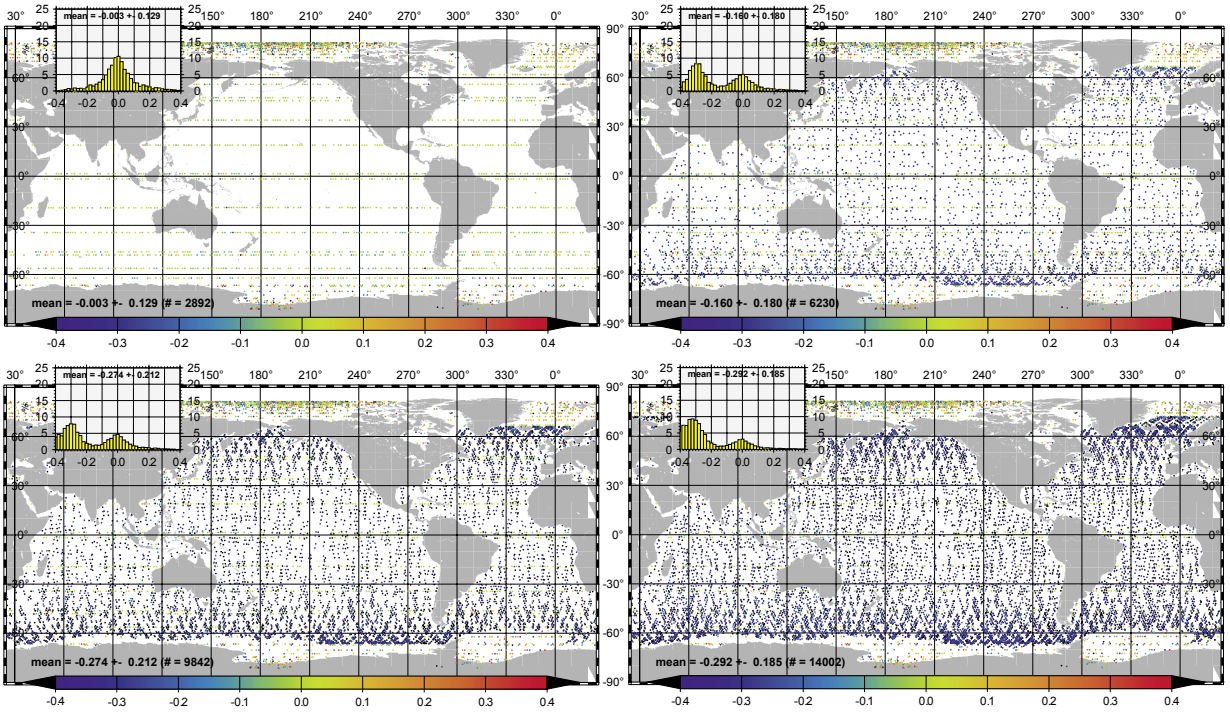

Fig. B3.2: Spatial distribution of ENVISAT crossovers with time difference $\Delta t_{ij} < 2$ days. The upper left panel shows the distribution of ENVISAT single-satellite crossovers only - with an inconvenient geographical coverage. The other panels show how this distribution improves after gradually adding dual-satellite crossovers which ENVISAT performs with T/P-EM (upper right), with Jason1 (lower left), and with GFO (lower right). The rather large relative range biases between ENVISAT and the other altimeter systems create the double peaked histogrammes and cause the dominance of the dark blue colour for dual-satellite crossover differences.

Tab. B3.1: Mean and rms of single satellite crossover (diagonal cells) and dual satellite crossover (off-diagonal cells). Units are m. The upper row gives values before, the lower row values after crossover adjustment. The last row gives the total number of crossovers for each mission.

T/P-EM	Jason1	GFO	ENVISAT
0.00 ±0.08 0.00 ±0.07	-0.18 ±0.07 0.00 ±0.06	0.04 ±0.08 0.00 ±0.07	-0.33 ±0.08 0.01 ±0.07
	0.00 ±0.06 0.00 ±0.06	-0.14 ±0.08 0.00 ±0.06	-0.47 ±0.07 0.00 ±0.06
		0.01 ±0.07 0.00 ±0.07	-0.29 ±0.09 0.00 ± 0.07
			0.00 ±0.13 0.00 ±0.13
16813	17705	18233	14316

For both crossover and consecutive differences a downweighting with increasing time difference (but with different half weight width) was applied. The crossover differences were also weighted proportional to $\cos^2\phi$, because the density of crossovers increases with latitude ϕ. Finally, the standard deviation of crossover differences (derived from interpolating the sea surface heights) was used for an additional weighting.

Table B3.1 compiles mean and rms values for single and dual satellite crossovers – before and after the crossover adjustment. A 1 cm decrease of the rms values was mainly achieved for dual satellite crossovers which in general have smaller time differences and get higher weights than single satellite crossovers. The rms of dual satellite crossovers between GFO and Jason1 and between ENVISAT and GFO decreased by 2 cm. The rms of single satellite crossovers improved only for T/P-EM by 1 cm.

The rank defect was solved by fixing first a single error component. After the adjustment, the mean of all T/P-EM error components was subtracted. In this way, the T/P-EM orbit was used as a mean reference, which is justified by the generally accepted assumption that the orbit of T/P-EM is the most precise one. The final error components of all other altimeter missions automatically capture the rather large relative range biases between T/P-EM and the other missions (as indicated by the change of mean values in table B3.1 before and after the adjustment).

Figures B3.3 and B3.4 show the result of the common crossover adjustment of all altimeter missions. There are individual passes where the estimated errors differ significantly from neighbouring passes, but also large scale patterns with similar errors at differ-

Fig. B3.3: Estimated errors of the radial component for T/P-EM (left) and Jason1 (right). Ascending passes (top) and descending passes (bottom) show errors with significant large scale pattern at different geographical regions.

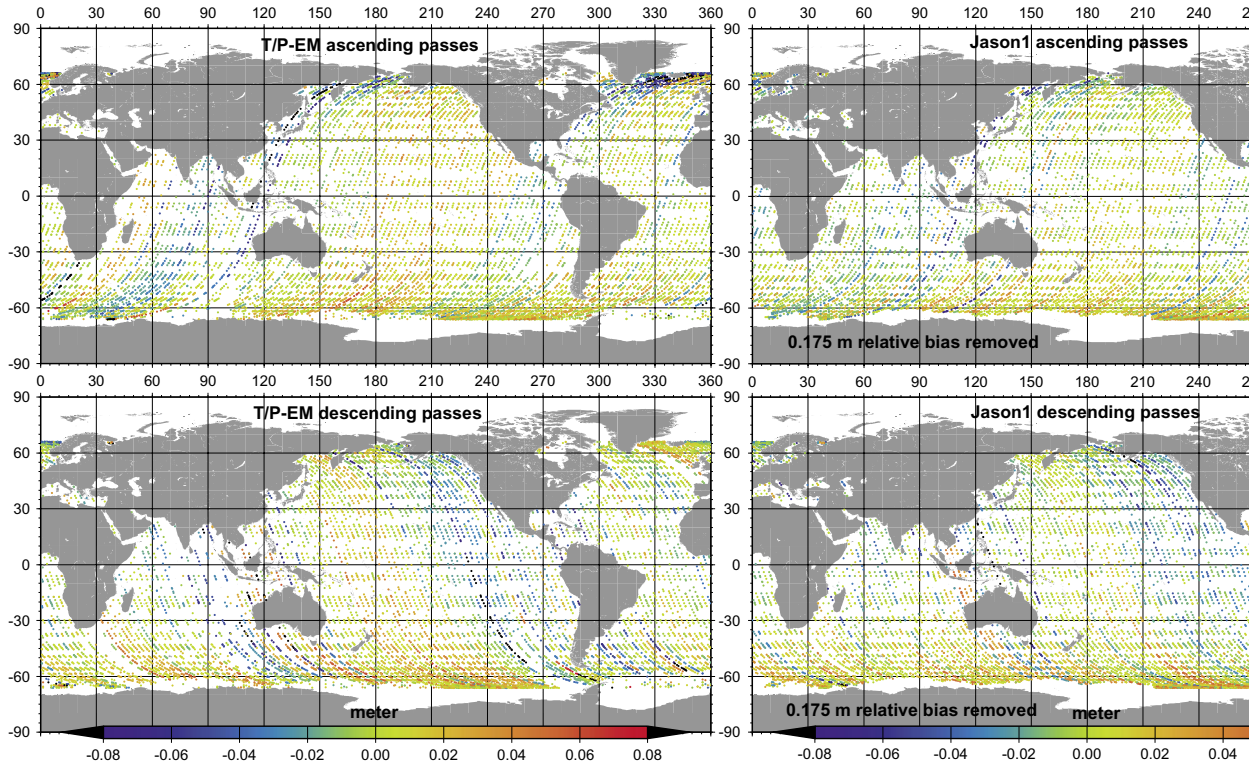

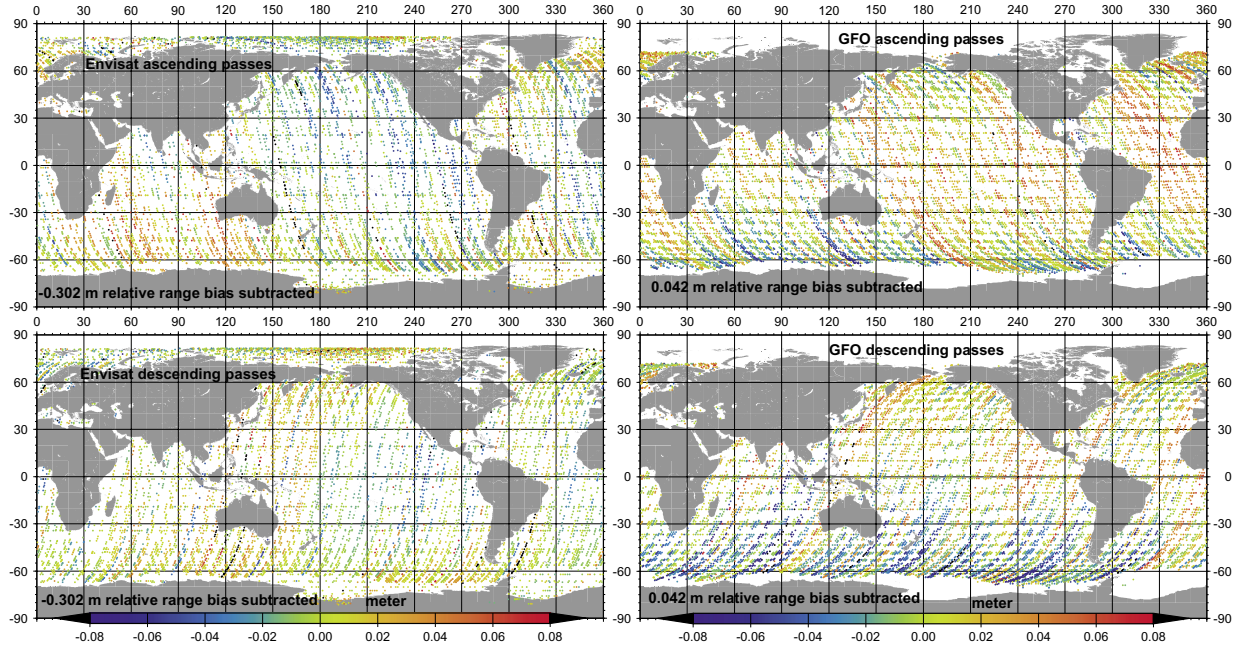

Fig. B3.4: Estimated errors of the radial component for ENVISAT (left) and GFO (right). Ascending passes (top) and descending passes (bottom) show errors with significant large scale pattern at different geographical regions. Especially striking are the northern and southern hemisphere errors of the descending passes of GFO.

ent geographical regions. Ascending and descending passes show a completely different error pattern. This is an indication that the orbits of all missions still carry the signature of errors of the gravity field used for orbit integration. It is known that gravity field errors map to geographical patterns which are different for ascending and descending passes. To first order, the error pattern may also be explained by inconsistencies in the center of origin implied by the satellite orbit.

The errors of Jason1, ENVISAT and GFO shown in figures B3.3 and B3.4 are reduced by their mean values to show more clearly their geographical variation. The mean values are caused by relative range biases between the (uncalibrated) altimeter missions. In order to estimate these range biases together with center-of-origin shifts that could explain – to first order – the error pattern, the model

$$x_i + v_{x_i} = \Delta r + \Delta x \cos\phi \sin\lambda + \Delta y \cos\phi \cos\lambda + \Delta z \sin\phi$$

was fitted to the error components x_i of every mission. Table B3.2 shows the values of the estimated parameters.

As a powerful tool to estimate altimeter system inconsistencies, DCA will be applied to all multi-mission periods such that all missions can be used for a common mapping of the sea surface.

Tab. B3.2: Relative range biases Δr and center of origin shifts Δx, Δy, Δz (m) estimated from the error components x_i obtained by DCA. The range biases and the Δz-shift are correlated due to the dominance of oceans on the southern hemisphere. GFO and ENVISAT have shifts of more than 1 cm for the z and y components respectively.

mission	T/P-EM	Jason1	GFO	ENVISAT
σ_0	±0.026	±0.018	±0.027	±0.030
relative range bias Δr	-0.003	0.173	0.045	-0.301
Δx-shift	-0.005	-0.003	0.001	0.002
Δy-shift	-0.003	0.001	-0.005	0.012
Δz-shift	-0.009	-0.008	-0.015	-0.004
number of error components	19821	21318	21974	16879

B4 Investigations to Unify Height Systems

The unification of national height systems is still subject to detailed investigations. Definition and realization of a unique global height reference surface are topics that have to be clarified by conventions and recommended procedures. In addition, every country has to decide on the type of its height system (normal or orthometric heights, geopotential numbers, ellipsoidal heights). DGFI contributes to the studies of the IAG Intercommission Project 1.2, "Vertical Reference Systems", is involved in the Project on the South American Reference System , Phase III, and performs relevant investigation within COSSTAGT, a project to estimate the absolute sea surface topography in coastal areas.

By levelling, geometric height differences are "measured" along the local plumb line. Because an equipotential surface is always perpendicular to the plumb line it would be a natural candidate for a global height reference surface. Such a surface is uniquely defined by an equipotential number, W_0. Although it is well known that the mean sea level is *not* coinciding with an equipotential surface, it appears natural to relate heights to the mean sea level (people at the coast want to know how much they are living above sea level). This, however, is a contradiction: to count heights from sea level, but refer them everywhere to an equipotential surface. Today, there is at least a qualitative knowledge about the sea surface topography (SSTop), the deviations between geoid and mean sea level (compare the SSTop estimate, shown in the previous annual report). A meaningful synthesis of this contradiction was already given in 1872 by Listing: The geoid was specified as that particular equipotential surface that most closely approximates the mean sea level.

Listing geoid: an equipotential surface approximating mean sea level

Listings definition of the geoid is, however, "academic" and does not answer practical questions:

- What gravity field should be used to realize the equipotential surface? There are a number of gravity field models that differ in resolution and accuracy.
- How should the mean sea level be realized? From altimetry it is well known that the mean sea level is not static, but changing by some decimeters – with opposite signs in different regions of the world. Altimetry is not able to map the mean sea level at high latitudes and in regions that are seasonally covered by ice.
- How should the deviations between geoid and mean sea level be measured? A least squares minimization of differences computed for a global grid? What grid spacing should be used?

Determination of W_0

In principle, the determination of W_0 is straightforward: Use a mean sea surface height model and a state-of-the-art gravity field model and compute on a global grid the potential at the gridded sea surface heights. Then, a weighted mean of the potential values can be taken to define W_0. Some computations have been performed in order to find out to what extent the determination of W_0 depends on the grid spacing, the extension in latitude and the choice of the gravity field model.

Offset of national height systems

As soon as a particular equipotential surface has been specified by definition of W_0, the offset of national height systems relative to the global height reference surface has to be determined. Traditionally, national height systems are defined through a long-term mean of tide gauge registrations. There are several approaches to estimate the offset between the tide gauge zero point and the selected equipotential surface: A precise geocentric positioning of the tide gauge may be used to compute the potential value W_i at the tide gauge zero point and to transform the (small) geopotential differences $\Delta W = W_0 - W_i$ by means of Bruns' formula to a vertical distance. However, W_i will be affected by short wavelength errors of the gravity field. The approach could be extended to all points with both levelled heights and geocentric coordinates. A precise local geoid computation could provide the short wavelength information of the gravity field – and the knowledge about the absolute sea surface topography would allow to determine the desired offset. To take advantage of any redundancy, a combination of these approaches is highly recommended.

COSSTAGT project

The primary objective of the COSSTAGT project is to estimate the SSTop and its low-frequency variability in selected coastal areas (above all around tide gauge zero points) through combination of altimeter observations, surface- and space-borne gravity data, precise point positioning and registrations of tide gauges. The SSTop shall be estimated by a most precise description of both sea level and the geoid in a common geocentric reference. Any attempt to estimate the SSTop in coastal areas has to consider the close interrelationship between altimetry, tide gauges, global positioning and the geoid, as illustrated in figure B4.1.

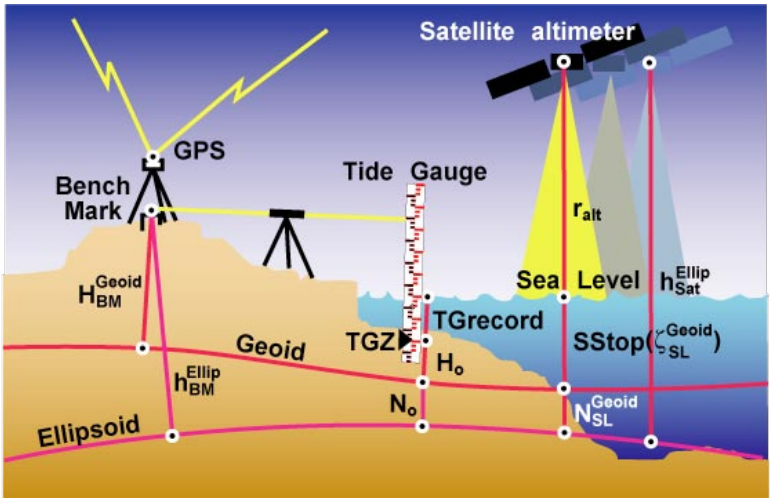

Fig. B4.1: Interrelationship between altimetry, tide gauges, global positioning, and the geoid.

Tide gauge records are complementary to altimetry: they measure at individual points, but provide quasi continuous sea level records with highest precision – in general for much longer time periods than altimetry. Tide gauge data have not only been used to define the zero point of national height systems; They are also used to estimate global sea level rise and to control the long-term stability of altimeter systems.

There are close relationships between tide gauge records and altimetric sea level time series. It is, however, not obvious that both time series describe the same oceanographic signal. Geodetic control by global navigation systems is a fundamental requirement to avoid that undetected vertical tectonic motions at tide gauges are interpreted as apparent sea level rise (or fall). DGFI therefore contributes to the TIGA project (see project D3) in order to estimate vertical velocities at tide gauges by a dedicated processing of continuous GPS observations.

Tidal Analysis at the Patagonian shelf

Coastal altimeter observations on the other hand are degraded in accuracy because the radar echo is falsified whenever it is reflected on a non-ocean surface. Large changes of environmental conditions at the coast are not taken into account, and global ocean tide models are still unable to predict tidal water levels at the coast. The improvement of coastal tides was a focus of the last years' work.

For the tidal analysis the Patagonian shelf was selected. It is an extended area with extreme tidal water levels (figure B4.2) and part of the SIRGAS project area. The decadel time series of TOPEX/Poseidon (T/P) allows a reliable dealiasing and analysis of the major tidal constituents. Of particular interest was the question whether the residual ocean tide corrections, estimated along both the ground tracks of T/P (up to cycle 364) and the shifted ground tracks of the extended TOPEX/Poseidon mission (T/P-EM, from cycle 368 on) are consistent with each other and can be extrapolated and applied to other altimeter missions – above all to the sunsynchronous ERS and ENVISAT missions (which are not at all able to sense solar tide constituents like S_2).

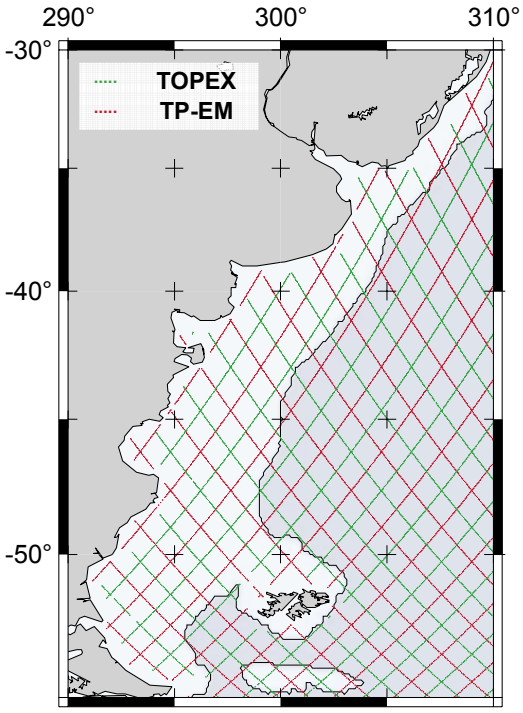

Fig. B4.2: The Patagonian shelf was used to estimate residual shallow water tides along the original T/P ground tracks (green) and the shifted ground tracks of the extended mission T/P-EM (red).

For the analysis the altimeter data were first enhanced and in a second step reorganized. After upgrading

- ocean tide corrections with GOT99.2b (Ray 2000),
- the new SSB model for TOPEX/Poseidon (Chambers 2003),
- the CLS01 mean sea surface (Hernandez & Schaeffer 2002),
- and the radial component of T/P and T/P-EM by crossover analysis,

sea surface height anomalies (SSHA) were computed and resampled to along-track bins with lengths of several kilometres (see also project D7). Residual amplitudes and phases of M2 were then estimated by a least squares tidal analysis of the binned SSHA:

$$SSHA_i(\varphi,\lambda,t) = A_i(\varphi,\lambda)\cdot f_i(t)\cdot\cos(\omega_i t + V_i(t) + u_i(t)) + B_i(\varphi,\lambda)\cdot f_i(t)\cdot\sin(\omega_i t + V_i(t) + u_i(t))$$

where A_i , B_i are cosine and sine coefficients, f_i and u_i are nodal corrections in amplitude and phase respectively, and $\omega_i t + V_i(t)$ are frequency and astronomical phase lag. Figure B4.3 shows a vector representation of the cosine and sine coeffcients and also the amplitudes $H_i = \sqrt{A_i^2 + B_i^2}$.

In order to verify the analysis and to measure the gain achieved by the residual tide constituents, the corrections were not only

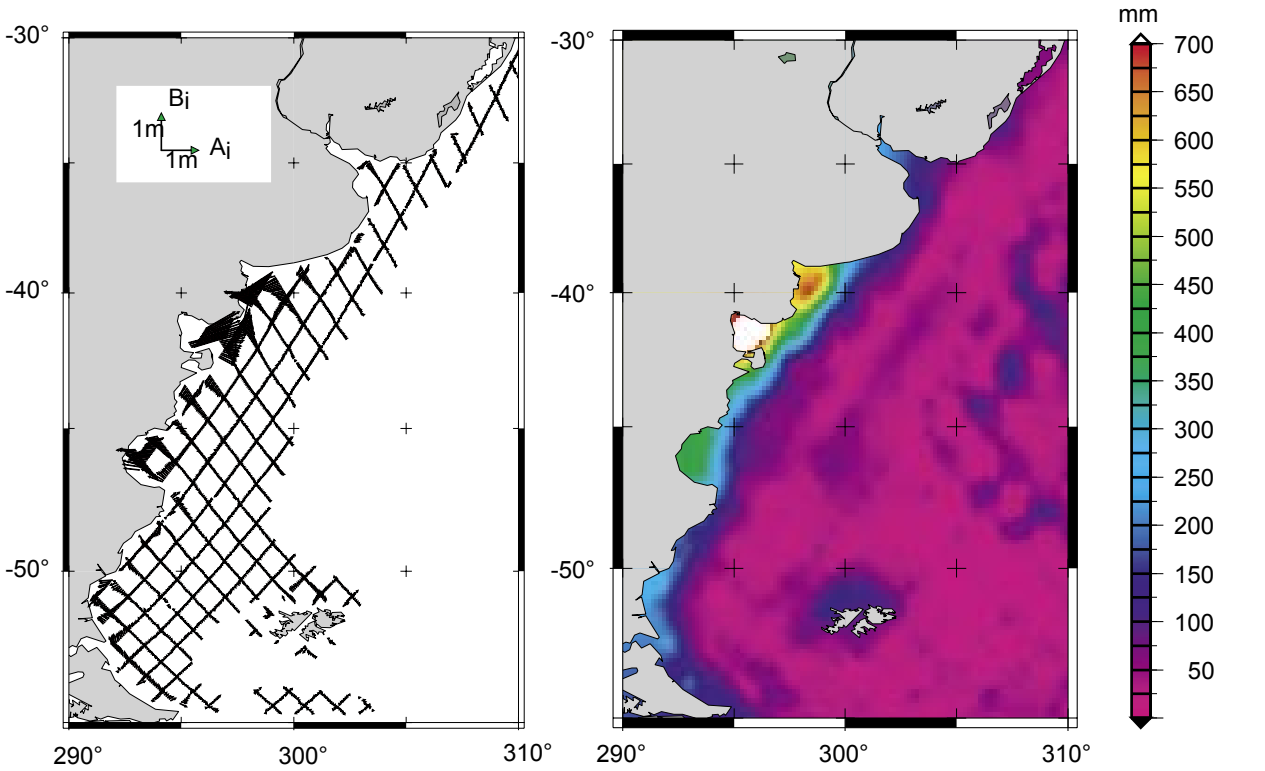

Fig B4.3: The vector representation of the coefficients Ai and Bi (left panel) for the M2 tidal constituent indicates the consistency of results derived from the "old" and "new" ground tracks of T/P and demonstrates the smooth development of residual tides towards the coast. The amplitudes of the M2 resdiual tides (right panel) show values up to and above 50 cm.

applied to TOPEX/Poseidon but also to ERS2 (which implies a spacial interpolation). Harmonic analysis of the M2 alias periods and statistics of satellite crossovers, both before and after correction, verified that considerable improvements were achieved at a small band along the coast. Figure B4.4 demonstrates the improvements for two individual profiles observed by TOPEX/ Poseidon and ERS2.

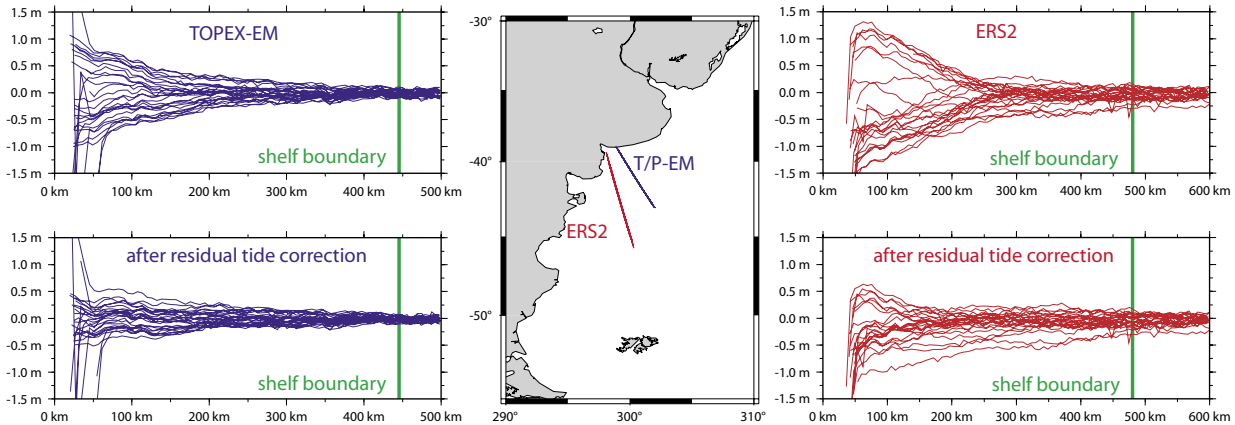

Fig. B4.4: A sequence of profiles for TOPEX-EM (left hand) and ERS2 (right hand) before (top panels) and after (bottom panels) correction with the residual tides show considerable improvements over the Patagonian shelf.

C Dynamic Processes

Variations of the Earth's geometrical shape, its gravity field and its rotation can be observed by modern space-geodetic techniques with high accuracy. For the explanation of the respective geodetic parameters on sub-daily to decadal time scales, independent approaches from theory and modelling are required. The understanding of dynamic processes in the Earth system is fundamental for the realization of geodetic reference systems and the combination of heterogeneous space-geodetic observations. The present research activities at DGFI comprehend numerical modelling of mass redistributions in the Earth system and their effects on gravity field and rotational dynamics. In order to improve the accuracy of satellite observations, the total electron content of the ionosphere is investigated using a wavelet approach. Besides, analysis techniques for time series of geodetic and geophysical parameters are developed.

C1 Impact of Mass Redistributions on Surface, Rotation, and Gravity Field of the Earth

Fluctuations of Earth rotation, reflected by polar motion and changes in length-of-day, are integral quantities which are associated with mass redistributions and motions occurring in the Earth's subsystems. The largest effects are due to tidal deformations of the solid Earth and mass redistributions within the atmosphere and the oceans. Variations of Earth rotation caused by these excitations are additionally superposed by free oscillations of the Earth, i.e. the Chandler wobble and the nearly diurnal free wobble. It is well known that the amplitude of the Chandler wobble would diminish due to friction without further excitation. However, time series derived from geodetic observations do not show any damping. The reason for the perpetuation of the Chandler amplitude is still not well understood.

Dynamic Earth system model DyMEG

In order to increase the understanding of both the geophysically induced global mass transports and the dynamical response of the Earth, the non-linear dynamic Earth system model DyMEG has been developed at DGFI (cf. preceding annual reports). The model is forced by consistent time series of variations of the Earth's tensor of inertia and relative angular momenta which are deduced from atmospheric and oceanic reanalyses or circulation models. Two independent consistent model combinations are considered. First, atmospheric data based on the reanalyses of the National Centers of Environmental Prediction (NCEP) are applied in combination with the ocean circulation model ECCO. Both models cover a range of 23 years from 1980 until 2002. Second, the atmospheric model ECHAM3-T21 GCM is used in combination with the ocean model OMCT for circulation and tides. The latter models cover a range of 20 years from 1975 until 1994. Both combinations are consistent representations of dynamics and mass motions in the subsystems atmosphere and ocean since the respective atmospheric forcing fields are used for the computation of ocean dynamics.

Numerical results for polar motion from DyMEG are significantly related with geodetic observations. The model time series for polar motion resulting from atmospheric and oceanic forcing are displayed in figure C1.1. For NCEP-ECCO (a), the correlation coefficients with the geodetic observations (c) are 0.98 for the x and 0.99 for the y component. The respective rms-values are 29.5 mas and 23.3 mas. In the case of ECHAM3-OMCT (b), the

correlation coefficients amount to 0.95 and 0.94 for *x* and *y* components respectively, the corresponding rms-values are 70.8 mas and 75.8 mas. Here, the agreement is slightly lower since the annual atmospheric variability is overestimated by ECHAM3. As clearly visible, both model combinations lead to an undamped polar motion of DyMEG. Signal analyses of the resulting time series by means of wavelet transformation feature stable energy in the Chandler frequency band. Hence, the consistent atmospheric and oceanic forcing is capable of exciting the Chandler amplitude over more than two decades.

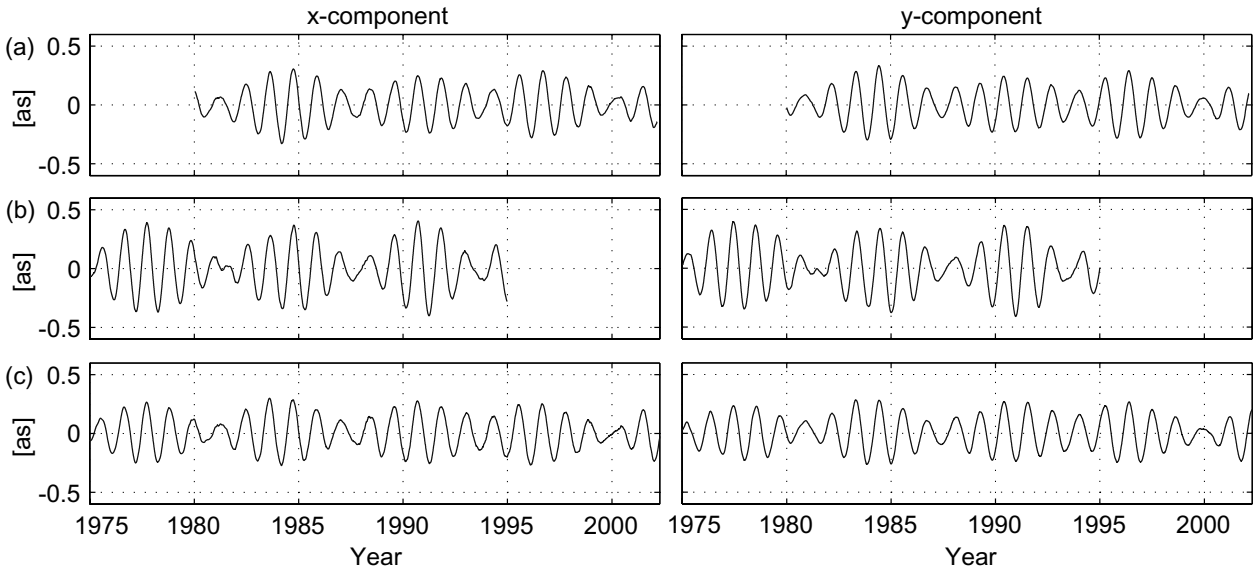

Fig. C1.1: Model results for polar motion applying atmospheric and oceanic excitations. (a) NCEP-ECCO, (b) ECHAM3-OMCT, (c) geodetic observation C04. Linear trends have been removed.

Separated atmospheric and oceanic forcing

Experiments with separated atmospheric and oceanic excitations demonstrate that mass variations in both subsystems contribute significantly to polar motion. As spectral analyses give no hint for increased excitation power in either spectra of atmospheric and oceanic excitations in the Chandler frequency band, obviously no explicit excitation near the Chandler frequency is necessary to perpetuate the Earth's free wobble. Ongoing stochastic weather phenomena yield a flat distribution of excitation power in the atmospheric and oceanic time series over the whole spectrum (white noise) which seems to be just sufficient to provoke a resonant reaction of the rotating Earth via rotational deformations. In order to assess the noise level of the four excitation series, the angular momentum functions were analysed with respect to the signal energy contained in a symmetric band of ±30 days around the Chandler period (400-460 days). This bandwidth was chosen in order to avoid spectral leakage from the annual into the Chandler band, which might adulterate the results. As polar motion of DyMEG is dominated by temporal variations of the elements ΔI_{13} und ΔI_{23} of the Earth's tensor of inertia, other deviation moments as well as relative angular momenta were neglected in this study. For the analysis, an elliptic Cauer-filter was applied.

The computations of polar motion with separated atmospheric and oceanic forcing span the time interval between 1.1.1980 and 31.12.1994 which is covered by all four excitation series. This was done in order to avoid discrepancies between the results which are due to differing initial conditions and thus might lead to misinterpretations. Figure C1.2 shows the resulting polar motion (*x* components) for the four band-pass filtered atmospheric and oceanic excitations (upper panels). Due to the circular trait of the Chandler wobble, the *y* components look alike. In addition, the integral signal energy is displayed, which is contained in the prograde Chandler band of the respective angular momentum time series between 400 and 460 days (lower panel). It has been determined from the filtered excitations by means of wavelet transformation.

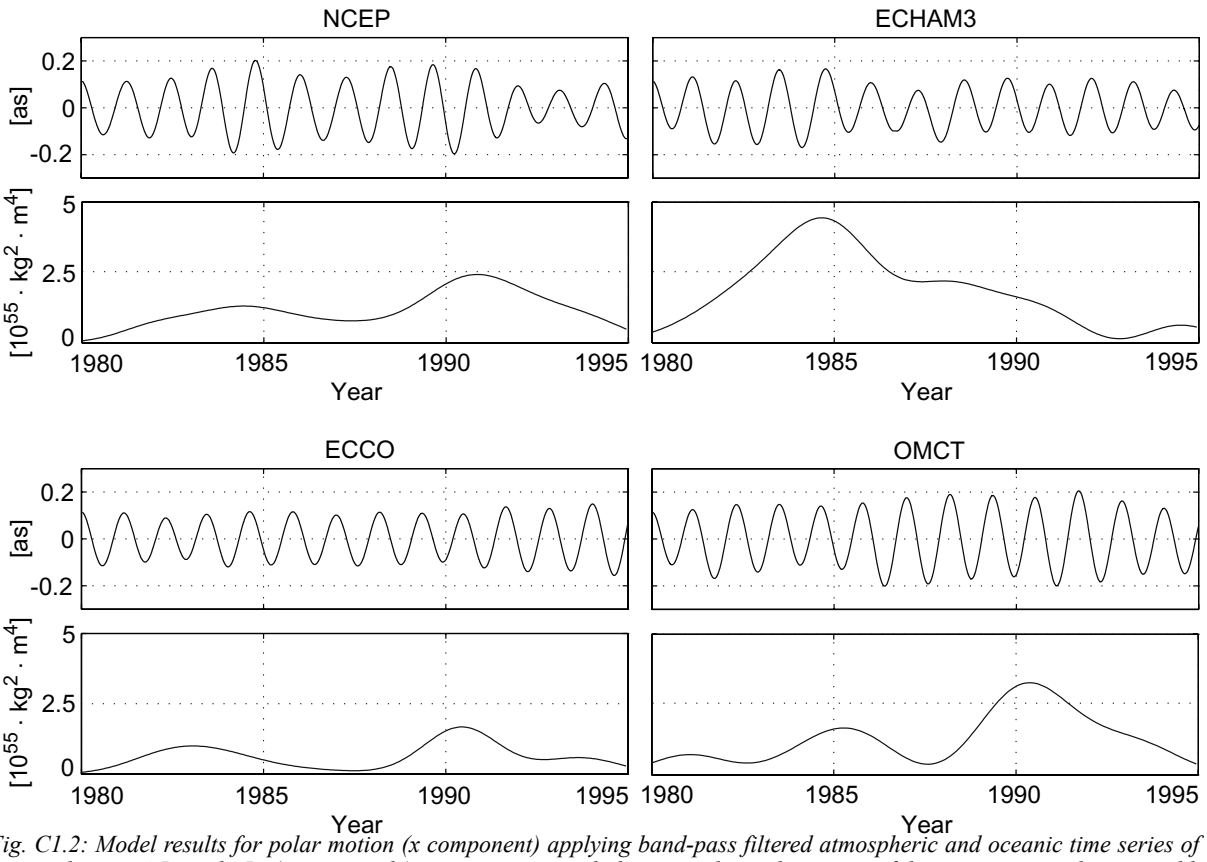

Fig. C1.2: Model results for polar motion (x component) applying band-pass filtered atmospheric and oceanic time series of the tensor elements ΔI_{13} and ΔI_{23} (upper panels) in comparison with the integral wavelet energy of the excitations in the spectral band between 400 and 460 days (lower panels).

In all polar motion series, the Chandler amplitude does not increase or decrease continuously, but features fluctuations which are linked to the instantaneous energy level of the excitations. The highest Chandler amplitudes are achieved for NCEP and OMCT while the ECCO run shows a rather weak amplitude. Both atmospheric data sets show higher energy levels than the corresponding ocean models. The energy of ECHAM3 is higher than the energy of NCEP, the level of OMCT is higher than the one of ECCO.

In the case of NCEP and ECHAM3, the maxima of the energy and the maxima of the Chandler amplitude coincide. For OMCT

and ECCO, the temporal agreement of energy and amplitude is not so conspicuous. Obviously not only the amount of excitation energy in the Chandler band but also the instantaneous phase relations of the excitations and the Chandler wobble are very important. Hence, the knowledge of the absolute amount of excitation energy is not sufficient for a definite conclusion of the resulting Chandler amplitude. Nevertheless, this experiment revealed that the energy of the atmospheric and oceanic excitations is high enough to counteract the damping of the Chandler wobble.

White noise Chandler wobble excitation

In a second experiment, equally distributed random numbers (white noise) from the interval [-1,+1] (Units [kg m²]) were set for the excitation. This purely synthetic excitation was multiplied by a constant factor l which corresponds to a variation of the noise level. Instead of ΔI_{13} and ΔI_{23}, two of these random time series were introduced into DyMEG. As expected, no reaction of the gyro becomes obvious for small values of l. For $l = 1 \cdot 10^{27}$, first effects on the free rotation of DyMEG are visible as the damping is attenuated. For $l = 1 \cdot 10^{29}$ the white noise is fully capable of exciting the Chandler wobble. The results of two model runs with different random excitations (both with $l = 1 \cdot 10^{29}$) are displayed in figure C1.3. Analogous to figure C1.2, the integral wavelet energy in the Chandler band (400-460 days) is shown, too.

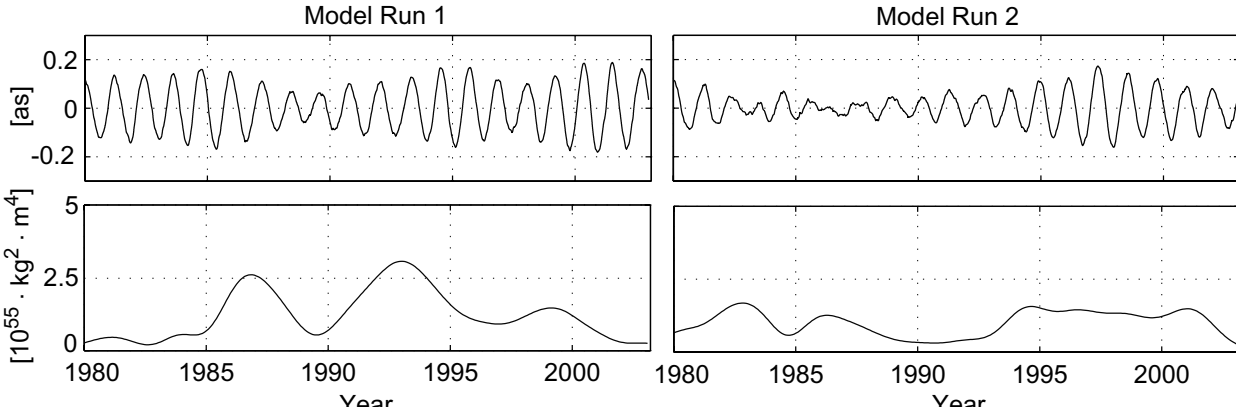

Fig. C1.3: Model results for polar motion (x component) applying two different time series of equally distributed random numbers from the interval [-1·10²⁹, +1·10²⁹] kg m² instead of the tensor elements ΔI_{13} and ΔI_{23}.

As clearly visible, the Chandler wobble is excited by the white noise. The noise level, which is necessary for the perpetuation of the Chandler amplitude corresponds to the noise level which is described by the atmospheric and oceanic excitations (figure C1.2). As above, the maxima of the energy and the maxima of the Chandler amplitude do not always coincide. Hence, this result supports the assumption, that not the energy level alone, but also the instantaneous phases of the random excitations are very important for the excitation of the Chandler wobble. Which atmospheric and oceanic processes are responsible for the noise, cannot be resolved in detail. Presumably purely stochastic atmospheric variations (weather) contribute essentially to the noise. As atmosphere and oceans interact, the stochastic signal is carried forward from the atmosphere into the oceans.

An essential part of this project was funded by DFG grant DR 143/10.

C2 New Analysis Techniques for Observations of Dynamic Processes

Structure of the ionosphere

The ionosphere is generally defined as a thick shell of electrons and ions, which envelops the Earth from about 60 to 1000 km height. As can be seen from figure C2.1, there exist four relatively destinct regions, namely the D layer between 60 and 90 km, the E layer from 90 to 130 km and the F layer, which is additionally devided into the F1 layer between 130 and 210 km and the predominant F2 layer from 210 to 1000 km. In the latter the maximum value NmF2 of the space- and time-dependent electron density profile is located at height hmF2. This height marks the border between the bottomside and the topside of the ionosphere. Since the Sun is the main source of the ionization, any variation of the solar radiation or the geometry with respect to the Earth yields large changes in the electron content distribution. This feature implies that the electron density is mainly characterized by diurnal variations. The red and the black curve in figure C2.1 illustrate the variation of an electron density profile between day and night time.

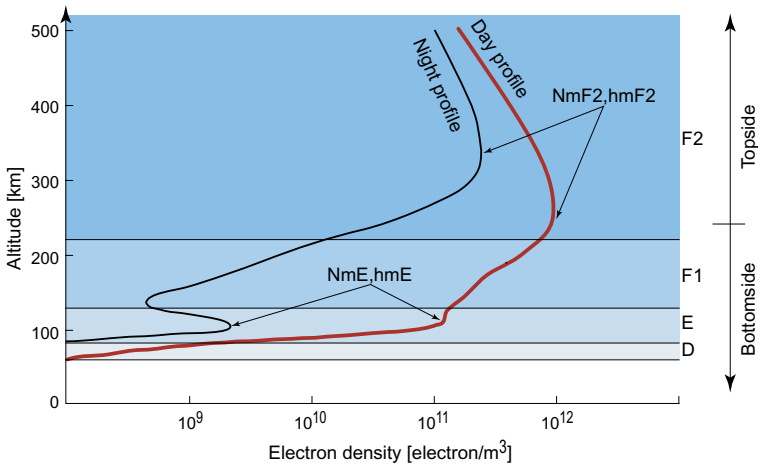

Fig. C2.1: Day and night profiles of the ionospheric electron density. The maximum value NmF2 of the electron density is located at height altitude hmF2 in the F2 layer.

Electron density distribution

The diurnal variations are the reason why the electron distribution is usually not described in an Earth-fixed, but in a Sun-oriented coordinate system. For *regional modelling* with respect to the Earth, however, we cannot uphold up this concept and have to consider the entire spectrum of variations. Besides the diurnal variations, at least semi-diurnal and annual periods as well as periodical variations of about eleven years due to the solar cycle have to be taken into account. Furthermore, there exist latitudinal variations like the Appleton-Hartree (equatorial) anomalies in the low latitudes and short-term variations in the auroral regions in the high latitudes. But besides these expected variations many other more unpredictable phenomena related to the activity of the Sun may occur, e.g. geomagnetic storms. In order to describe the deterministic part of the electron density distribution both theoretical and empirical models are applied.

The International Reference Ionosphere (IRI) for instance is a climatological model and comprises several profiles for plasma parameters. Our investigations, however, are based on the *NeQuick model*, which is an empirical model generating profiles of the electron density. This model was mainly developed by the

Aeronomy and Radio Propagation Laboratory (ARPL) of the International Centre of Theoretical Physics (ICTP) in Trieste/Italy.

Wavelet Model of Ionosphere

In the last years the new possibility to estimate the electron distribution by GPS measurements has opened a very active and promising field of ionospheric research. While ground-based two-dimensional ionospheric maps mean a substantial progress in ionospheric weather research, applications and forecast, the radial geometry of the ground-based observations limits their capability for providing information on the vertical electron distribution. Using simulated data it was demonstrated that this limitation can be overcome by the introduction of more or less horizontal cuts through the ionosphere, performed by space-borne GPS receivers flying on low-Earth orbiting (LEO) satellites such as GPS-Met, CHAMP, GRACE or SAC-C. Two- and three-dimensional snapshots representing the global ionosphere were obtained combining ground- and space-based real observations.

Our objective is to derive a *regional space-time model of the electron density distribution* mathematically based on wavelet strategies and physically controlled by the NeQuick model. The parameters of this Wavelet Model of the Ionosphere (WMI) shall be estimated by means of GPS observations on terrestrial stations and LEO satellites. In addition pseudo observations from the NeQuick model are introduced in order to stabilize the estimation process. The fundamental so-called geometry-free observation equation for the determination of the electron content of the ionosphere from GPS phase or code measurements was presented in the last year's annual report on page 42. To be more specific, these observations provide informations about the the so-called slant total electron content (STEC), which is defined as the integral of the space- and time-dependent electron density along the ray-path between the transmitter in the satellite and the receiver, either on ground or in space. Usually the STEC values are transformed into so-called vertical total electron content (VTEC) values using a certain mapping function. Besides STEC the observation equation contains moreover the inter-frequency differential delays in receiver and satellite.

The NeQuick model describes the electron density distribution $N(\mathbf{x},t)$ in a given point P with position vector $\mathbf{x}$ and for any time t by a function that depends – among other parameters – mainly on the quantities NmF2 and hmF2 introduced before, i.e. $N(\mathbf{x},t;\mathrm{NmF2},\mathrm{hmF2})$. Our approach is based on the linearization of the equation for the computation of the electron density from the NeQuick model with respect to the parameters NmF2 and hmF2, i.e.

$$N(\mathbf{x},t;\mathrm{NmF2},\mathrm{hmF2}) = N_o(\mathbf{x},t) + \left.\frac{\partial N(\,)}{\partial \mathrm{NmF2}}\right|_o \mathrm{dNmF2}(\mathbf{x},t) + \left.\frac{\partial N(\,)}{\partial \mathrm{hmF2}}\right|_o \mathrm{dhmF2}(\mathbf{x},t)$$

The terms of zeroth order, i.e. the values $N_o(\mathbf{x},t)$, are computed with the approximate values $\mathrm{NmF2}|_o$ and $\mathrm{hmF2}|_o$ derived from the NeQuick model. The partial derivatives

$$\frac{\partial N(\,)}{\partial \mathrm{NmF2}} \quad \text{and} \quad \frac{\partial N(\,)}{\partial \mathrm{hmF2}}$$

with respect to the unknown parameters NmF2 and hmF2 were calculated and kindly provided by P. Coisson from ICTP. The space- and time-dependent corrections dNmF2($\mathbf{x}$,t) and dhmF2($\mathbf{x}$,t) can be modelled either

- globally, e.g. by means of a *spherical harmonics approach*, or
- regionally, e.g. by means of a *wavelet approach*.

Since we are interested in regional modelling, we prefer the second approach, i.e. a wavelet expansion, which is already successfully applied in gravity field representations (project B2). However, in order to keep the numerical efforts within a limit we intend to replace the spherical wavelet approach by the so-called tensor wavelet approach, which is often used in digital image processing. To be more specific, one-dimensional scaling and wavelet functions were combined to construct the base functions of multi-dimensional detail spaces.

Parameter Estimation

In the parameter estimation step we have to solve not only for the wavelet coefficients but also for the inter-frequency differential delays of all the receivers and satellites. Since they cannot be estimated independently, the coefficient matrix of the linear model shows a rank deficiency. Hence, additional constraints will be introduced. Depending on the chosen wavelet approach an additional rank deficiency problem may occur. Bayesian statistics is one method to solve this regularization problem.

The main features of our proposed WMI can be summarized as follows: Our method yields

- up-to-date corrections to the monthly values of the electron density and the height of the F2 peak provided by an a priori model or a climatologic data base
- spatially and temporally varying vertical electron density profiles,
- any STEC value by integrating the model results along the desired ray-path,
- VTEC values not falsified by deficiencies of the mapping function used to transform STEC into VTEC.

The results of a high-resolution WMI will be of great importance e.g. for altimetry satellite missions like GFO or Cryosat, which are not equipped with dual-frequency altimetric sensors. First numerical results of WMI will be presented in the near future.

Long-Term Prediction of Earth Rotation Parameters by ANFIS

During the last year the work on the prediction of Earth rotation parameters (ERP), i.e. the length of day (LOD) and polar motion, by means of Adaptive Network based Fuzzy Inference Systems (ANFIS) has been extended from the short-term case reaching up to 40 days in the future to the long-term case reaching up to one year in the future. ANFIS are based on Fuzzy Logic and consist of a modelling part in terms of fuzzy inference system (fuzzification, rule base, defuzzification) and a training and validation part.

As data basis the ERP C04 time series of the International Earth Rotation and Reference Systems Service (IERS) with daily values were again used. The effects of the tides of the solid Earth and the oceans as well as seasonal variations of the atmosphere were reduced from the time series before the analysis. The residual series were used for both training and validation of the network. For optimization purposes different network architectures were studied and tested. In contrast to the results of the studies on short-term prediction the best recommendation for both LOD and polar motion was obtained as

$$\{x(t-4k), x(t-3k), x(t-2k), x(t-k)\} \rightarrow x(t)$$

This means that the predicted value for a time t is a weighted combination of the values of four previous days with the weights determined by the ANFIS. The index k indicates the number of days in future for which the value has to be predicted like, e.g., $k = 365$ for one year. Hence, the weighted average of the values of the previous four years is used for prediction.

Figure C2.2 shows the results of the one-year prediction of the y component of polar motion which fit rather well to the given time series except some deviations about 1997.5 and 2000 which could not be explained. Figure C2.3 shows the corresponding results for LOD. In addition, table C2.1 shows the results of a com-

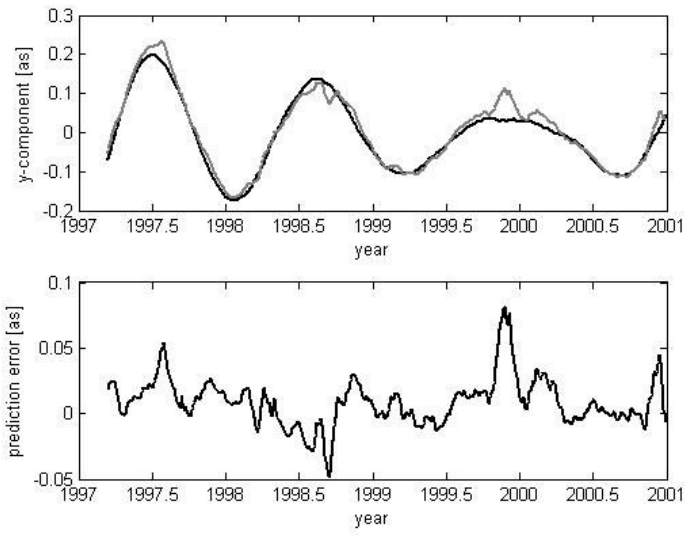

Fig. C2.2: (Top) One-year prediction results of the y component of polar motion (gray), the corresponding actual time series (black) and (bottom) the corresponding prediction errors.

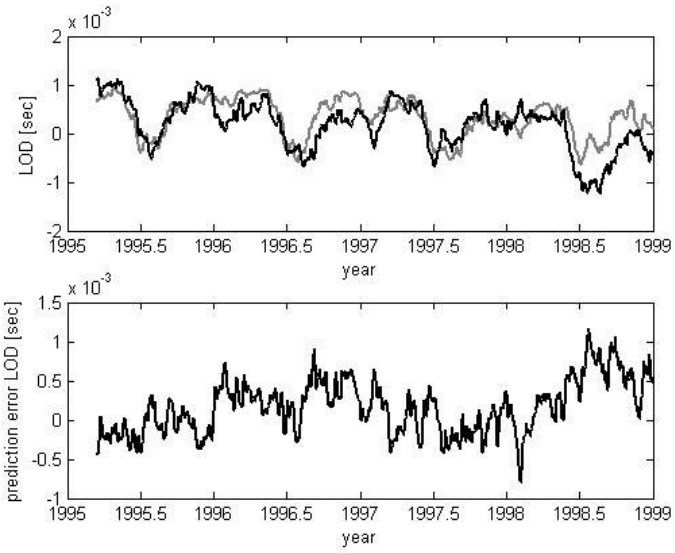

Fig. C2.3: (Top) One-year prediction results of LOD (gray), the corresponding time series (black) and (bottom) the corresponding prediction errors.

Tab. C2.1: Comparison of values predicted by ANFIS and comparison with the results from a prediction with an Artificial Neural Network (ANN)

	Polar Motion		LOD	
Prediction day	**ANFIS**	**ANN**	**ANFIS**	**ANN**
	RMS^{pm} [mas]	RMS^{pm} [mas]	RMS^{LOD} [ms]	RMS^{LOD} [ms]
1	0.24	0.29	0.017	0.019
2	0.55	0.57	0.045	0.049
3	0.84	0.95	0.067	0.074
4	1.25	1.30	0.088	0.097
5	1.64	1.79	0.115	0.121
10	3.17	3.25	0.188	0.193
15	4.75	4.70	0.251	0.246
20	6.37	6.28	0.259	0.251
25	8.02	7.78	0.267	0.249
30	9.12	8.89	0.275	0.245
35	10.28	10.14	0.281	0.263
40	11.32	10.96	0.290	0.258
180	20.98	23.67	0.296	0.361
270	22.75	24.51	0.313	0.386
360	23.92	25.09	0.303	0.347

parison of the prediction rms between ANFIS and an independent solution by Schuh et al. using Artificial Neural Networks (ANN). Obviously the quality of the prediction of the two techniques has an equal level.

As in the previous studies, the ANFIS model was rather easy to establish. The significant restriction for applications is due to the computer run-time which strongly depends on the complexity of the model. For this reason only four values in the past were used.

C3 Analysis of Time Series of Geophysical Processes

The work on the analysis of time series has been continued. In the following we first present some results of the Fourier analysis of station positions and datum parameters obtained from space geodetic solutions. In the second part we deal with the wavelet analysis of nutation series in order to investigate the Free Core Nutation.

Time series Fourier analysis of space geodetic solutions

With increasing accuracy of the space geodetic techniques time-variable effects of station positions and datum parameters (e.g. TRF origin) become detectable. We analysed time series for these parameters obtained from daily VLBI and weekly SLR, GPS and DORIS solutions with respect to various aspects, such as non-linear motions (e.g. seasonal signals) and systematic biases (see (project D1). Reasons for non-linear motions are manifold, e.g. loading effects, large earthquakes, mass redistibutions within the Earth's system. A major goal of the time series analysis is to study and reduce remaining discrepancies between different space techniques and solutions, what is essential for a reasonable geophysical interpretation of the results.

Time series of translation parameters

Satellite techniques such as SLR, GPS and VLBI are sensitive to the center of mass through the orbit dynamics and thus allow to estimate the origin of the terrestrial reference frame (TRF). Figure C3.1 shows the time series of weekly translation parameters obtained from similarity transformations of the weekly solutions w.r.t. ITRF2000. The results reflect common (global) variations of the technique-specific station networks w.r.t. ITRF2000 station positions and velocities. The results are sensitive to the network geometry and to changes w.r.t. the selected stations used for the transformations. SLR provides the most stable results for the translation parameters and reveals a significant annual signal with amplitudes of a few millimeters (table C3.1). The GPS and DORIS results are less stable compared to SLR, especially for the *z*-component. The large offset in the *z*-component of DORIS in 1998 was caused by SPOT-4 data problems. The seasonal signals obtained from SLR agree well with geophysical model results and with other studies (table C3.2). The amplitudes of the annual variations of the *z*-component obtained from the GPS degree-one approach are probably too large.

Tab. C3.1: Amplitudes of the annual signals obtained from the different solutions.

Source	Seasonal signal (amplitude)		
	x [mm]	*y* [mm]	*z* [mm]
SLR			
DGFI	3.1 ± 0.6	3.0 ± 0.6	4.5 ± 1.3
ASI	4.1 ± 1.2	4.5 ± 1.1	3.7 ± 2.3
GPS			
SIO	0.5 ± 0.9	5.2 ± 1.4	9.8 ± 9.2
JPL	3.5 ± 1.5	7.8 ± 1.7	19.1 ± 4.1
CODE	2.3 ± 1.1	3.6 ± 0.9	5.0 ± 2.6
DORIS			
IGN	5.9 ± 1.8	4.7 ± 1.4	1.1 ± 0.7

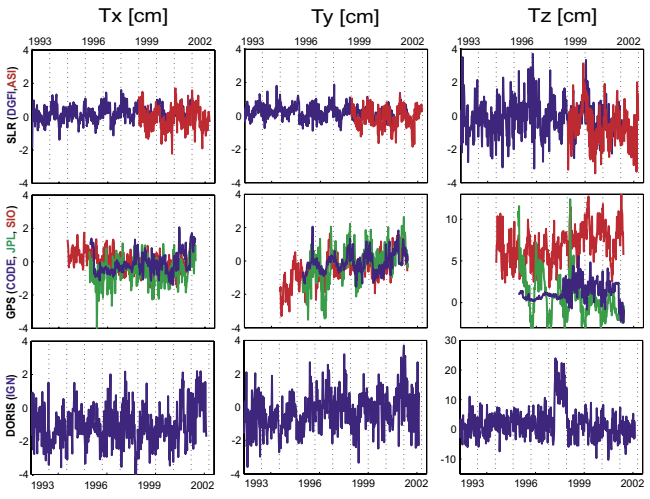

Fig. C3.1: Time series of weekly translation variations [cm].

Tab. C3.2 Seasonal signal of geocenter variations derived by models and GPS degree-one approach (from Dong, 2003).

source	*x*-component		*y*-component		*z*-component	
	A [mm]	Φ [deg]	A [mm]	Φ [deg]	A [mm]	Φ [deg]
geophysical model (Dong et al., 1997)	4.2	224	3.2	339	3.5	235
geophysical model (Chen et al., 1999)	2.4	244	2.0	270	4.1	228
GPS degree-one approach (Blewitt et al., 2001)	2.3 ± 0.3	184 ± 3	4.8 ± 0.3	285 ± 3	11.0 ± 0.2	214 ± 1
GPS degree-one approach (Dong et al., 2003)	2.1 ± 0.3	224 ± 7	3.3 ± 0.3	297 ± 6	7.1 ± 0.3	232 ±3

Time series of site positions

The position time series obtained from the space geodetic solutions reveal non-linear effects for a large number of sites. Many stations show seasonal variations caused among others by loading effects, e.g. increased winter loading of soil moisture, snow and atmospheric loading. Furthermore stations located in deformation zones may by affected be co-seismic displacements and post-seismic deformation processes caused by large earthquakes (see last year's annual report). As an example we present the time series for the GPS station Hafelekar (HFLK), Austria, located in the Alps (height 2334 m). Figure C3.2 shows annual signals in the north and height component, which are probably caused by heating of the rocks in summer.

Time series of nutation

Next, nutation estimates w.r.t. the IAU2000A model (figure C3.3), determined at DGFI with the VLBI software OCCAM6.0 were analysed by means of wavelet techniques in order to detect the Free Core Nutation (FCN) of the Earth. The FCN as a rotational mode is due to the fact that the mantle and the core of the Earth are rotating differently at the flattened core-mantle boundary.

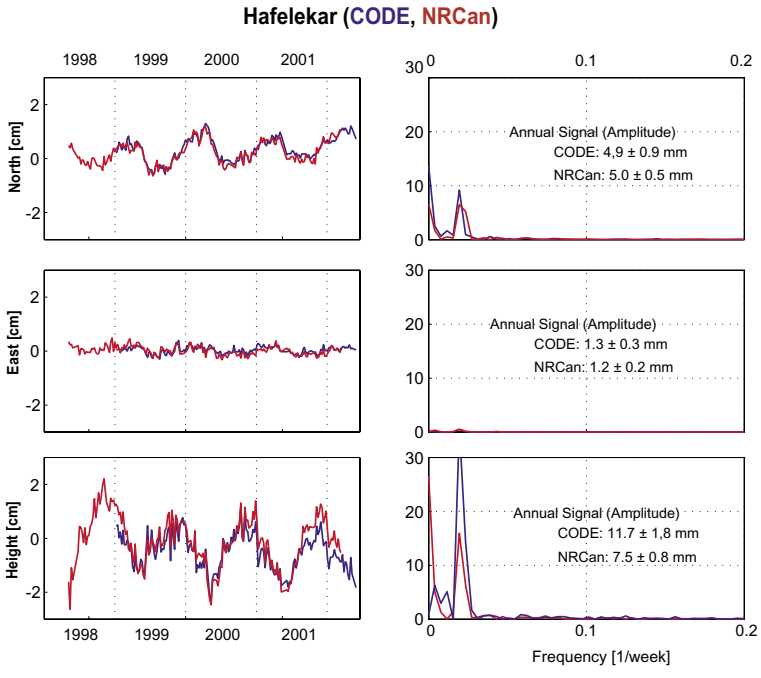

Fig. C3.2: Weekly position time series for GPS station Hafelekar (HFLK), Austria.

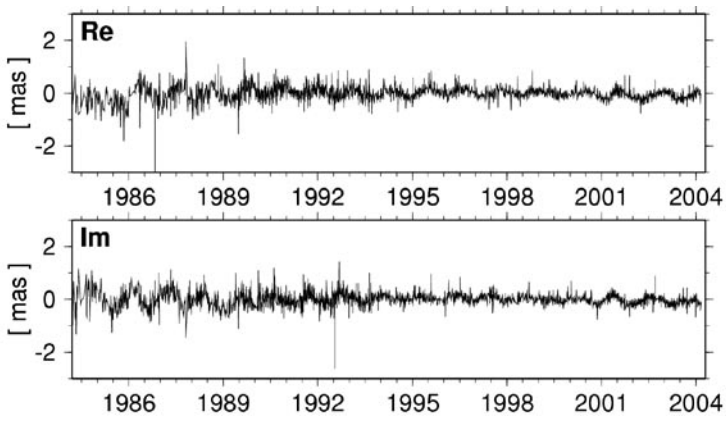

Fig. C3.3: Nutation estimates $d\varepsilon$ (Re) and $d\psi \sin \varepsilon_o$ (Im) w.r.t. the IAU2000A model, determined at DGFI with the VLBI software OCCAM 6.0.

Wavelet Analysis of nutation series

The figures C3.4 and C3.5 display the retrograde part of the corresponding wavelet scalogram, showing periods between 300 and 600 days. As wavelet function we used the Morlet function – already explained in detail in former annual reports of DGFI – with different values for the shape parameter σ (the higher this value is chosen the closer the Morlet wavelet transform approximates the Fourier transform). The scalogram shown in figure C3.4, determined with σ = 3, clearly shows an increase of the period (or phase) of the FCN from around 425 days to approximately 450 days. As can already be seen from the data series in figure C3.3, the maximum energy decreases with time. Both the variations of the period/phase and the amplitude are in good agreement with many other investigations based on different data sets determined with different VLBI softwares. However, this phenomenon does not completely coincide with theoretical predictions: while a variation of the amplitude of the FCN might be physically evoked by a variable excitation (e.g. by variable diurnal atmospheric fluctuations), its period must, from a theoretical point of view, be very stable at about 431.2 days.

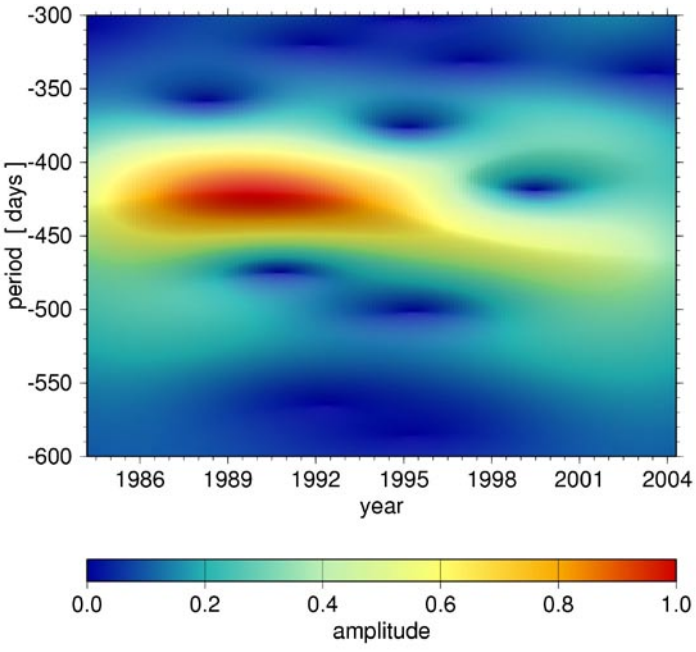

Fig. C3.4: Retrograde wavelet scalogram (normed) of the nutation series shown in figure C3.3, computed with shape parameter σ = 3. It shows an increase of the period (or phase) of the FCN from around 425 days to approximately 450 days, as well as a decrease of the maximum energy with time.

In order to study this phenomenon in more detail, we computed a more constrained wavelet transform of the nutation data set by setting the shape parameter σ to 10. As can be seen from figure C3.5 another explanation of the variation of the FCN arises: two close-by retrograde oscillations with periods of about 410 and 435 days might superpose each other. In principle, this agrees with the earlier DGFI hypothesis of a superposition of different oscillations, except that the periods of the these oscillations differ from the former investigations.

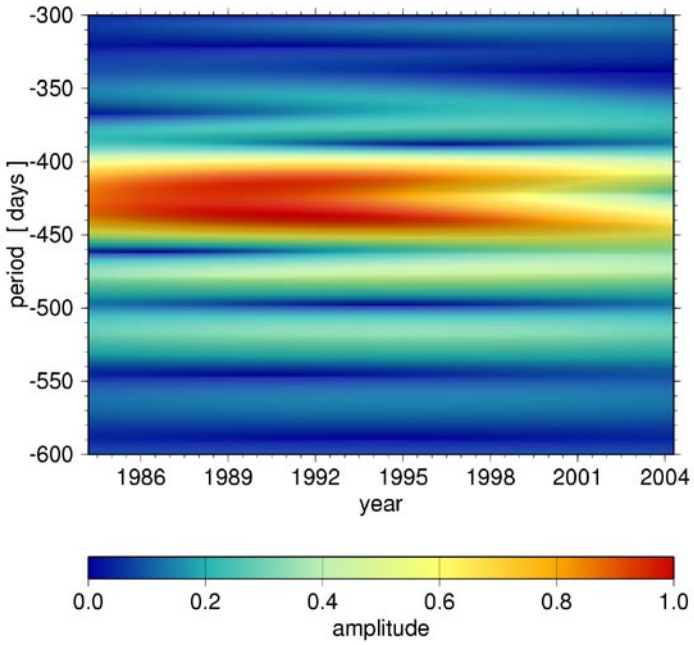

Fig. C3.5: Retrograde wavelet scalogram (normed) of the nutation series shown in figure C3.3, computed with shape parameter σ = 10. It suggests that the apparent variation of the FCN could also be evoked by two close-by retrograde oscillations with periods of about 410 and 435 days.

D International Services

DGFI contributes significantly to the international scientific cooperation by participating intensively in several scientific services of the International Association of Geodesy (IAG). By this means it provides its research results directly to the scientific community. On the other hand it gets direct access to the original data and results of other institutions and research groups for its own investigations. In the International Earth Rotation and Reference Systems Service (IERS) DGFI acts as a Combination Centre for the International Terrestrial Reference Frame (ITRF) and as a Combination Research Centre (CRC). In the International GPS Service (IGS) DGFI operates the Regional Network Associate Analysis Centre for South America (RNAAC-SIRGAS). For the International Laser Ranging Service (ILRS) DGFI holds one of the two global data centres, the EUROLAS Data Centre (EDC), and works as an Associate Analysis Centre (AAC). DGFI is an Analysis Centre of the International VLBI Service for Geodesy and Astrometry (IVS). Furthermore, DGFI investigates the possibilities and requirements for the establishment of an International Altimeter Service (IAS) and participates in the installation of IAG´s Global Geodetic Observing System (GGOS). In the frame of international cooperation, DGFI operates several permanent GPS stations for the realization of reference frames and monitoring crustal deformations, in particular at tide gauges.

D1 ITRS Combination Centre / IERS Combination Research Centre

DGFI serves as an ITRS Combination Centre and as an IERS Combination Research Centre (CRC) within the International Earth Rotation and Reference Systems Service (IERS). Within the Research Group on Satellite Geodesy (Forschungsgruppe Satellitengeodäsie, FGS), DGFI, FESG (Forschungseinrichtung Satellitengeodäsie, TU München) and GIUB (Geodätisches Institut, Universität Bonn) established a joint CRC. A major part of the work is funded by the programme GEOTECHNOLOGIEN of BMBF and DFG, Grant 03F0336C.

TRF realization 2003

Input are multi-year solutions with station positions and velocities of the different space geodetic techniques (VLBI, SLR, GPS and DORIS). The TRF computations were finished at the end of the year 2003. The input data, the combination methodology and first results were presented in the Annual Report 2002/2003. During the period 2003/2004 the work concentrated on a detailed analysis and validation of the TRF results.

TRF validation and accuracy assessment

The TRF computations provide valuable results to assess the current accuracy of the terrestrial reference frame. The combined intra-technique solutions were used to evaluate the TRF accuracy by comparing the space geodetic solutions with local ties and the velocity estimations of co-located instruments. Since GPS is the dominant technique regarding the number and spatial distribution of co-locations with the other techniques, the GPS solution was considered as a reference for this specific TRF accuracy evaluation. By co-locations and local ties selected within the inter-technique combination, the DORIS, SLR and VLBI solutions were referred to the GPS reference frame. This was done by adding the local tie components to the DORIS, SLR and VLBI station coordinates. Then, a 14-parameter Helmert transformation was applied between the GPS solution and the “transformed” solutions of the other techniques. A great advantage of this approach is that the transformation results do not depend on a specific TRF datum (e.g. ITRF2000), as the comparisons are performed in an (arbitrary) GPS reference frame. The transformation results between

GPS and the other techniques are summarized in table D1.1. In the case of VLBI and SLR, the discrepancies are in the order of a few millimetres for the transformation parameters, and the rms residuals of station positions and velocities of the co-located instruments are 5 mm and 1 mm/yr respectively. Larger discrepancies exist for co-locations between GPS and DORIS. The current accuracy is not satisfying for many co-location sites. Remaining biases between the contributing space geodetic solutions are a major error source.

Tab. D1.1: Helmert transformation results of the "transformed" DORIS, SLR and VLBI networks w.r.t. the GPS network. Shown are the translation, rotation, and scale parameters, as well as the rms values of station positions and velocities

H.-T. Results	DORIS	SLR	VLBI
Tx [mm]	-5.2 ± -9.6	2.7 ± 1.4	-0.4 ± 1.7
Ty [mm]	-0.6 ± 6.1	0.0 ± 1.3	-2.8 ±1.7
Tz [mm]	2.9 ± 6.4	-2.2 ± 1.3	3.1 ± 1.7
Rx [mm]	3.2 ± 6.3	-3.3 ± 1.6	-4.6 ± 2.2
Ry [mm]	-7.7± 9.8	-1.2 ± 1.6	1.8 ± 2.2
Rz [mm]	-9.9 ± 12.3	-2.2 ± 1.6	1.8 ± 2.2
Scale [mm]	-8.5 ± 5.3	1.9 ± 1.2	-4.7 ± 1.6
Pos RMS [mm]	12.1	4.1	5.4
Vel RMS [mm/yr]	1.60	0.87	0.92

Comparison with ITRF2000

The comparison of the TRF realization 2003 with ITRF2000 provides a first "quasi-independent" quality assessment and validation of the ITRS products. Figure D1.1 shows the station velocities of the DGFI solution compared to ITRF2000. The combined DGFI solution contains less sites than ITRF2000, since a number of stations with short observation time spans (e.g. less than one year), do not allow accurate and reliable velocity estimations. Enlargements for Europe and North America reveal significant differences for some stations. Figure D1.2 represents the rms residuals between both TRF realizations for station positions and velocities. The agreement for VLBI and GPS station positions is better than for the other techniques. The discrepancies are largest for DORIS. Figure D1.3 shows histograms for the distribution of station position and velocity differences between both TRF for the 369 common VLBI, SLR, GPS and DORIS stations in north, east, and height component. For about 60% of the stations the position and velocity differences are below 1 cm and 2.5 mm/yr, respectively. But on the other hand, there are too many stations (10%) with position and velocity differences larger than 5 cm and 10 mm/yr, which is not tolerable for a precise reference frame.

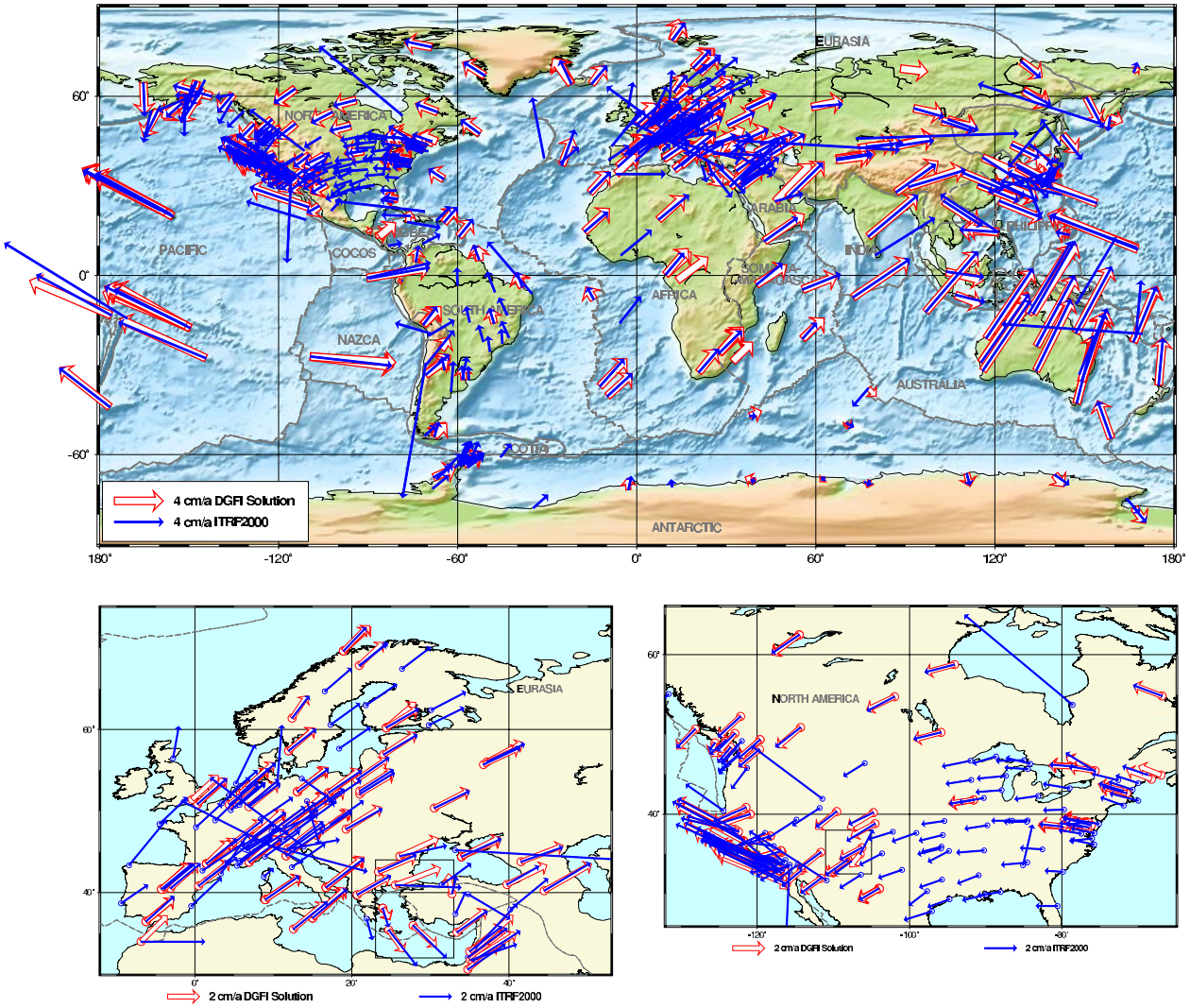

Fig. D1.1: Station velocities of the combined DGFI solution compared to ITRF2000. Enlargements are shown for Europe and North America.

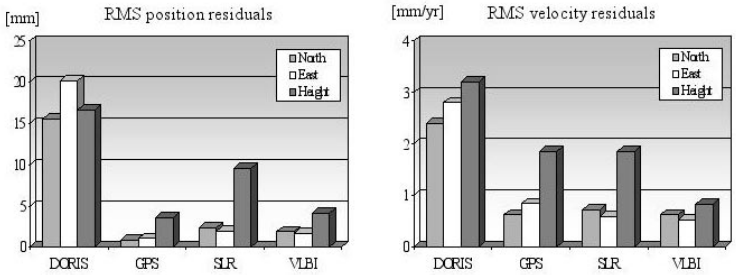

Fig. D1.2: Rms station position and velocity residuals in north, east, and up component obtained from a 14-parameter Helmert transformation between the combined DGFI solution and ITRF2000.

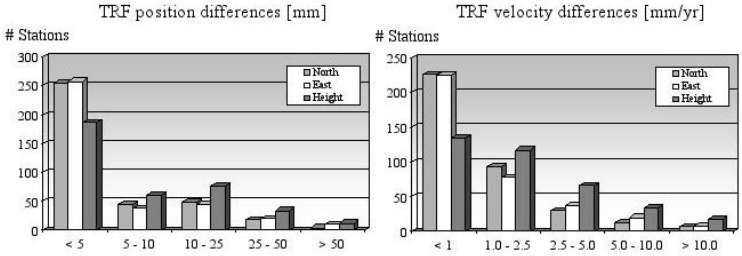

Fig. D1.3: Histograms representing the differences between the combined DGFI solution and ITRF2000 in station positions (left) and velocities (right) for the 369 common stations (75 VLBI, 69 SLR, 172 GPS and 53 DORIS).

TRF realization based on epoch normal equations

The high accuracy of the space geodetic observations is not reflected by current TRF realizations of the terrestrial reference system. Remaining systematic effects between techniques must be reduced and non-linear effects in site positions must be considered in future TRF realizations. A first TRF realization was computed on the basis of epoch (e.g. weekly/daily) normal equations using five years (1999-2004) of VLBI, SLR, GPS and DORIS data. This new approach has major advantages compared to past TRF realizations based on multi-year solutions with station positions and constant velocities. The position time series show non-linear motions and discontinuities for a large number of sites. Reasons can be manifold, such as seasonal signals caused by loading effects, effects of seismic deformation processes caused by earthquakes, equipment changes, changes of software, models and processing strategies. First results of this new approach are promising (figure D1.4).

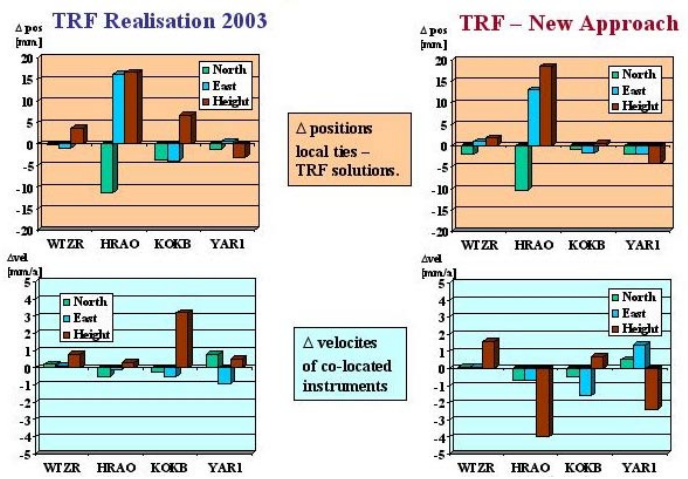

Fig. D1.4: Comparison of positions and velocities at co-location sites. New approach (right) vers. TRF realization 2003 (left).

IERS Combination Research Centre

The DGFI activities as IERS Combination Research Centre (CRC) are closely related to most of the projects in part A. The modelling of the different space geodetic observations (A1:GNSS, A2: SLR, A3:VLBI) contributes to the development of rigorous combination methods for the computation of future IERS products. Theoretical research related to the combination of space geodetic data, the development of refined combination methods, and the software enhancement are tasks of A4, which are the basis of the research activities of the CRC. The CRC work can be divided into four major topics:

- investigations related to TRF relevant issues,
- quasi-rigorous combination of VLBI, GPS (and SLR) using CONT02 data,
- activities within the IERS Combination Pilot Project.

TRF related investigations

The ITRS Combination Centre activities of DGFI included various investigations related to TRF relevant issues, such as:

- TRF datum: Solutions and normal equations of the different space techniques were analysed to study the covariance information of the datum parameters, such as the origin and scale (see A4, figure A4.1). In addition, the time series of the

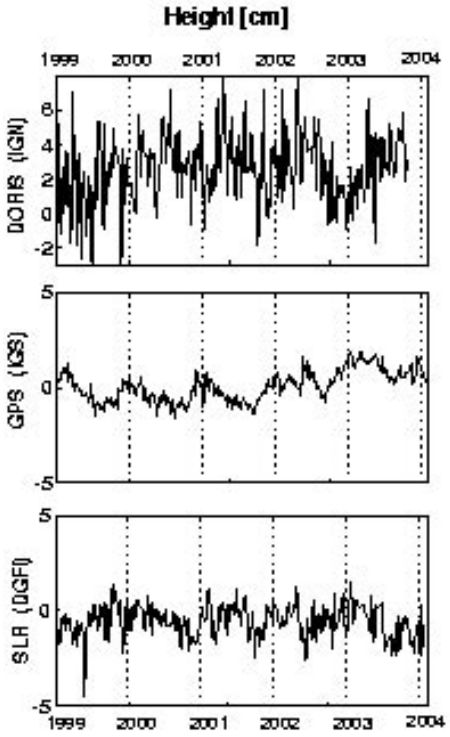

Fig. D.1.5: Station height variations for co-location site Yarragadee, Australia.

datum parameters contribute to identify strengths and weaknesses of the space techniques. The results of project A6 are essential to realise the kinematic datum for the TRF computations.

- Analysis of time series (see also C3): The time series of station positions and datum parameters, obtained from VLBI, SLR, GPS and DORIS solutions, were analysed w.r.t. non-linear signals (e.g. seasonal variations and jumps) and were compared at co-location sites to investigate remaining biases between the techniques. As an example, figure D1.5 shows the height variations for Yarragadee, Australia, obtained from weekly DORIS, GPS and SLR solutions. The inconsistencies between the techniques need further investigation.
- Combination methodology: Various issues were studied, such as the weighting for the intra- and inter-technique combination (e.g. variance component estimation, see A4), the modelling and parametrization of non-linear site motions, the implementation of local tie information, the handling of remaining biases between the techniques, the rigorous combination of site positions, Earth orientation parameters, and quasar coordinates (see A3).

CONT02 combination

This joint combination project, based on CONT02 VLBI data of eight telescopes for a 15-day period in October 2002, was initiated by DGFI and Forschungseinrichtung Satellitengeodäsie (FESG) at the beginning of 2003. First results were presented in the Annual Report 2002/2003. The activities were continued, aiming at a rigorous combination of the VLBI data with global GPS (SLR) data of the same time span, taking much care to use identical models and the same parametrization. All common parameters (e.g. station coordinates, EOPs, tropospheric zenith delays and gradients) were studied within this rigorous combination.

In a first step, station coordinates were combined using local tie information. The time series show for most of the co-location stations a smoothing effect, especially for the height component. In the next step, sub-daily EOP were analysed and combined. The results prove, that both techniques benefit from a combination. The rms values of the combined pole coordinates and UT1–UTC values are smaller than those of the single technique solutions. Further work focusses on the combination of tropospheric zenith delays (ZPD). A comparison of the estimates of the VLBI and GPS solutions show a very good agreement for their time dependent behaviour. Figure D1.6 shows the results for the station Hartebeesthoek, South Africa. The offsets between both techniques, caused by the height difference of the VLBI and GPS reference points, have to be modelled and considered in the combination. Table D1.2 presents the remaining discrepancies between the theoretical and the estimated ZPD differences. The largest differences are observed for GPS stations with radome. However, using the theoretical ZPD differences as “tropospheric ties” instead of the height components of the local ties, the repeatabilities of the station coordinates are in the same order of magnitude.

Tab. D1.2: Zenith path delay offsets between VLBI and GPS, compared to the theoretical values derived from the Saastamoinen troposphere model.

Station	GPS ZD [mm]	VLBI ZD [mm]	ΔZD [mm]	Saasta [mm]	ΔZD-Saasta [mm]	ΔH [m]	Radome
Ny Alesund	34.65	37.40	-2.75	1.1	-3.85	3.1	SNOW
Onsala	54.66	55.33	-0.67	4.3	-4.97	13.71	OSOD
Wettzell	97.91	98.97	-1.06	0.8	-1.86	3.1	-
Hartebeesthoek	142.96	144.97	-1.42	0.3	-1.72	1.54	Unkn
Algonquin	59.81	53.85	5.96	6.2	-0.42	23.11	-
Fairbanks	39.58	40.31	-0.73	3.5	-4.23	13.08	JPLA
Kokee Park	143.84	138.33	5.51	2.3	3.21	9.24	-
Westford	73.67	72.05	1.62	0.5	1.12	1.75	-

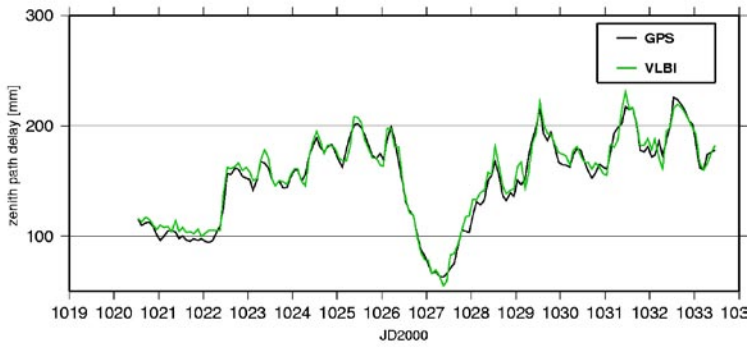

Fig. D1.6: Time series of tropospheric zenith delay corrections derived from GPS and VLBI data for station Hartebeesthoek, South Africa.

This proves the high stability of the two-hour tropospheric parameters derived from both techniques.

In addition to the microwave techniques, SLR normal equations were included in the CONT02 combination studies as well, but only with a daily resolution for the ERP. SLR delivers valuable information to realize the scale and origin of the combined network and contributes to a more stable realization of the reference system due to more co-located stations.

IERS Combination Pilot Project

The IERS Combination Pilot Project was initiated by the IERS Analysis Coordinator and the IERS Working Group on Combination in the beginning of 2004. This project aims at more consistent, routinely generated IERS products. “Weekly” SINEX solutions, which are available from the various technique services and contain station coordinates, EOPs, and, possibly, quasar coordinates, shall be rigorously and routinely combined into consistent weekly IERS products (SINEX files).

Within this project, DGFI provides individual SLR and VLBI solutions and combined SLR solutions for the intra-technique combination (step 1) and has been accepted by the IERS as a combination centre for the inter-technique combination (step 2). The presently available SINEX files were analysed regarding various issues, such as format and suitability for a rigorous combination. A suitable strategy for the weekly inter-technique combination, including input data check, and validation of results is under development. The procedure requires an updating of combination software and analysis tools, especially for the EOP combination.

D2 IGS Regional Network Associate Analysis Center

The DGFI has been acting as an IGS Regional Network Associate Analysis Centre for South America (IGS RNAAC SIR) since the start of the regional densification of the IERS Terrestrial Reference Frame (ITRF) initiated by the International GPS Service (IGS) in June 1996. Every week, a coordinate solution including all available data of this network is generated and delivered to the IGS global data centers.

RNAAC SIR network

The number of processed global and regional GPS stations in this region has again increased. The RNAAC network consists of 84 GPS stations (31 of them are regional) by the end of September 2004 (figure D2.1), including stations which deliver their data not always in time for the processing (AUTF, BHMA, COYQ, TGCV, VALP) or have finished operation (BARB, ESTI, INEG, MOIN, RCM5/6, RIOP, SLOR, SSIA, TEGU/TEG1). The stations Cartagena (CART) and Galapagos (GLPS) are online again, and Puerto Deseado (PDES) is still under construction.

New position and velocity solution

A new accumulated solution DGFI04P01 has been computed including the permanent GPS network of South America and a number of addional sites in the Antarctic, the Atlantic Ocean, the Pacific Ocean, the Caribbean Sea, and Central America. It covers the time period from July 1996 to July 2004 and provides position and linear velocity estimates of 64 stations which are included in at least 52 weekly solutions. The combined solution is based on the weekly SINEX files generated by DGFI as the IGS RNAAC SIR. IGS combined orbits and Earth orientation parameters were held fixed (IGSWWWWD.SP3 and IGSWWWW7.ERP). The solution is referred to IGb00 (IGS03P33_RS99.snx) by constraining positions and velocities of ASC1, CRO1, EISL, FORT, KOUR, LPGS, OHIG/OHI2, RIOG, and SANT. The reference epoch is 2003.0.

Figure D2.1 and D2.2 show the horizontal and vertical velocities. For sites with less than one year of observations only position coordinates are available. The big discrepancies between ITRF2000 and DGFI04P01 (e.g. in the vertical velocities at INEG, IMPZ, RIOP and VBCA) are due to the very short observation period of these stations in the ITRF2000 solution.

Weekly position solutions

In addition to the permanent service of the IGS RNAAC SIR the DGFI is now providing weekly position solutions in order to support all South and Central American countries in their national GPS surveys. The reference epoch of these weekly solutions is the middle of the corresponding week. They are available on the DGFI ftp server at pub/gps/DGF.

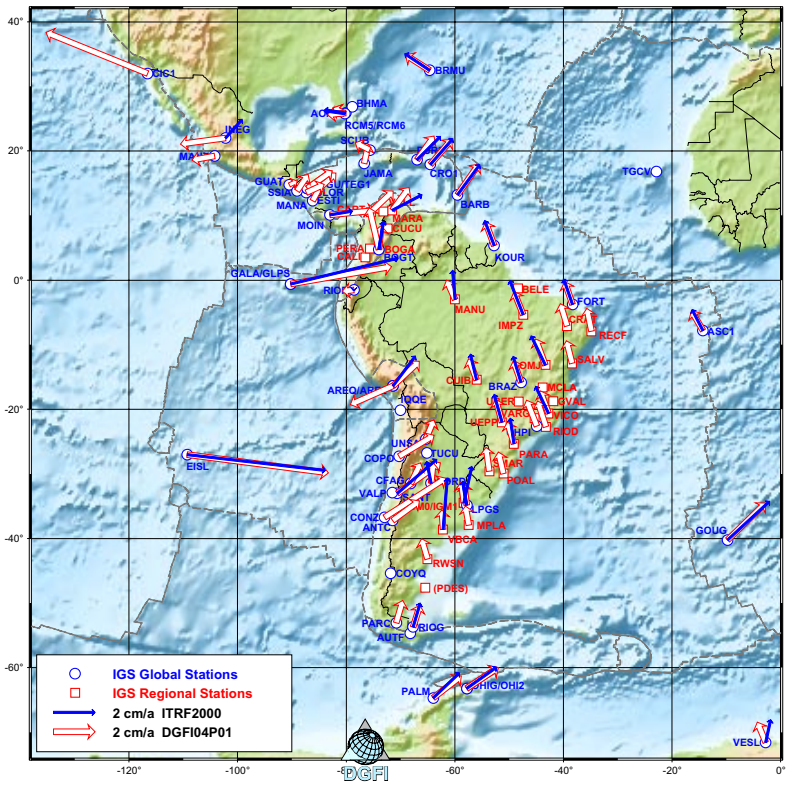

Fig. D2.1: IGS RNAAC SIR network and horizontal velocities from solution DGFI04P01.

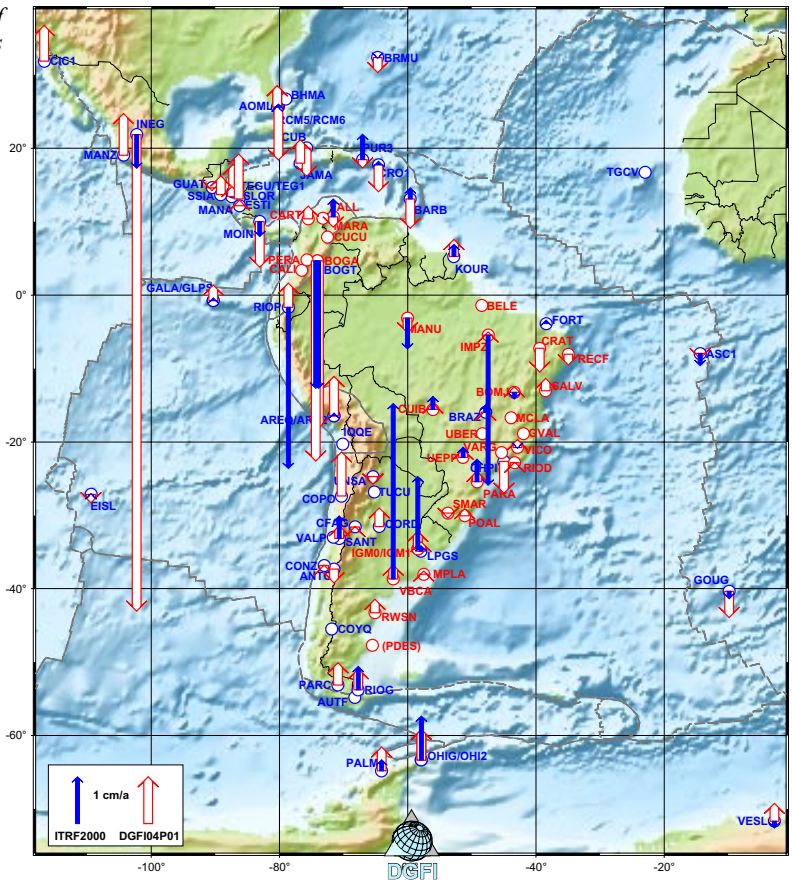

Fig. D2.2: Vertical velocities of IGS RNAAC SIR stations from solution DGFI04P01.

D3 Permanent GPS Stations

At present DGFI operates seven permanent GPS stations in co-operation with national institutions:

Argentina:	Mar del Plata (MPLA), Bahia Blanca (VBCA), Rawson (RWSN)
Colombia:	Cartagena (CART), Bogotá (BOGA)
Venezuela:	Maracaibo (MARA)
Faroe Islands:	Torshavn (TORS)

With the exception of BOGA and MARA, all stations serve for monitoring sea level changes. The station CART, which failed at the end of March 2003, resumed operational service by the end of July 2004.

Within the framework of the INTERREG III B Programme „Alpine Space“ of the European Commission, reconnaissance work for the installation of permanent GPS stations within the project GPSQUAKENET was done. The main criterion is a stable geological situation. So far, Oberjettenberg, Herzogstand and Hochgrat were identified as suitable (figure D3.1). Additionally, different types of receivers and the data transfer capabilities were tested.

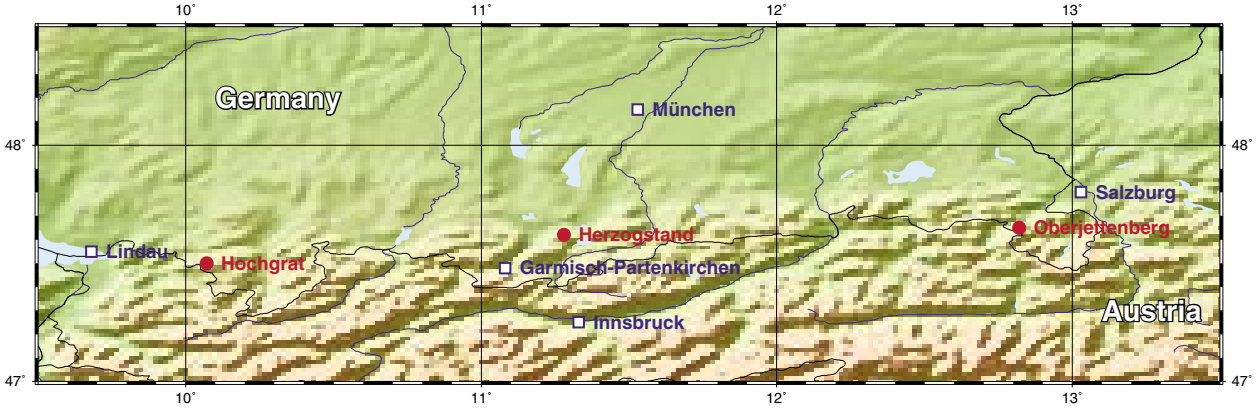

Fig. D3.1: Selected locations of the first three Alpine permanent GPS stations

TIde GAuge benchmark monitoring project (TIGA)

The observations from the stations in South America are integrated in the regional network of the IGS which is processed at DGFI (see D2). The measurements of permanent stations at tide gauges are processed in the framework of the IGS TIde GAuge benchmark monitoring project (TIGA).

DGFI processes a permanent GPS network covering the entire North and South Atlantic oceans. The network and the processing strategy were designed in 2002/2003 and described in the last annual report. To improve the network geometry, eleven additional stations were recently included (see figure D3.2).

After updating of the Bernese GPS software from version 4.2 to 5.0, the processing was changed to the new version. Weekly solutions generated with the old version were reprocessed. To estimate reliable velocities for all stations as soon as possible, it was decided to process one week of data per month backwards and every week forwards starting in January 2004. Until now 68

weeks covering 4 years are processed. Figure D3.3 gives an overview of the actual state of processing and the data availability of some stations.

Fig. D3.2: GPS network processed at DGFI in the frame of the TIGA project (red: DGFI permanent stations, green: newly added stations)

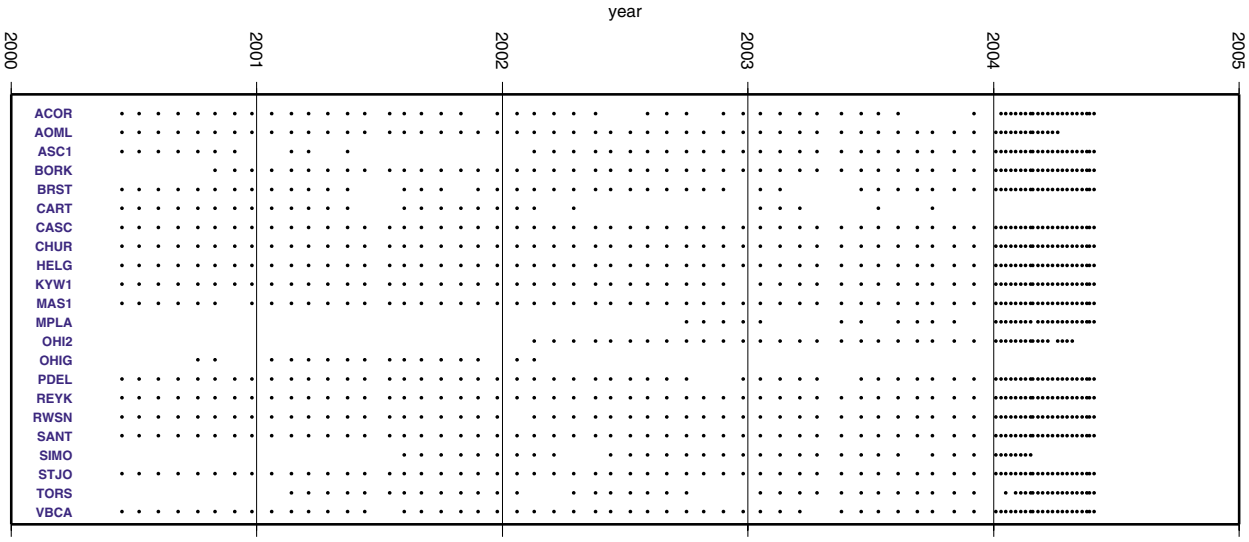

Fig. D3.3: Availability of GPS stations at tide gauges for the processed weeks

Consistency checks are performed comparing the daily and the weekly combined solutions. In a first run, an accumulated solution including all daily solutions is performed, setting up velocities for all stations. Stations so far supplying only very short time series are excluded from the combination. But transforming the daily solutions to the cumulative one, time series of coordinates are generated. Exemplarily, the time series for Rawson (RWSN) and Helgoland (HELG) are shown in figure D3.4. The corresponding rms values for all combined stations are given in table D3.1. The time series are analysed in order to detect jumps or systematic effects, which have to be modelled in the combination.

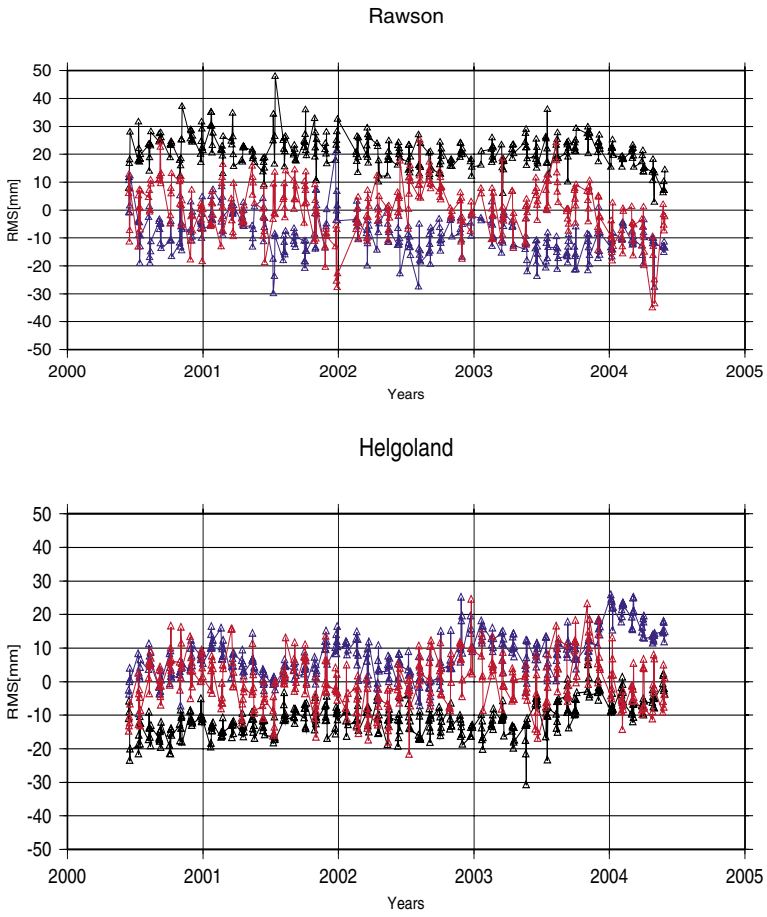

Fig. D3.4: Station position time series for Rawson and Helgoland (north=black, east=blue, up=red)

Tab. D3.1: Repeatabilities for selected GPS stations at tide gauges

Station		Daily repeatabilities [mm]		
		North	East	Up
BORK	**Borkum**	4.2	5.6	8.8
BRST	**Brest**	4.5	6.5	7.7
CASC	**Cascais**	4.8	6.7	8.0
CHUR	**Churchill**	7.1	8.8	10.7
HELG	**Helgoland**	5.0	6.6	7.8
KYW1	**Key West**	6.4	6.8	11.3
RWSN	**Rawson**	5.7	7.0	9.4
TORS	**Torshavn**	5.4	4.9	6.9
VBCA	**Bahia Blanca**	5.4	6.3	9.2

D4 ILRS Associate Analysis Centre

The work within this project concentrates on the processing and combination of satellite laser ranging data of the global SLR tracking network. During the ILRS Analysis Working Group (AWG) Meeting on April 22-23, 2004, in Nice, France, five groups have been nominated as official ILRS Analysis Centres: ASI (Agencia Spatiale Italiano), GFZ (GeoForschungsZentrum Potsdam), JCET (Joint Center for Earth Systems Technology, USA), NSGF (Natural Environment Research Council, *NERC*, Space Geodesy Facility, UK) and DGFI. During the ILRS-AWG Meeting in San Fernando, Spain on June 5, 2004, DGFI was nominated as official backup ILRS Combination Centre, ASI was nominated as offical primary ILRS Combination Centre. The activities can be devided in three major topics:

- Operational processing of SLR data to Lageos-1/2 and generation of weekly SINEX files with station positions and Earth orientation parameters (ILRS Analysis Centre);
- Operational combination of the individual SLR solutions (ILRS Combination Centre);
- Reprocessing of SLR data for various scientific investigations;
- Computation of an SLR multi-year solution.

ILRS Analysis Centre

The ILRS Analysis Centres are processing on an operational weekly basis SLR data to Lageos-1/2 and Etalon-1/2, and provide weekly loosely constrained solutions (SINEX files) with station positions and Earth orientation parameters (x-pole, y-pole and length of day). The processing at DGFI is performed with the DGFI software DOGS-OC. During the processing quality checks are performed, one is the computation of pass-wise range and time biases (see A2). The results for the biases are available at the DGFI homepage, http://ilrsac.dgfi.badw.de. Figure D4.1 shows the mean differences of the weekly station positions from the individual solutions and the ASI combined solution for 2004. The spherical (3-dimensional) station position differences are in the order of 1 cm for most of the weekly solutions, only the NSGF solutions differ by about 2 cm from the combined ASI solution. For some weeks the NSGF solutions show bigger discrepancies (3-4 cm), which seems to affect also the combined solutions. Therefore it should be considered to develop outlier criteria for the combination to ensure that the combined ILRS solution is better and more reliable than any of the individual contributions.

ILRS Combination Centre

DGFI serves as official ILRS Backup Combination Centre since June, 2004. It uses the same procedures and constraints as the ILRS Primary Combination Centre, which has been taken over by ASI, Italy. Both centres are obliged to weekly compute a combined SLR solution as official product of the ILRS. The products are stored at the data centres of CDDISA and EDC. Both combination centres use software versions for automated processing. The software development and combination procedure of DGFI is described in project A4.

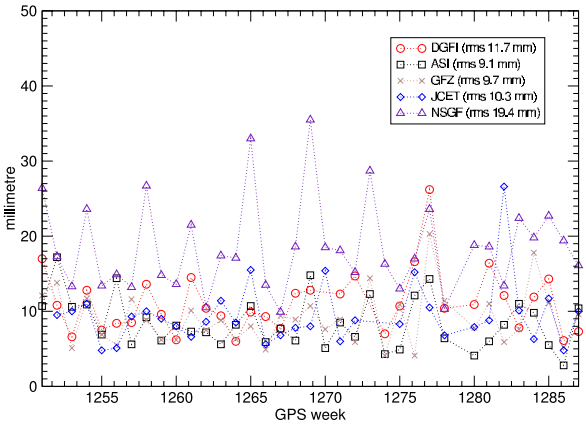

Fig. D4.1: Weekly r.m.s. differences of station coordinates for all contributing solutions w.r.t. the official combined ILRS station coordinates.

The official weekly products are:

- Combined solution for station coordinates and EOP. DGFI delivers a SINEX file with a minimal constraints solution and with an unconstrained normal equation system, ASI computes a loosely constrained solution.
- Combined solution for EOP aligned to ITRF2000. DGFI takes the EOP part of the above combined solution argueing that the minimum constraints solution is indirectly an alignment to ITRF2000, because the a priori coordinate values are taken from ITRF2000 . ASI aligns the above loose constraints solution to ITRF2000 by Helmert transformation and computes new EOP on the basis of the Helmert transformed coordinates. (see figures D4.2 and D4.3).

Reprocessing of SLR data

DGFI has started to reprocess all SLR tracking data from January 1981 to 2004 to LAGEOS-1 and from October 1992 to 2004 to LAGEOS-2 with the latest version of the DOGS software and consistent modelling. The amount of data is more or less constant since 1984 with some fluctuations. Figure D4.4 shows the number of normal points for both LAGEOS satellites for weekly arcs, as well as the number of edited observations. Intensive tracking campaigns can be anticipated as small peeks in the fig-

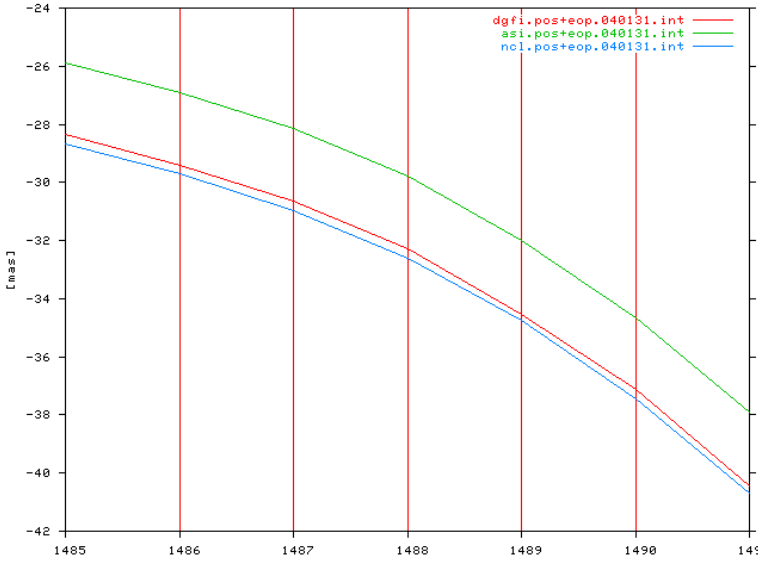

Fig. D4.2: EOP of ASI (green) and DGFI (red) for week January, 25 – 31. The values are taken from the combined solution for station coordinates and EOP

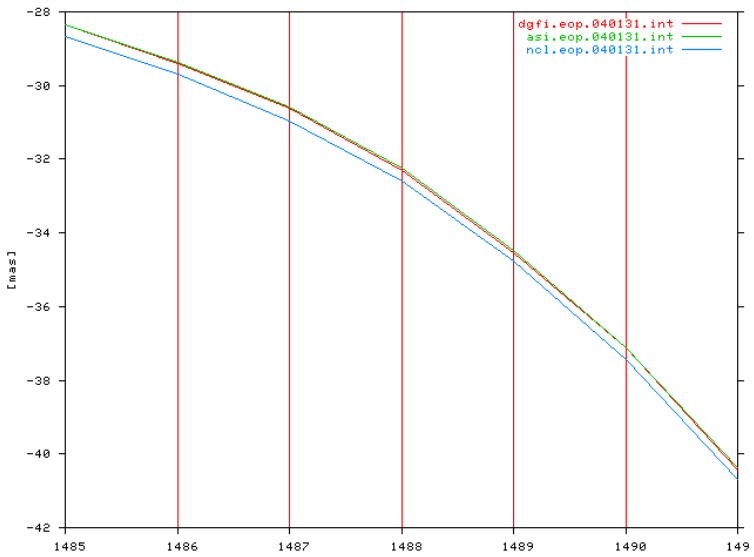

Fig. D4.3: EOP of ASI (green) and DGFI (red) for week January, 25 – 31.The values are taken from the combined solution for EOP only

ure. Figure D4.5 indicates that during the first years (1981-1984) the tracking precision improved rapidly. Until 1993 the accuracy level was about 2-3 cm. Since the launch of LAGEOS-2 the 1 cm level was nearly reached, but for some weeks the accuracy was degraded depending on the stations tracking. At that time not the whole SLR network was on the highest tracking performance. Since 2000 all stations have reached a high tracking performance, so the weekly r.m.s. is below 1 cm for both satellites. In 2004 some new tracking stations provide SLR data with not yet fully operational tracking systems.

SLR multi-year solution

A major goal of the reprocessing is to compute a consistent multi-year SLR solution, which can serve as reference for various activities, e.g. bias estimation for the tracking stations, the operational weekly computations and combinations of SLR solutions, the weekly inter-technique combination in the framework of the IERS Combination Pilot Project, and for the computation of a refined terrestrial reference frame (see D1). It has to be considered that the ITRF2000 does not include the newer SLR tracking stations, and furthermore for some stations the ITRF2000 position and ve-

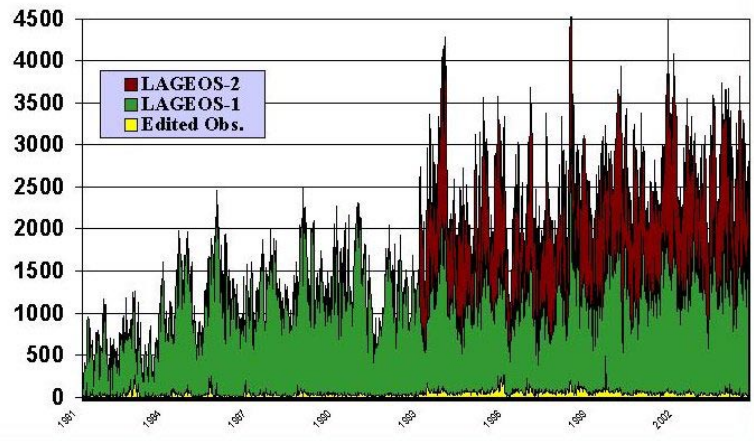

Fig. D4.4: Number of LAGEOS-1 and -2 normal points and edited observations for weekly arcs.

Fig. D4.5: Weekly r.m.s. orbital fit [cm].

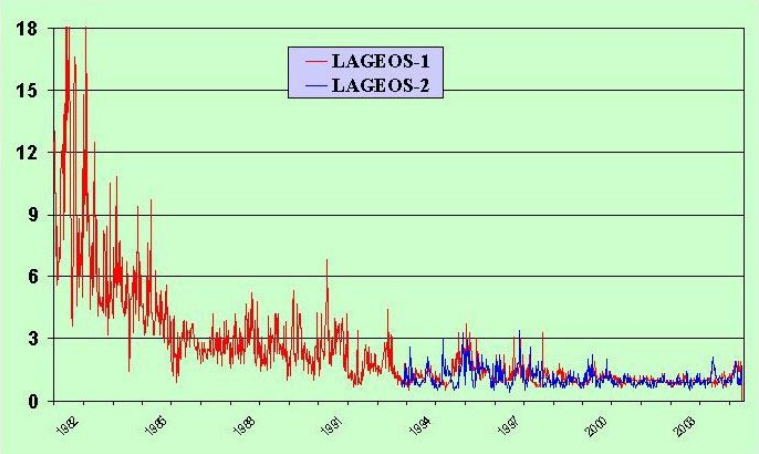

locity estimations are unreliable. The computations are an iterative procedure based on weekly single satellite arcs starting with ITRF2000 station coordinates (for the newer SLR tracking we used the results of DGFI solutions) and IERS EOPC04 earth orientation parameters. In a first step we checked for outliers and pass biases on arc basis. In the second step we analysed the weekly arcs looking for discontinuities in the time series of the weekly station positions, which can be caused by earthquakes, instrumental or unknown station problems.The edited arcs were used to compute a series of J2 values (see A2), and to generate weekly unconstrained normal equations for both satellites. As a first result we accumulated 5.5 years to generate a SLR solution (1999-2004), which was also used for a refined TRF computation at DGFI (see D1). Figure D4.6 shows this new SLR solution compared to ITRF2000 for Europe and parts of Asia. By the end of this year a new 24 years solution of SLR tracking stations will be available.

Fig. D4.6: Station velocities of 5-years SLR solution (blue) compared to ITRF2000 (red).

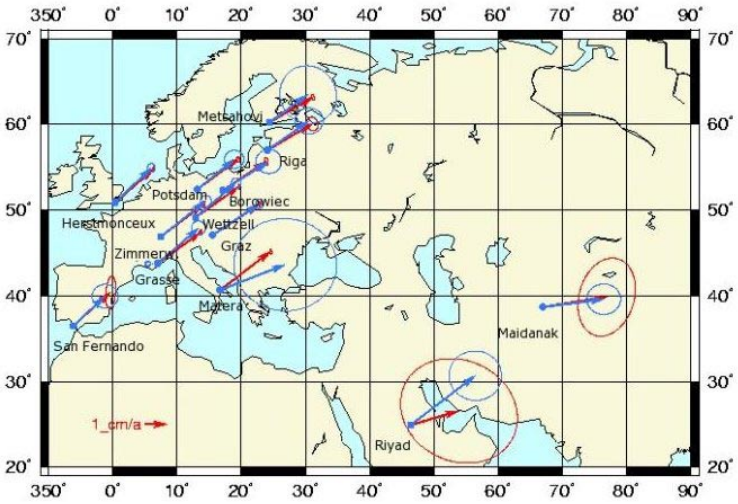

D5 ILRS Global Data Centre / EUROLAS Data Centre

Since November 1998, the beginning of the International Laser Ranging Service (ILRS), DGFI runs the ILRS Global Data Centre in addition to the EUROLAS Data Centre (EDC). The second ILRS Global Data Centre is at CDDIS/NASA. Changes and new activities are highlighted in this report.

ILRS

Since the implementation of the SLRmail and SLReport exploders at EDC in November 1995 1259 SLRmails (an increase of 125) and 4379 SLReports (an increase of 1205) were received and distributed to interested users. On August 15, 2003 EDC installed the URGENT Mail exploder (transition from HTSI to EDC), and 30 URGENT Mails are circulated to a permanently updated distribution list. The SLRmail and SLReport distributions lists are also updated on request.

The ILRS Analysis Centres send now regularly their ILRS products (positions, earth rotation parameters (EOPs) and summary files) to the Global Data Centres. These products are available at the EDC ftp server. As a back-up and to be sure that all products are available at EDC a mirror of the CDDIS/NASA data base for these ILRS products was installed. Corresponding to an agreement of the ILRS Data Formats and Procedures Working Group the access to the data is the same at both ILRS Global Data Centres. This applies also to the product full-rate data. First steps for equalizing the whole structure at EDC and CDDIS are done. The current SLR network with its three sub-networks is shown in figure D5.1.

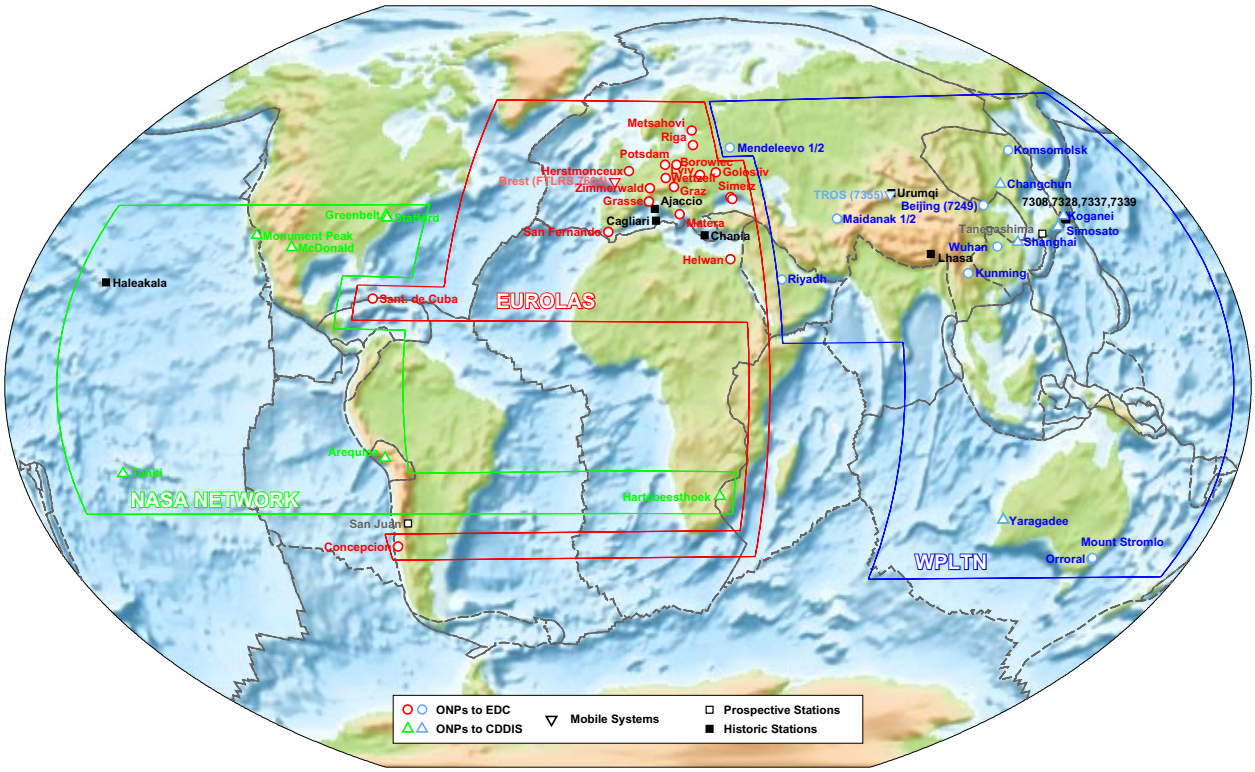

Fig. D5.1: Current SLR network with its three sub-networks supporting ILRS

Observation Campaigns

The ILRS Governing Board decides about finishing, continuing or agreeing of new SLR campaigns. The JASON-1 - TOPEX Tandem, ETALON-1/2, and ENVISAT campaigns will continue, LARETS and Gravity Probe-B are appointed as new campaigns.

Due to a budget cut at NASA Headquarters the NASA sites delivered less observation passes in 2004. Nevertheless the NASA SLR stations continue to provide valuable contributions to the ILRS (see table D5.1)

Tab. D5.1: Decreasing number of passes of NASA sites in 2004. (Haleakala and Arequipa stopped observation in July and February 2004 resp.)*

SITE	YEAR	JAN	FEB	MAR	APR	MAY	JUN	JUL	AUG	SEP	SUM
7080MDOL	2003	443	244	396	377	282	270	94	285	307	2698
	2004	137	148	184	187	221	151	193	116	134	1471
7105GODL	2003	506	380	513	572	226	262	378	425	633	3895
	2004	507	255	158	161	127	107	191	291	192	1989
7110MONL	2003	808	675	954	194	202	1005	681	652	1159	6330
	2004	780	198	218	258	644	459	769	483	548	357
7124THTL	2003	52	25	222	158	216	36	143	71	70	993
	2004	53	27	45	48	41	131	100	75	111	631
7210HALL*	2003	429	473	421	312	482	507	318	466	584	3992
	2004	496	246	112	194	95	57	0	0	0	1200
7403AREL*	2003	56	61	81	205	268	136	213	190	172	1382
	2004	6	0	0	0	0	0	0	0	0	6
7501HARL	2003	80	279	594	642	654	571	327	805	547	4499
	2004	180	207	244	354	579	113	121	246	120	2164

Observed Satellite Passes

In the time period from October 2003 to September 2004 45 SLR stations observed 31 satellites (including the four moon reflectors). Table D5.2 shows the EDC data base content at August 31, 2004. This content is compared with the content of the CDDIS data base, and has to be updated at EDC and/or CDDIS in case of discrepancies.

Tab. D5.2: Content of ILRS/EDC data base at September 30, 2004 for the product normal points (including Lunar Laser Ranging (LLR) observations to four moon reflectors)

Satellite	number of passes		Satellite	number of passes		Satellite	number of passes	
	increase 04	2004		increase 04	2004		increase 04	2004
ADEOS		671	**GLONASS-70**		1430	**LAGEOS-1**	8280	61426
AJISAI	9822	82433	**GLONASS-71**		2617	**LAGEOS-2**	6961	53931
BEACON-C	6123	32212	**GLONASS-72**		3260	**LARETS**	3272	3272
CHAMP	1493	6576	**GLONASS-74**		39	**LRE/H2A**		75
DIADEME-1C		1393	**GLONASS-75**		300	**METEOR-3**		409
DIADEME-1D		1585	**GLONASS-76**		301	**METEOR-3M**	342	1284
ENVISAT	4670	12887	**GLONASS-77**		343	**MOND-1**	39	320
ERS-1		10524	**GLONASS-78**		2712	**MOND-2**	26	214
ERS-2	5030	43177	**GLONASS-79**		3237	**MOND-3**	305	1983
ETALON-1	1582	9470	**GLONASS-80**		4466	**MOND-4**	12	582
ETALON-2	1547	9676	**GLONASS-81**		275	**REFLECTOR**	6	3728
FIZEAU		4243	**GLONASS-82**		244	**RESURS-01-3**		2011
GEOS-3		2237	**GLONASS-84**	1286	5272	**STARLETTE**	7439	61548
GFO-1	3538	22855	**GLONASS-86**	24	1204	**STARSHINE-3**		48
GFZ-1		5606	**GLONASS-87**	1181	3299	**STELLA**	3911	39758
GLONASS-62		963	**GLONASS-88**	5	14	**SUNSAT**		1864
GLONASS-63		1952	**GLONASS-89**	1499	2634	**TIPS**		1849
GLONASS-64		81	**GPS-35**	597	5147	**TOPEX/POS.**	8983	75391
GLONASS-65		397	**GPS-36**	653	4547	**WESTPAC-1**		5620
GLONASS-66		1544	**GRACE-A**	1596	4423	**ZEIA**		146
GLONASS-67		4299	**GRACE-B**	1483	3855			
GLONASS-68		875	**GRAVITY PROBE-B**	181	181			
GLONASS-69		945	**JASON-1**	6739	19073	**Sum of all**	**88625**	**640933**

D6 IVS Special Analysis Centre

IVS OCCAM working group

The goal of the IVS (International VLBI Service for Geodesy and Astrometry) OCCAM working group is to constantly improve the VLBI software OCCAM, which is used at DGFI to analyse VLBI observations. The main members of the group are scientists from Geoscience Australia (Canberra, Australia), the Vienna University of Technology (Vienna, Austria), the St. Petersburg University, the Institute of Applied Astronomy (both St. Petersburg, Russia) and DGFI. The version 6.0 of the software was officially released in February 2004 during the IVS General meeting in Ottawa, Canada. Since then, the software was upgraded in many parts (see also A3), mainly in very close cooperation with the Vienna University of Technology, reconceiled during two small working meetings, one in March (Vienna) and one in July 2004 (Munich).

Reliability measures for geodetic VLBI products

The reliability of geodetic VLBI products depends essentially on the checkability of the observation data and the reference frame points. First investigations to clarify the potential influence of non-detectable errors in terrestrial and celestial reference frames on VLBI products were done using the CONT02 campaign (for further information on CONT02 see projects A3 and D1). This showed that proper reliability measures for VLBI products can be derived in a rigorous way using statistical test theory as background (see figures 6.1 and 6.2). But, although the accomplished reliability analysis of the CONT02 campaign was well-suited for the illustration of the procedure, it is rather recommended to assess a large number of different VLBI sessions in the outlined way to achieve a thorough evaluation of existing reference frames.

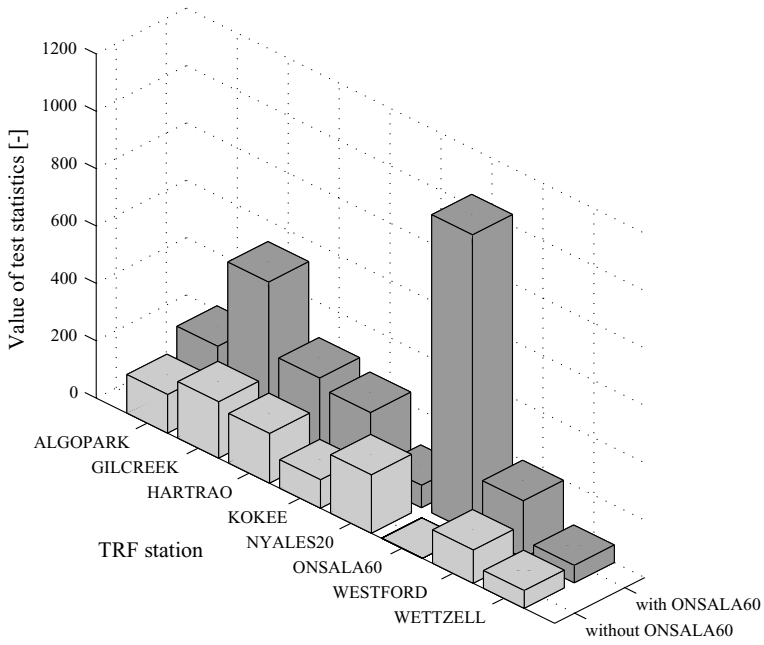

Fig. 6.1: Test statistic values if one respective station is discarded from the datum definition. If ONSALA60 is discarded before testing, the values of the other stations are reduced and homogenized significantly.

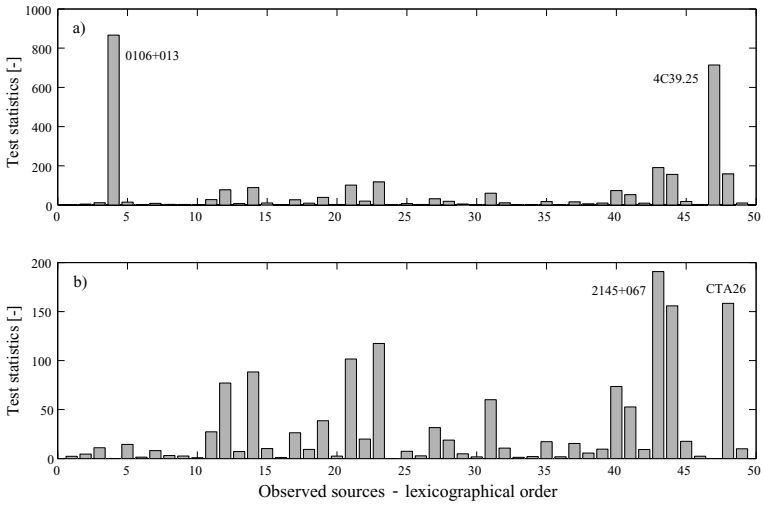

Fig. D6.2: Test statistic values if one respective radio source is discarded from the datum definition (note the different ranges on the y-axis), some sources with significant test values are named:
a) Datum defined using all radio sources,
b) Datum defined as in a), but without the sources 0106+013 and 4C39.25.

Further contributions to the IVS

The updated version of OCCAM is now embedded in an environment of scripts and programs which allow to do high quality analysis of actual VLBI data on an operational basis as well as for many scientific purposes (options to estimate all parameters common to geodetic and astrometric VLBI solutions, automation of many processes, pre- and post-fit analysis of the data etc.). This enables DGFI to contribute to the IVS as operational analysis center in the near future, as well as to take part in the IVS Pilot Projects on timeseries of baseline lengths and in the IERS Combination Pilot Project by contributing session-wise VLBI SINEX files to the IVS.

D7 Developments for an International Altimeter Service

The objective of the IAG intercommission project ICP1.1 "Satellite Altimetry" is to study rational, feasibility and scope of an International Altimeter Service, IAS. One of the first initiatives was the establishment of an IAS-Planning Group (IAS-PG) which shall develop a detailed implementation plan for an IAS, serving the altimeter user community with an utmost long time series of harmonized multi-mission altimeter observations with up-to-date geophysical corrections and consolidated geocentric reference and with related sea level products. The IAS-PG was established at the Eighth Meeting of the GLOSS Group of Experts in Paris, October 2003, and got a formal endorsement of the GLOSS programme, executed under the umbrella of the International Oceanographic Commission (IOC). Endorsements of other bodies (e.g. IAPSO) are being sought.

International Altimeter Service Planning Group (IAS-PG)

The nomination of members of IAS-PG was a trade-off between the requirement to have all space agencies, processing centres, and scientific groups properly represented and the need to limit the size of the group in order to work efficiently.

Web pages for IAS-PG were established within the Internet representation of IAG, Commission 1. At the same time a mailing list was realized in order to facilitate the communication among the members of the group. The mailing list is important because the group is not funded – business meetings are to be attached to international conferences related to altimetry.

An IAS-PG business meeting was held at the EGU Scientific Assembly in Nice, May 2004. Discussions included

- programmes, projects and already existing or forthcoming observation systems related to a future IAS,
- general functionality and objectives of an altimeter service,
- the compilation of user requirements,
- possible demonstration or pilot products, and
- status reports on the US Pathfinder project, the ERS reprocessing, on ICESat, and the ESA Oxygen O_2 concept.

IAS-PG has to report to IAG, GLOSS and other bodies related to satellite altimetry and shall provide – as a final deliverable – an implementation plan for the realization of an IAS.

OpenADB development continued

In addition to the coordination of the IAS-PG the development of OpenADB was continued. OpenADB, an open altimeter data base with a generic data format, the capability of fast parameter updates and the potential to generate data base extracts with user defined content and format, is a demonstration project for a future altimeter service. It shall prove that major drawbacks of existing altimeter mission data (the inhomogeneous format and out-of-date record parameters) can be avoided.

The compilation of altimeter mission data and the transformation to the mission independent OpenADB format is an ongoing activity. The current status of altimeter data holdings is summarized in table D7.1. Access to ERS and ENVISAT data is ensured through two ESA accepted proposals, dedicated to the cross-calibration

Tab. D7.1: Status of altimeter mission data, transformed to the OpenADB system

Mission (phases)	Repeat [days]	Mission data				Transformation to OpenADB			
		Source	Access	Media CD/DVD/ ftp	Volume [GByte]	Cycles	Volume/ cycle [MByte]	Total volume [GByte]	Interface/ Activity
GEOSAT (GM)	-	NOAA	free	10/-/-	~6.5	~25	~100	2.3	ready/evaluation
GEOSAT (ERM)	17		free			68	~70	3.9	ready/evaluation
ERS-1 (A,C)	3	CERSAT	PI only						
ERS-1 (B,D)	35								
ERS-1 (E/F)	168								
TOPEX/Pos.	10	CNES	free	120/-/-	78.0	364	~66	23.0	ready/completed
T/P-EM	10	NASA	free	-/-/FTP	11.0++	67	~66	4.2	ready/completed
ERS-2	35	CERSAT	A0416	80/-/-	52.0	77	~121	~11.0	ready/evaluation
GFO	17	NOAA	free	-/3/FTP	9.0 ++	97	~74	6.7	ready/ongoing
ENVISAT	35	ESA	A0416	-/32/-	150.5 ++	27	~153	4.1	developm/ongoing
JASON-1	10	NASA	free	-/2/FTP	26.0 ++	90	~45	4.0	ready/ongoing

of ERS-2 and ENVISAT (A0416) and the cross-calibration of CryoSat (AOCRY2707) with other altimeter systems equipped with traditional pulse limited radar sensors (launch in 2005) .

New sea state bias model for TOPEX/Poseidon

The OpenADB altimeter data is gradually enhanced. The long term stability of TOPEX/Poseidon suffered from a sea state bias model, empirically derived from side A data only (side A sensor components degraded in 1996 and were replaced by side B components). Chambers provided a new sea state bias model taking into account the different sensor performance for side A and side B. The OpenADB data has been updated accordingly.

Binned sea surface height anomalies (ssha)

For the comparison with tide gauge registrations a new product has been created for the OpenADB data structure, facilitating time series analysis of the altimeter data. It is similar to the "stacked" data files created within NASAs Pathfinder project: a nominal ground track is used to define – relative to the equator crossing – fixed small along-track bins with a length chosen such that for each repeat cycle at least one altimeter observation is located inside the bins. For every observation point the sea surface height is computed (applying environmental and geophysical corrections) and – after subtracting a static mean sea surface – compiled as sea surface height anomalies (ssha) into the bins. Figure D7.1 shows a time series of sea surface height anomalies for a particular bin located at the Patagonian shelf. Analysis of these time series allow, for example, to estimate residual shallow water tides (compare project B4).

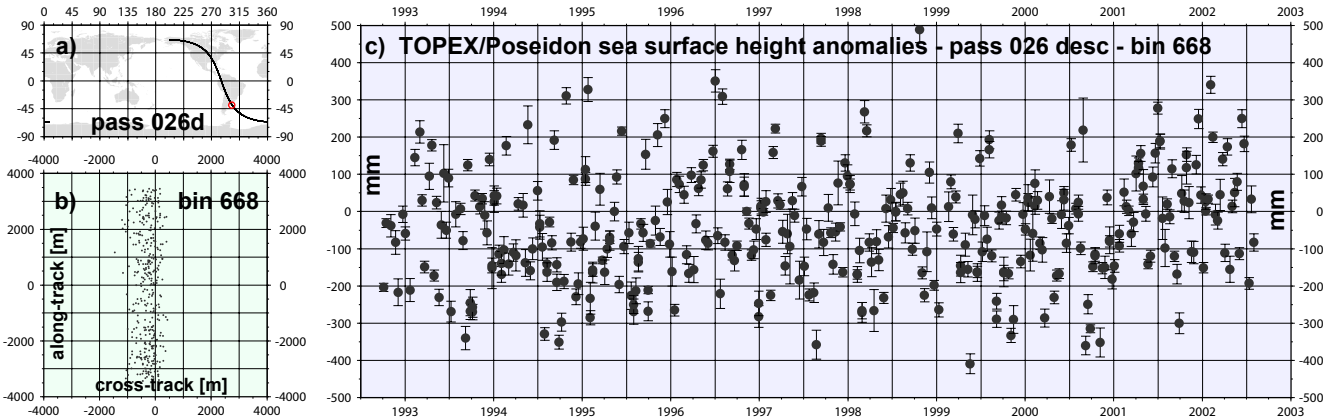

Fig. D7.1: Time series of TOPEX/Poseidon sea surface height anomalies (ssha) for a small along-track bin at the Patagonian shelf (see panel a). The location of the ssha within the bin is shown in panel b) with along-track and cross-track deviation [km] from the nominal ground track. Panel c) shows the ssha time series. The large scatter is due to residual shallow water tides, which are not properly modelled by global ocean tide models .

D8 Contribution to GGOS

The International Association of Geodesy (IAG) installed the Global Geodetic Observing System (GGOS) during the General Assembly of the International Union of Geodesy and Geodynamics (IUGG) in Sapporo, Japan, July 2003. The main objectives of GGOS are the representation of Geodesy in international bodies and the coordination of observations, models, data processing and parameter estimation in all areas of geodesy. The different geodetic techniques shall be integrated in order to achieve consistent and reliable products for the Earth's geometry and kinematics, the Earth's orientation and rotation, and the Earth's gravity field. DGFI participates in GGOS by its functions in various services of the IAG (see D1 to D7) and by contributing to the GGOS objectives.

In 2004 IAG has become a participating organization in the inter-governmental ad-hoc Group on Earth Observations (GEO). GEO was established by a declaration of thirty-three nations plus the European Commission during the Earth Observation Summit held in Washington, DC, on July 31, 2003. It signifies the political commitment to move towards the development of a comprehensive, coordinated, and sustained Earth observation system. GEO will seek in its work to improve coordination of strategies for Earth observations, to involve and assist developing countries, exchange in situ, aircraft, and satellite observations, and to prepare a 10-year implementation plan. IAG nominated each two representatives to GEO Sub-groups including a DGFI scientist in the Sub-group for capacity building.

GGOS also strives for becoming an official partner in the United Nations' Integrated Global Observing Strategy (IGOS). IGOS is a strategic planning process that links research, long-term monitoring and operational programmes in a framework for decisions and resource allocation providing governments with information for decision-making. IGOS is developed by a partnership including the Committee on Earth Observation Satellites (CEOS), World Climate Research Programme (WCRP), International Group of Funding Agencies for Global Change (IGFA), and the three Global Observing Systems (G3OS) for climate (GCOS), oceans (GOOS), and terrestrial observations (GTOS). GGOS submitted in 2004 a concept note for a „Dynamic Earth" theme within IGOS and was encouraged to develop a formal proposal for this new theme. DGFI is involved in this development.

E Information Services and Scientific Transfer

The results of scientific research need to be made available to the scientific community as well as to the public. Therefore adequate procedures for publication and for promoting a better understanding of science have to be developed and applied. Besides the publications in scientific journals and series, the DGFI maintains an information system in the internet. Moreover, the DGFI has an intensive data exchange with various scientific organizations. Adequate structures for managing this exchange on internal as well as external basis are to be installed and permanently tested and improved. This exchange especially refers to the contribution to and collaboration in large international projects and services, which can only be accomplished by the cooperation of many institutions.

Members of the staff of the DGFI participated in numerous congresses and other meetings, they gave lectures and submitted reports and publications. Further on, the DGFI is represented by its co-workers in numerous national and international bodies. The information exchange is extended by working visits at other institutes as well as scientific guests working temporarily at the DGFI.

E1 Geodesy Information System GeodIS

GeodIS is an information system for geodesy. Since some years it is maintained by DGFI with the objective to compile information about the most important areas of physical geodesy, namely geometry and reference systems, Earth rotation and orientation and the gravity field. This information is prepared for the Internet and is made available under the location

http://www.dgfi.badw.de/~geodis/ .

The intention of GeodIS is not to teach readers about geodesy or to substitute a text book on geodesy but to help people in finding information on and data of geodesy they are interested in. As an example, GeodIS provides a summary about the relevant scientific organizations and the international services with direct links to the corresponding homepages. Such a comprehensive summary is elsewhere not available.

Fig. E1.1: Home Page of the GeodIS information system

E2 DGFI Home Page

The DGFI home page is maintained in order to inform about the research performed at the institute and about the scientific results that were achieved. The home page is available under the location

http://www.dgfi.badw.de

The home page represents structure and content of the research program, gives short information about the ongoing research projects and the national and international projects, DGFI is involved in. The multiple contributions of DGFI to international services is represented.. The homepage also provides a list of papers and reports published by the employees and compiles all their posters and presentations. An increasing number of publications and posters is made available in electronic form, mostly with the portable document format (pdf), a de-facto standard for the exchange of electronic documents. Figure E2.1 shows the current bilingual layout, realised with the Open Source content management system Typo3.

Fig. E2.1: The bilingual layout of the DGFI home page

Content Management System (CMS)

The use of a content management system for the Internet presentation was a necessary step.There was an increasing number of pages that are to be developed and maintaned with the requirement for a uniform layout. There are also growing demands to include interactive and dynamic content, e.g. queries to data base systems like MySQL. All these requests could only be solved by a growing expertise on HTML, CSS, MySQL and PHP. Training each of the scientists on these script languages became as impossible as a delegation of the growing work to one specialist.

Typo3

This conflict was solved by installation and use of the Typo3 content management system. This system administrates the pages of an Internet site by a data base system, ensures a common layout by predefined templates and provides simple interfaces to

the editors - the scientist responsible for the page content. With Typo3, the scientists can now use any browser to create, modify or delete pages - without experiences in HTML, CSS and additional languages.

The selection of Typo3 turned out to be right: Typo3, an Open Source project, is one of the most actively developed management systems, applied by a growing number of commercial sites. It provides comfortable functions to handle graphics - a necessary feature for the presentation of scientific results. Typo3 also allows to maintain several independent internet sites in parallel, a feature that is intensively used at DGFI: Typo3 is not only used for the DGFI home page, but also for IAG, Commission 1, the home page of the Deutsche Geodätische Kommission (DGK), and even the Intranet (see project E3 below).

Internet Site for IAG, Commission 1

The leading role of DGFI scientists within the scientific organization of the International Association of Geodesy, IAG, in particular the responsibilities for IAG, Commision 1 (President and Chair of Intercommision Projects and of Study Groups) requested a selfstanding internet presentation for IAG, Commission 1. Based on the experiences with the DGFI home page, the content management system Typo3 was used to realise this new site within short time. The IAG, Commission 1 home page is available under

http://iag.dgfi.badw.de/

The layout is similar to that of the IAG home page. There are numerous sub-pages for subcommissions, inter-commission projects and study groups as well as links to other commissions of IAG, the IAG services and to COSPAR, the Council for Space Research. The start page of the IAG, Commission 1 home page is shown in figure E2.2.

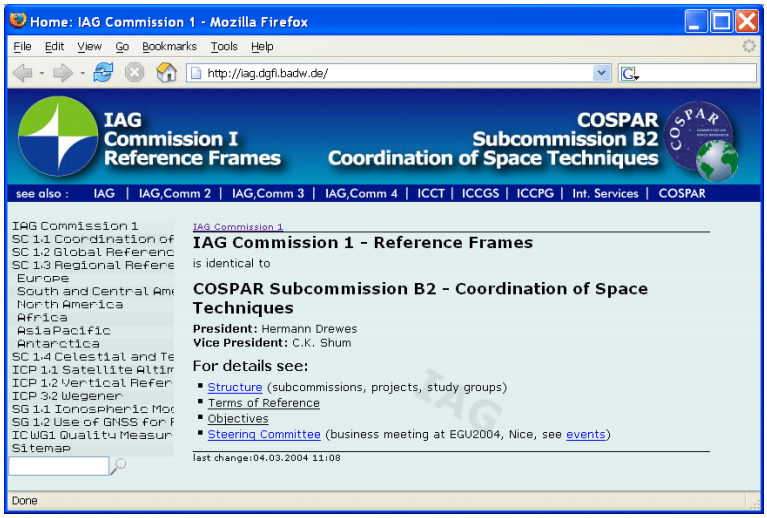

Fig. E2.2: The IAG, Commission 1 home page

Internet Site for Deutsche Geodätische Kommission (DGK)

The home page of the Deutsche Geodätische Kommission (DGK) was also redesigned on the basis of Typo3. The site is available at location

http://dgk.badw.de/

It informs about the structure of DGK, membership and working groups, the research institutes in Germany, and above all the numerous publications of DGK. The layout of the new DGK site is shown in figure E2.3

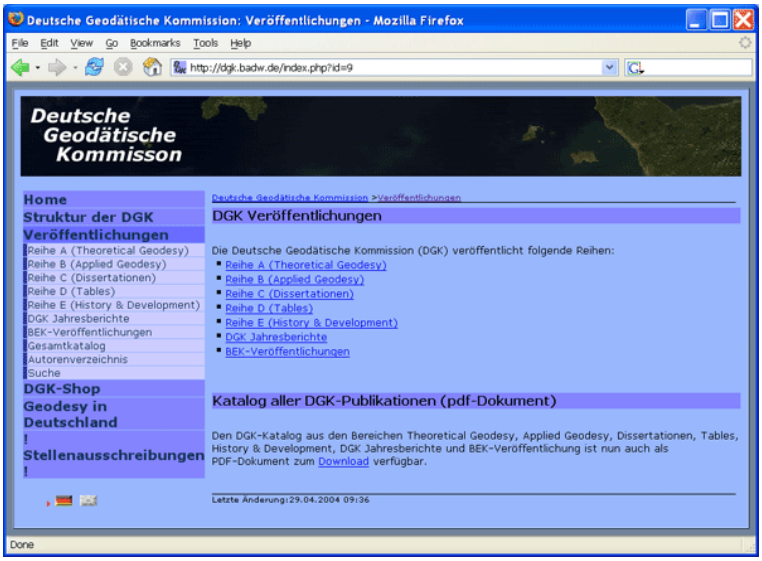

Fig. E2.3: Layout of the DGK home page after redesign with Typo3

The list of publications is now administrated by means of a MySQL data base system. The catalog of DGK publications is available in electronic form, created from the data base entries and dynamically updated as soon as new publications are edited. A comfortable search function for the DGK publications has been installed that allows to look for author(s), year or period of years, keywords and substrings within the title of publication. New DGK publications shall be more and more provided in electronic form (as pdf file). The catalog indicates which publications are available as electronic documents.

Finally, a rudimentary shopping system has been developed that allows to select and order DGK publications.

E3 Intranet

The DGFI Intranet has to provide a reliable access to the Internet for Emails and the World Wide Web (WWW). Furthermore it enables the acces to shared disc spaces, backup devices, printers and CD/DVD burners. Another aspect is the Intranet server which allocates actual information to all colleagues. Because of an increasing demand on computing capacity three additional Linux-PCs have been added as computing server to the Intranet.

Intranet server

Like the DGFI Internet server, the Intranet server (a Linux-PC using Apache-2 Webserver) has been ported to use the content management system TYPO3. This enables every associate to change contents on the server pages.

Backup device

For the archiving of fundamental data or for the backup of whole user discs the IBM TSM (Tivoli Storage Manager) located at the computing center LRZ (Leibniz Rechenzentrum) is used. A fast computer link of 100 Mbits/sec. enables together with a special software fast backup and restore operations. The overall capacity of the system is 260 TByte using 7 robot systems with tape drives and databank interface. To speed up the data transfer into the system a disc cache of 2200 GByte completes the TSM system. Presently LRZ considers a replacement of the system because the capacity is close to the limit.

The following list shows the present use of the TSM by DGFI

- number of nodes 3 ,
- number of backup files: 2.489.311 ,
- disc space used for backup: 500.842 MByte ,
- number of archived files: 7.152.852 ,
- disc space used for archiving: 1.591.852 MByte ,
- data transfer per month: 3.299 MByte.

Backup is the transfer of a whole disk to the TSM system to restore the disk in case of disk failure. In this case older files will be overwritten. Archiving is the explicit transfer of datasets to the archiving system. In this case many versions of the same file can be stored. To remove files from the TSM, they have to be explicitly deleted.

E4 Publications

Acuña, G., W. Bosch: Absolute comparison of satellite altimetry and tide gauge registrations in Venezuela. In: Hwang, C., C.K. Shum, J. Li (Eds.): Satellite Altimetry for Geodesy, Geophysics and Oceanography, IAG Symposia, Vol. 126, 261-270, Springer, 2003.

Akyilmaz, O., H. Kutterer: Prediction of Earth orientation parameters by fuzzy inference systems. DGFI Report No. 75, München 2003.

Angermann, D., D. Thaller, M. Rothacher: IERS SINEX combination campaign. Proceedings of IERS workshop on combination research and global geophysical fluids. IERS Technical Note 30, 94-101, 2003.

Angermann, D., B. Meisel, M. Krügel, M. Müller, V. Tesmer: Time series of site positions and datum parameters. Proceedings of IERS workshop on combination research and global geophysical fluids. IERS Technical Note 30, 199-201, Verlag des Bundesamtes für Kartographie und Geodäsie, Frankfurt a.M., 2003.

Boehm, J., H. Schuh, V. Tesmer, H. Schmitz-Hübsch: Tropospheric zenith delays determined by VLBI as a contribution to climatological studies. In: Schwegmann, W., V. Thorandt (Eds.): Proceedings of the 16th Working Meeting on European VLBI for Geodesy and Astrometry, Bundesamt für Kartographie und Geodäsie, Leipzig/Frankfurt am Main, 237-245, 2003.

Bosch, W.: Geodetic application of satellite altimetry. In: Hwang, C., C.K. Shum, J. Li (Eds.): Satellite Altimetry for Geodesy, Geophysics and Oceanography, IAG Symposia, Vol. 126, 3-22, Springer, 2003.

Bosch, W.: Session JSP05 - worldwide sea level change. In: Müller, J. (Hrsg.): Berichte zur XXIII. Generalversammlung der IUGG - Assoziation für Geodäsie, ZfV (129) 12-13, 2004.

Drewes, H.: Challenges for SLR in the realization of the terrestrial reference frame, modelling of the Earth‘s gravity field, Earth rotation and geodynamics, positioning and applications. In: ILRS Annual Report 2002, 5-7, NASA/TP-2003-212239, 2003.

Drewes, H.: Symposium U8 - geosciences: the future. In: Müller, J. (Hrsg.): Berichte zur XXIII. Generalversammlung der IUGG - Assoziation für Geodäsie, ZfV (129) 8-10, 2004.

Drewes, H., D. Angermann: Remarks on some problems in the combination of station coordinate and velocity solutions. Proceedings of IERS workshop on combination research and global geophysical fluids. IERS Technical Note 30, 30-32, Verlag des Bundesamtes für Kartographie und Geodäsie, Frankfurt a.M., 2003.

Drewes, H., Ch. Reigber: The IAG Project “Integrated Global Geodetic Observing System (IGGOS)“ - Setup of the Initial Phase. In: Vandenberg, N., K. Baver (Eds.): IVS 2004 General Meeting Proceedings, 32-37, NASA/CP-2004-212255, 2004.

Eder, K., T. Geiss, H. Hornik, H. Rentsch, H. Tremel: Neukartierung und DGM-Aufbau für das Tujuksu Gletschergebiet im Tian Shan. Zeitschrift für Gletscherkunde und Glazialgeologie, Band 38, Heft 2, 129-138, 2002.

Fabert, O.: Effiziente Wavelet Filterung mit hoher Zeit-Frequenz-Auflösung. DGK, Reihe A, Heft 119, München, 2004.

Gerstl, M.: Numerical aspects of combination at the observation equation and normal equation level. Proceedings of IERS workshop on combination research and global geophysical fluids. IERS Technical Note 30, 89-93, 2003.

Hornik, H.: Resolutionen der Internationalen Union für Geodäsie und Geophysik (Zusammenstellung und Übersetzung). In: Müller, J. (Hrsg.): Berichte zur XXIII. Generalversammlung der IUGG - Assoziation für Geodäsie, ZfV (129) 24-28, 2004.

Hornik, H.: Struktur der IUGG und IAG für den Zeitraum 2003-2007 (Zusammenstellung und Übersetzung). In: Müller, J. (Hrsg.): Berichte zur XXIII. Generalversammlung der IUGG - Assoziation für Geodäsie, ZfV (129) 28-31, 2004.

Huber, S., K. Kaniuth: On the weighting of GPS phase observations in the EUREF network processing. Mitteilungen des Bundesamtes für Kartographie und Geodäsie 33, 355-358, 2004.

Husson, V., C. Noll, W. Seemüller: Infrastructure. In: ILRS Annual Report 2002, NASA/TP-2003-212239, 29-30, 2003.

Ilk, K.H., J. Flury, R. Rummel, P. Schwintzer, W. Bosch, C. Haas, J. Schröter, D. Stammer, W. Zahel, H. Miller, R. Dietrich, P. Huybrechts, H. Schmeling, D. Wolf, J. Riegger, A. Bardossy, A. Güntner: Mass transport and mass distribution in the Earth system - Contribution of the new generation of satellite gravity and altimetry missions to geosciences. GOCE Projektbüro, TU München und GFZ Potsdam, 2004.

Kaniuth, K., S. Vetter: GPS Estimates of Postglacial Uplift in Fennoscandia. ZfV (129), 168-175, 2004.

Kaniuth, K., S. Huber: Modelling vertical site displacements due to atmospheric pressure loading with the Bernese sofware - a demonstration using EUREF data. Mitteilungen des Bundesamtes für Kartographie und Geodäsie 33, 89-95, 2004.

Krügel, M., V. Tesmer, D. Angermann, D. Thaller, M. Rothacher, R. Schmid: CONT02 campaign - combination of VLBI and GPS. In: Vandenberg, N., K. Baver (Eds.): IVS 2004 General Meeting Proceedings, NASA/CP-2004-212255, 418-422, 2004.

Kutterer, H.: The role of parameter constraints in VLBI data analysis. In: Schwegmann, W., V. Thorandt (Eds.): Proceedings of the 16th Working Meeting on European VLBI for Geodesy and Astrometry, Bundesamt für Kartographie und Geodäsie, Leipzig/Frankfurt am Main, 171-179, 2003.

Kutterer, H.: Symposium G02 - advanced space technology. In: Müller, J. (Hrsg.): Berichte zur XXIII. Generalversammlung der IUGG - Assoziation für Geodäsie, ZfV (129), 17-18, 2004.

Kutterer, H., R. Heinkelmann, V. Tesmer: Robust outlier detection in VLBI data analysis. In: Schwegmann, W., V. Thorandt (Eds.): Proceedings of the 16th Working Meeting on European VLBI for Geodesy and Astrometry, Bundesamt für Kartographie und Geodäsie, Leipzig/Frankfurt am Main, 247-255, 2003.

Rummel, R., H. Drewes, H. Hornik: Deutsche Geodätische Kommission/Deutsches Geodätisches Forschungsinstitut. Jahrbuch 2003 der BAdW, 251-258, München, 2004.

Schön, S.: Analyse und Optimierung geodätischer Messanordnungen unter besonderer Berücksichtigung des Intervallansatzes. DGK, Reihe C , Heft 567, München, 2003.

Schön, S., H. Kutterer: Imprecision in geodetic observations - case study GPS monitoring network. In: S. Stiros and S. Pytharouli (Eds.): Proceedings of the 11th FIG International Symposium on Deformation

Measurements. May 25-28, 2003. Thira/Santorini, Greece. Geodesy and Geodetic Applications Laboratory, Department of Civil Engineering, Patras University. Publication No. 2: 471-478, 2003.

Seitz, F., J. Stuck, M. Thomas: Consistent atmospheric and oceanic excitation of the Earth‘s free polar motion. Geophysical Journal International (157), 25-35, 2004.

Tesmer, V.: Refinement of the stochastic VLBI model: first results. In: Schwegmann, W., V. Thorandt (Eds.): Proceedings of the 16th Working Meeting on European VLBI for Geodesy and Astrometry, Bundesamt für Kartographie und Geodäsie, Leipzig/Frankfurt am Main, 207-218, 2003.

Tesmer, V.: Das stochastische Modell bei der VLBI-Auswertung. DGK, Reihe C, Heft 573, München, 2004.

Tesmer, V., H. Kutterer: An advanced stochastic model for VLBI observations and its application to VLBI data analysis. In: Vandenberg, N., K. Baver (Eds.): IVS 2004 General Meeting Proceedings, NASA/CP-2004-212255, 296-300, 2004.

Tesmer, V., H. Kutterer, H. Drewes: Simultaneous estimation of a TRF, the EOP and a CRF. In:Vandenberg, N., K. Baver (Eds.): IVS 2004 General Meeting Proceedings, NASA/CP-2004-212255, 311-314, 2004.

Titov, O., V. Tesmer, J. Boehm: OCCAM v.6.0 software for VLBI data analysis. In: Vandenberg, N., K. Baver (Eds.): IVS 2004 General Meeting Proceedings, NASA/CP-2004-212255, 267-271, 2004.

Torres J., H. Hornik (Eds.): International Association of Geodesy / Section I – Positioning; Subcommission for Europe (EUREF); Publication No. 12 – Report on the Symposium of the IAG Subcommission for Europe (EUREF) held in Ponta Delgada, 5 – 8 June 2002 – Reports of the EUREF Technical Working Group, Bundesamt für Kartographie und Geodäsie, No. 29, Frankfurt a.M., 2003.

E5 Posters and Oral Presentations

Angermann, D.: Terrestrial reference frame results derived from a combination of "weekly" GPS, VLBI, SLR and DORIS normal equations, EGU 2004 General Assembly, Nice, France, 26.04.2004.

Angermann, D.: Realisierung des terrestrischen Referenzsystems, Geodätisches Kolloquium, FH Oldenburg, 10.06.2004.

Angermann, D.: Towards a rigorous combination of space geodetic data, GEOTECHNOLOGIEN Statusseminar, Potsdam, 05.07.2004.

Angermann, D., B. Meisel, M. Krügel, V. Tesmer, R. Miller, H. Drewes: Analysis of site position time series derived from space geodetic solutions. AGU Fall Meeting, San Francisco, USA, 08.-12.12.2003 (Poster).

Angermann, D., M. Krügel, B. Meisel, M. Gerstl, H. Drewes: TRF realizations at DGFI, GEOTECHNOLOGIEN Statusseminar, Potsdam, 05.07.2004 (Poster).

Bosch, W.: Do we need an international altimeter service?, GLOSS Expert Meeting No. 8, IOC (UNESCO), Paris, France, 16.09.2003.

Bosch, W.: Sea level anomalies - affected by variations of the reference frame?, EGU 2004 General Assembly, Nice, France, 26.04.2004.

Bosch, W.: Decoding and extracting altimeter data with binread, EGU 2004 General Assembly, Nice, France, 28.04.2004 (Poster).

Bosch, W.: Temporal and spatial variability of the bias between TOPEX- and GPS derived TEC. EGU 2004 General Assembly, Nice, France, 29.04.2004.

Bosch, W.: Validation of marine gravity data using GRACE gravity field models, Joint CHAMP/GRACE Science Meeting, GFZ, Potsdam, 05.07.2004 (Poster).

Bosch, W.: Using EIGEN-GRACE02S to investigate defectiveness of altimeter gravity data, IAG International Symposium Gravity, Geoid and Space Missions, GGSM2004, Porto, Portugal, 30.08.-01.09.2004 (Poster).

Bosch, W.: Simultaneous crossover analysis for contemporary altimeter missions, ENVISAT Symposium, Salzburg, Austria, 07.09.2004.

Drewes, H.: Sistemas de referencia geocéntrico en el mundo. XXI Congreso Brasileiro de Cartografía, Belo Horizonte, Brasil, 01.10.2003.

Drewes, H.: Avances en la realización de los sistemas de referencia terrestres. Instituto Geográfico Augustín Codazzi, Bogota, Colombia, 10.10.2003.

Drewes, H.: Die Arbeiten des DGFI in den Jahren 2002/2003. DGK Vollsitzung, München, 27.11.2003.

Drewes, H.: Rezente Krustenbewegungen im Mittelmeer und in der Karibik - Kooperationsprojekte der ETH Zürich und des DGFI. Kolloquium H.-G. Kahle, Zürich, Switzerland, 20.01.2004.

Drewes, H.: Forschungsschwerpunkte des DGFI und Projekte auf dem Gebiet rezenter Krustenbewegungen. DGK Arbeitskreis „Rezente Krustenbewegungen", Hannover, 23.04.2004.

Drewes, H.: The reference frame for the Alpine Space GPS Network. INTERREG II B “Alpine Space GPS QUAKENET“ Kick-off Meeting, Trieste, Italia, 21.05.2004.

Drewes, H.: Realisierung terrestrischer Referenzsysteme durch die Dienste der IAG. Geodätisches Kolloquium, Univ. Innsbruck, Austria, 26.05.2004.

Drewes, H.: IAG’s Global Geodetic Observing System (GGOS) in its initial phase. SLR Workshop, San Fernando, Spain, 07.06.2004.

Drewes, H.: The ITRF for science and practice in the future. Geotechnologien Status-Seminar, Potsdam, 05.07.2004.

Drewes, H.: IAG’s Global Geodetic Observing System (GGOS). COSPAR 35th Scientific Assembly, Paris, France, 21.07.2004.

Drewes, H.: Geodätische Astronomie, optische Satellitengeodäsie, Very Long Baseline Interferometry - und was dann?. Festveranstaltung Prof. Dr. James Campbell, Bonn, 30.07.2004.

Drewes, H.: Deformaciones sésmicas y asésmicas de la corteza terrestre en América Central y del Sur determinadas por métodos geodésicos espaciales. Primer Congreso Latinamericano de Sismología, Armenia, Colombia, 20.08.2004.

Drewes, H.: Deformaciones de la corteza terrestre en América del Sur y su importancia para los sistemas de referencia terrestre. Instituto Geográfico Agustín Codazzi, Bogotá, Colombia, 27.08.2004.

Drewes, H.: El sistema de observación geodésico global de la Asociación Internacional de Geodesia (IAG): Universidad Distrital Francisco José de Caldas, Bogotá, Colombia, 31.08.2004.

Heidbach, O., H. Drewes: Model of the interseismic velocity field of the South American continent. EGU 2004 General Assembly, Nice, France, 27.04.2004 (Poster).

Kelm, R.: Quality control and combination. ILRS/AWG Workshop No.9, Kötzting, 26.10.2003.

Kelm, R.: DGFI weekly SLR intra-technique combination. ILRS Analysis Working Group Meeting, Nice, France, 23.04.2004.

Kelm, R.: Extended modelling for “weekly“ inter-technique combination. EGU 2004 General Assembly, Nice, France, 26.04.2004.

Kelm, R.: DGFI updated weekly SLR intra-technique combination. ILRS Analysis Working Group Meeting, San Fernando, Spain, 05.06.2004.

Kelm, R., B. Meisel: Statistical analyses for the combination of different geodetic space techniques. GEOTECHNOLOGIEN Statusseminar, Potsdam, 05.07.2004 (Poster).

Krügel, M.: Analysis of local ties from multi-year solutions of different techniques. IERS Workshop on site co-location, Matera, Italy, 23.10.2003.

Krügel, M., V. Tesmer, D. Angermann, D. Thaller, M. Rothacher, R. Schmid: Rigorous combination of GPS and VLBI to study reference frame related issues. IGS Workshop, Bern, Switzerland, 01.-05.03.2004 (Poster).

Krügel, M., D. Thaller: FESG and DGFI results of the CONT02 campaign. GEOTECHNOLOGIEN Statusseminar, Potsdam, 05.07.2004 (Poster).

Kutterer, H.: Prediction of earth rotation parameters using adaptive fuzzy inference systems. Arbeitstreffen zum Thema “Modellbildung der Erdrotation” im Rahmen des DFG-Forschungsvorhabens “Rotation der Erde”, Technische Universität Wien, 09.10.2003.

Kutterer, H.: Reliability measures for geodetic VLBI products. Third IVS General Meeting, Ottawa, Canada, 11.02.2004.

Meisel, B.: Comparison and combination of DORIS data with other space techniques. IOS Plenary Meeting, Paris, France, 04.05.2004.

Meisel, B.: Refined approaches for terrestrial reference frame computations. 35th COSPAR Scientific Assembly, Paris, France, 21.07.2004.

Meisel, B., D. Angermann, H. Drewes, M. Gerstl, H. Müller: Realization of the TRF origin by different satellite techniques. AGU Fall Meeting, San Francisco, USA, 08.-12.12.2003 (Poster).

Meisel B., D. Angermann, M. Krügel, R. Miller, D. Frey: Seasonal signals in GPS, VLBI, SLR and DORIS site position time series. EGU 2004 General Assembly, Nice, France, 28.04.2004 (Poster).

Meisel, B., D. Angermann, M. Krügel, H. Müller, V. Tesmer: Time series analysis of station coordinates and datum parameters. Geotechnologien Statusseminar, Potsdam, 05.07.2004 (Poster).

Müller, H.: Station coordinates and Earth orientation operational solution. ILSR/AWG Workshop No.9, Kötzting, 26.10.2003.

Müller, H.: Contribution to the ILRS AWG Benchmarking Pilot Project. ILSR/AWG Workshop No.9, Kötzting, 27.10.2003.

Müller, H.: Multi year SLR solution. 14th Int. Workshop on Laser Ranging, San Fernando, Spain, 07.06.2004.

Müller, H.: Results of the SLR tracking data quality control during the operational processing. 14th Int. Workshop on Laser Ranging, San Fernando, Spain, 09.06.2004.

Savcenko, R., W. Bosch: Shallow-water tide analysis with complementary tracks of Jason1 and T/P-EM. EGU 2004 General Assembly, Nice, France, 28.04.2004 (Poster).

Savcenko, R., W. Bosch: Residual tide analysis in shallow-water using T/P and T/P-EM. IAG International Symposium Gravity, Geoid and Space Missions, GGSM2004, Porto, Portugal, 02.-03.09.2004 (Poster).

Schmidt, M.: Multi-scale representation of the gravity field based on satellite and terrestrial data. Faculty of Aerospace Engineering, TU Delft, the Netherlands, 05.12.2003.

Schmidt, M.: Gravity field determination using multiresolution techniques. 2nd International GOCE User Workshop, Frascati, Italy, 08.03.2004.

Schmidt, M.: A method for ingesting observed TEC into an empirical ionospheric model. EGU 2004 General Assembly, Nice, France, 27.04.2004.

Schmidt, M.: Multi-resolution representation of regional gravity data. IAG International Symposium Gravity, Geoid and Space Missions, GGSM2004, Porto, Portugal, 02.09.2004.

Schmidt, M., O. Fabert, J. Kusche, C.K. Shum, S.-C. Han: Multi-resolution representation of regional gravity data sets. EGU 2004 General Assembly, Nice, France, 28.04.2004 (Poster).

Schön, S., H. Kutterer: Towards a realistic uncertainty budget for GPS heights. AGU Fall Meeting 2003, San Francisco, 12.12.2003 (Poster).

Seitz, F.: A dynamic model for the investigation of atmospheric and oceanic influences on Earth rotation. Lectures on present research in advanced geodesy, Institut für Geodäsie und Geophysik der Technischen Universität Wien, Austria, 08.10.2003.

Seitz, F.: Ein nichtlineares Systemmodell zur konsistenten Untersuchung von Rotation, Oberflächengestalt und Schwerefeld der Erde. Arbeitstreffen zum Thema „Modellbildung der Erdrotation“ im Rahmen des DFG-Forschungsvorhabens „Rotation der Erde“, Technische Universität Wien, Austria, 09.10.2003.

Seitz, F.: Consistent atmospheric and oceanic excitation of the Earth’s free polar motion. Workshop Forcing of polar motion in the Chandler frequency band: A contribution to understanding interannual climate variations, Luxembourg, 21.04.2004.

Tesmer, V.: An advanced stochastic model for VLBI observations and its application to VLBI data analysis. Third IVS General Meeting, Ottawa, Canada, 11.02.2004.

Tesmer, V.: CONT 02 campaign - combination of VLBI and GPS. Third IVS General Meeting, Ottawa, Canada, 11.02.2004.

Tesmer, V.: VLBI solution DGFI04R01: Simultaneous estimation of a TRF, CRF and the EOP using the software OCCAM. EGU 2004 General Assembly, Nice, France, 26.04.2004.

Tesmer, V.: Consistent VLBI solution DGFI04R02P: Simultaneous estimation of a TRF, CRF and the EOP. GEOTECHNOLOGIEN Statusseminar, Potsdam, 05.07.2004 (Poster).

Tesmer, V., H. Drewes, H. Kutterer: Simultaneous estimation of a TRF, the EOP, and a CRF. Third IVS General Meeting, Ottawa, Canada, 09.-11.02.2004 (Poster).

E6 Membership in Scientific Bodies

International Council for Science (ICSU)
- International Lithosphere Program (ILP) (Bureau Member: H. Drewes)
- Committee on Space Research (COSPAR): Subcommission B2 International Coordination of Space Techniques for Geodesy and Geodynamics (President: H. Drewes)

International Union of Geodesy and Geophysics (IUGG)
- IUGG Representative to Panamerican Institute for Geography and History, PAIGH (H. Drewes)
- IUGG Representative to United Nations Cartographic Office (H. Drewes) International Association of Geodesy (IAG)
- IAG Commission 1: Reference Frames (President: H. Drewes)
- IAG-Representative to Sistema de Referencia Geocéntrico para las Américas, SIRGAS (H. Drewes)
- Inter-commission Project 1.1: Satellite Altimetry (Chairman: W. Bosch)
- Inter-Commission Committee on Theory (ICCT) Working Group "Inverse Theory and Global Optimization" (M. Schmidt)
- Subcommission 1.3a: IAG Reference Frame Sub-commission for Europe (Secretary: H. Hornik)
- Subcommission 1.3a: IAG Reference Frame Sub-commission for Europe, Technical Working Group (H. Hornik)
- Working Group 1.2.3 and Inter-Commission Committee on Theory (ICCT) Working Group 3: Integrated theory for crustal deformation (B. Meisel)
- Study Group 1.1: Ionosphere Modelling (M. Schmidt)
- Study Group 1.3 and Inter-Commission Committee on Theory (ICCT) Working Group: Quality measures, quality control, and quality improvement (M. Krügel)
- Study Group 2.3: Satellite Altimetry: data quality improvement and coastal applications (W. Bosch)
- Project Integrated Global Geodetic Observing System, IGGOS (Secretary: H. Drewes)
- International Laser Ranging Service (ILRS): Governing Board (H. Drewes, W. Seemüller)
- International Laser Ranging Service (ILRS): Analysis Working Group (D. Angermann, R. Kelm, H. Müller)
- International Laser Ranging Service (ILRS): IERS Working Group on Combination (D. Angermann)
- International Laser Ranging Service (ILRS): Working Group Site Survey and Co-location (D. Angermann)
- International Laser Ranging Service (ILRS): Data Formats and Procedures Working Group (Chairman: W. Seemüller)
- International VLBI Service for Geodesy and Astrometry (IVS) – Special Analysis Center (H. Drewes, V. Tesmer)

Group on Earth Observation (GEO)
- Subgroup 2: Capacity Building (IAG Delegate: H. Drewes)

European Space Agency (ESA)
- Radar Altimeter 2 Science Advisory Group, RA2SAG (W. Bosch)

Centre National d'Etudes spatiales (CNES) / National Aeronautics and Space Administration (NASA)
- Ocean Surface Topography Science Team for Jason (Joint Altimetry Satellite Oceanography Network) (W. Bosch)

Consortium of European Laser Stations EUROLAS
- Member in the EUROLAS Board of Representatives (W. Seemüller)
- EUROLAS Secretary (W. Seemüller)

Deutsche Geodätische Kommission (DGK)
- "Ständiger Gast" (H. Drewes)

– Working Groups “Rezente Krustenbewegungen”, “Theoretische Geodäsie” (several collaborators)

Deutsche Forschungsgemeinschaft (DFG)
– Deutscher Landesausschuß für das Internationale Lithosphärenprogramm (H. Drewes)

Deutscher Verein für Vermessungswesen (DVW), Gesellschaft für Geodäsie, Geoinformation und Landmanagement
– Working Group 10 „Experimentelle, angewandte und theoretische Geodäsie” (H. Drewes)

E7 Participation in Meetings, Symposia, Conferences

GLOSS Techn. Workshop on New Technical Developments in Sea and Land Level Observing Systems, IOC (UNESCO), Paris, France, 14.-16.09.2003 (Bosch)

GLOSS Experts Meeting No. 8, IOC (UNESCO), Paris, France, 16.-17.09.2003 (Bosch)

XXI Congreso Brasileiro de Cartografía, Belo Horizonte, Brasil, 30.09.-03.10.2003 (Drewes)

IERS Geotechnologien Project Meeting, Bonn, 06.-07.10.2003 (Angermann, Kelm, Krügel, Meisel, Tesmer)

Working Meeting "Modellbildung der Erdrotation", Technische Universität Wien, Austria, 09.-10.10.2003 (Kutterer, Seitz)

IERS Workshop on site co-location, Matera, Italy, 23.-24.10.2003 (Angermann, Drewes, Krügel)

ILRS Analysis Working Group Workshop No.9, Kötzting, 26.-27.10.2003 (Angermann, Gerstl, Kelm, Müller)

ILRS Technical Workshop, Kötzting, 28.-31.10.2003 (Drewes, Müller, Seemüller)

Coordinators Meeting DFG Priority Research Programme "Mass Transport and Mass Distribution in the Earth System", Immenstaad, 03.-04.11.2003 (Bosch)

SAPOS Symposium, Frankfurt/M., 03.-05.11.03 (Krügel)

GOCE-CryoSat Workshop, Fa. Astrium, Friedrichshafen, 04.-05.11.2003 (Bosch)

EUREF Technical Working Group Meeting, Frankfurt a.M., 10.-11.11.2003 (Hornik)

Coordinators Meeting DFG Researchers´ Group „Erdrotation und globale dynamische Prozesse", Technische Universität Dresden, 14.11.2003 (Kutterer)

Science Working Team Meeting: From TOPEX/Poseidon to Jason, Arles, France, 18.-21.11.2003 (Bosch)

Deutsche Geodätische Kommission, Annual Meeting, München, 26.-28.11.2003 (Drewes, Hornik)

International Lithosphere Programme Bureau Meeting, San Francisco, USA, 07.12.2003 (Drewes)

AGU Fall Meeting 2003, San Francisco, 08.-12.12.2003 (Drewes, Meisel, Schön)

European Partners in IGGOS (EPIGGOS) Constitution Meeting, Potsdam, 14.01.2004 (Drewes)

Interreg III B "Alpine Space" Meeting, Milano, Italy, 14.-15.01.2004 (Drewes)

Third IVS General Meeting, Ottawa, Canada, 09.-11.02.2004 (Drewes, Kutterer, Tesmer)

Fifth IVS Analysis Workshop, Ottawa, Canada, 12.02.2004 (Kutterer, Tesmer)

Interreg III B "Alpine Space - GPS Quakenet" Scientific Meeting, München, 16.-17.02.2004 (Angermann, Drewes, Seemüller, Stuber)

Geotechnologien Project IERS/ITRF, Frankfurt a.M., 26.-27.02.2004 (Angermann, Drewes, Kelm, Krügel, Meisel, Tesmer)

IGS Workshop, Bern, Switzerland, 01.-05.03.2004 (Krügel, Tesmer)

2nd International GOCE User Workshop, Frascati, Italy, 08.03.2004 (Schmidt)

EUREF Technical Working Group Meeting, Budapest, Hungary, 22.-23.3.2004 (Hornik)

FGS Workshop 2004 on "Ringlaser Gyroscopes and Earth Rotation", Wettzell, 24.-25.03.2004 (Richter, Seitz)

OCCAM Working Meeting, Wien, Austria, 24.-26.03.2004 (Tesmer)

FGS Directing Board Meeting, Wettzell, 25.03.2004 (Bosch, Drewes)

Workshop "Forcing of polar motion in the Chandler frequency band: A contribution to understanding inter-annual climate variations", Luxembourg, Luxembourg, 21.-23.04.2004 (Seitz)

ILRS Analysis Working Group Meeting, Nice, France, 22.-23.04.2004 (Kelm, Müller)

DGK "Arbeitskreis Rezente Krustenbewegungen", Hannover, 23.04.2004 (Drewes)

EGU 2004 General Assembly, Nice, France, 25.-30.04.2004 (Angermann, Bosch, Drewes, Fabert, Kelm, Schmidt, Tesmer)

IERS Working Group 2 Meeting "Site survey and co-location", Nice, France, 26.04.2004 (Angermann)

IAG-ICP1.1 Business Meeting of the International Altimeter Service Planning Group, IAS-PG, Nice, France, 27.04.2004 (Bosch)

IAG Commission 1 "Reference Frames" Steering Committee Meeting, Nice, France, 28.04.2004 (Angermann, Bosch, Drewes, Schmidt, Tesmer)

IERS Working Group 3 Meeting "Combination", Nice, France, 29.04.2004 (Angermann, Tesmer)

IAG Executive Committee Meeting, Nice, France, 30.04.2004 (Drewes)

IDS Plenary Meeting, Paris, France, 03.-04.05.2004 (Meisel)

DGK Coordination Meeting „Geodäsie-Studium Concepción", Frankfurt/Main, 07.05.2004 (Drewes)

COSSTAGT Business Meeting, BKG, Frankfurt, 12.05.2004 (Bosch)

INTERREG III B "Alpine Space GPS QUAKENET" Kick-off Meeting, Trieste, Italy, 20.-21.05.2004 (Drewes)

EUREF Technical Working Group Meeting, Bratislava, Slowakia, 01.06.2004 (Hornik)

EUREF Symposium, Bratislava, Slovakia, 02.-05.06.2004 (Hornik)

ILRS/AWG Workshop Nr. 11, San Fernando, Spain, 05.06.2004 (Kelm, Müller)

ILRS Data Formats and Procedures Working Group Meeting, San Fernando, Spain, 07.06.2004 (Seemüller)

14th International Workshop on Laser Ranging, San Fernando, Spain, 07.-11.06.2004 (Drewes, Müller, Seemüller)

ILRS Governing Board Meeting, San Fernando, Spain, 09.06.2004 (Drewes, Seemüller)

ILRS General Assembly, San Fernando, Spain, 11.06.2004 (Müller, Seemüller)

Status Seminar Geotechnologien, Potsdam, 05.07.2004 (Angermann, Drewes, Krügel, Meisel)

Coordinators Meeting DFG Priority Research Programme, GFZ, Potsdam, 06.07.2004 (Bosch, Schmidt)

IAG-GEO Business Meeting, GFZ, Potsdam, 08.07.2004 (Bosch)

Joint CHAMP/GRACE Science Meeting, GFZ, Potsdam 05.-08.07.2004 (Bosch, Drewes, Seitz)

COSPAR 35th Scientific Assembly, Paris, France, 18.-25.07.2004 (Drewes, Meisel)

GGSM2004 Gravity, Geoid and Space Missions, Porto, Portugal, 30.08.-03.09.2004 (Bosch)

Intercommission Project 1.2 Vertical Reference Frames - Business Meeting, 31.08.2004, Porto, Portugal (Bosch)

ENVISAT Symposium, Salzburg, Austria, 06.-10.09.2004 (Bosch)

Geotechnologien Project IERS/ITRF, DGFI München, 13.-14.09.2004 (Angermann, Drewes, Gerstl, Krügel, Meisel, Seemüller, Tesmer)

Coordinators Meeting DFG Priority Research Programme, TUM, IAPG, 14.09.2004 (Bosch)

Official ILRS Combination Centers Meeting, Matera, Italy, 14.-16.09.2004 (Kelm)

COSSTAGT Project Meeting, DGFI, München, 23.-24.09.2004 (Bosch, Savcenko, Schmidt, Tesmer)

E8 Guests

09.10.2003: Dr. Saandar Mijidorj, MONMAP, Mongolia.

28.-31.10.2003: Dr. John Dawson, AUSLIG, Australia.

03.03.-31.08.2004: Juan Carlos Baez, Universidad de Concepción (UdeC), Concepción, Chile (presently at University Curitiba, Brasil) for research stay in GPS positioning.

22.03.-16.04.2004: Laura Sánchez, Instituto Geográfico Agustín Codazzi, Bogotá, Colombia.

10.05.-09.11.2004: Regiane Dalazoana, Universidade Federal do Paraná (UFPR), Curitiba, Brasil.

24.-28.05.2004: Prof. Silvio Freitas, Universidade Federal do Paraná (UFPR), Curitiba, Brasil.

02.06.-21.07.2004: Prof. Joao Francisco Galera Monico, Universidade Estadual Paulista (UNESP), Presidente Prudente, Brasil.

30.06.-01.07.2004: Dr. Johannes Böhm, TU Wien, Austria.

28.07.2004: Dr. Collin Fossu, Univ. Kumasi, Ghana.

13.-17.09.2004: Roberto Luz, Universidade Federal do Paraná, Curitiba, Brasil.

Prof. MSc Gustavo Acuña, Universidad del Zulia, Maracaibo, Venezuela, worked at DGFI in the frame of his PhD study at Technische Universität München.

Prof. Claudio Brunini, Universidad Nacional de La Plata, stayed at DGFI from 01.06. to 30.11.2003 with a grant of the Alexander von Humboldt Foundation.

F Personnel

F1 Number of Personnel

The total staff of DGFI during the 2003/2004 period was (incl. DGK office):

- from regular budget:

  12 scientists
  11 technical and administrative employees
  1 worker
  5 student helpers with an average of 306 hours/year
  1 scientific assistant with an average of 120 hours/year
  2 students in practical courses
  3 minor time employees

- from project funds:

  5 scientific employees

F2 Lectures at Universities

The following DGFI scientists had lectureships at universities:

Hon.-Prof. Dr. H. Drewes: “Geodetic Geodynamics“, Techische Universität München, WS 2003/2004

PD Dr.-Ing. habil. H. Kutterer: „Ausgleichungsrechnung III“, Universität Karlsruhe (TH), WS 2003/04

Dr.-Ing. B. Richter: „Geodätische Bezugssysteme“, Universität Stuttgart, WS 2003/04

F3 Graduations

The following doctoral graduation was completed:

05.12.2003: Dipl.-Ing. Volker Tesmer: Das stochastische Modell bei der VLBI-Auswertung. Technische Universität München.